Generation of Microbubble Foam Using a Packed Column

by

James Alfred Suggs

Thesis submitted to the Faculty of the

Virginia Polytechnic Institute and State University

in partial fulfillment of the requirements for the degree of

Master of Science

in

Chemical Engineering

APPROVED:

Donald L. Michelsen, Chairman

Felix Sebba

Kenneth Konrad

September, 1987

Blacksburg, Virginia

Generation of Microbubble Foam Using a Packed Column

by

James Alfred Suggs

Donald L. Michelsen, Chairman

Chemical Engineering

(ABSTRACT)

A technique for generating microbubble foams from a dilute surfactant solution using a column packed with millimeter sized glass beads is examined. The investigation requires the fabrication of a test unit capable of producing microbubble foam at 40 L/min and design and fabrication of a packed bed device. The work also introduces an improved method for photographing and viewing microbubble foams immediately after they are formed. This method can be used to quantitatively characterize the bubbles in the foam. Microbubble foams with a majority of bubbles less than 90 microns (μ) in diameter and with few bubbles greater than 150 μ were produced with the packed column device. The experimental results indicate that increased shearing forces resulting from increased volumetric flowrate and increased air fraction, enhance the generation of bubbles less than 90 μ in size. Further, stable microbubbles can be produced with surfactant (sodium dodecylebenzenesulfonate) concentrations as low as 200 ppm; and, the use of recycle produces a dramatic decrease in the size of all bubbles produced. Economically, the packed bed technique is superior to the spinning disk technique, the current microbubble foam generation method. This fact is partially due to the absence of an adequate large scale spinning disk device. In application, surfactant costs hamper the feasible use of a packed bed generation device. If, however, an application is used which begins with a surfactant laden solution, then the packed bed method becomes competitive.

Acknowledgements

I would like to recognize and sincerely thank many of my colleagues at Virginia Tech who, by their help, support, and friendship, have made my graduation possible. First, thanks go to Tim Longe and Jeff Smith, my officemates of a year and a half, for putting up with me as well as for offering their advice on subjects ranging from plumbing to philosophy. Second, thanks to the grad students that began the graduate program the same time I did; especially for their friendship, ears, and wisdom.

I also extend thanks to Billy Williams and Wendell Brown, the chemical engineering shop personnel, for the skill and help they provided in the construction of my research equipment.

I also want to acknowledge and thank Dr. Michelsen for serving as my advisor and for giving me the opportunity to design my project freely from scratch: but most importantly, for all the help and criticism he provided throughout the project, especially during the writing of my thesis. I also thank Dr. Konrad and Dr. Sebba for serving on both my graduation and examination committees, and for answering all the little questions that came up. Thanks is also extended to the U.S. Environmental Protection Agency, Union Pacific, and the Commonwealth of Virginia for providing the financial support for the project.

Finally, I should mention Dr. Adel of the Mining and Minerals Engineering Department for his help with the image analysis.

Table of Contents

List of Illustrations

List of Tables

1.0 Introduction

Aqueous foams are being used successfully throughout industry, especially in the areas of mineral, particulate, and oil flotation, dust suppression, petroleum production, and fire fighting. Recently, however, the development of techniques for producing consistent fine microbubbles could expand applications and perhaps improve the uses of foams in industry. One new microbubble foam development is known as Colloidal Gas Aphrons (CGA). First investigated by Sebba [1], CGA are typically characterized as a highly stable, 50 to 65% dispersion of fine 25 to 50 micron sized bubbles. The wide range of potential applications for these microbubble foams include: many flotation separation processes (removal of ash forming material from coal), enhanced oxygen transfer in gas-liquid systems (biological reactors), removal of oils from sand (scouring), and, use as an in-situ oxygen source (in-situ biodegradation of hazardous wastes).

Considerable laboratory work has been completed using CGA to address these problems, but only limited pilot-scale testing has been conducted. Large scale testing and commercialization has been restricted by the inability to produce these microbubbles in greater quantities. To date CGA generation has been limited to a technique known as the spinning disk method. This method, first developed in 1984 [2], involves the use of a small metal disk rotating in excess of 4000 RPM between two carefully positioned baffles in a container filled with dilute surfactant solution. This

technique produces "batches" of CGA and is amenable to continuous batch operation but with production limited to 4 L/min.

Efforts to scale-up the spinning disk method are hampered due to the problem of generating the necessary high shear in larger vessels. Conceptually, a series of many spinning disk generators operating in parallel could provide higher production rates, however, this idea is not practical or cost effective. With this obstacle to spinning disk scale-up in mind, it was reasoned that a fundamentally new generation technique would be required.

A preliminary goal of this thesis was to review microbubble foam generation techniques and to select a particular technique for study. An examination of the problems faced in producing microbubble foams indicated that mixing and high shear generation play a vital role in foam generation. An idea familiar to the chemical engineer is that of the packed column, a piece of equipment that provides static mixing and, at high flows, the means for providing high shear. There are many cases in which foams are generated with packed columns (supporting their mixing performance), but none examine the high flow situation necessary to produce microbubble foam. As a packed bed has a simple construction, no moving parts, and can be readily scaled to different sizes, it was chosen as the new method to be studied for producing microbubble foams.

The overall objective of this thesis was to study the production of microbubble foam in a packed bed. In particular, the specific objectives were:

1. To produce microbubble foam using a packed bed generation device in greater amounts than currently available,
2. To determine what variables significantly influence the character of microbubble foam produced with a packed bed device, and,
3. To evaluate the economic feasibility of using a packed bed generation device, especially in terms of future applications.

In order to accomplish these objectives, several minor goals were introduced. A portable microbubble foam generation pilot unit for testing various generation techniques needed to be designed and fabricated, and a packed bed generation device also needed to be designed and fabricated. Also,

before a reliable study of any microbubble foam generation technique could be undertaken an improvement in the means of quantitatively characterizing foam was required. Currently, microbubble foams are judged by a visual inspection of the product, or by transferring a sample to a microscope slide. Both methods are unreliable for accurate determination of the bubble size, thus another objective of the thesis was to develop a method that rapidly characterizes microbubble foam.

The following gives a short overview of the contents of the thesis. In Chapter 2.0, background information on aqueous foams, CGA, and packed beds is presented. Chapter 3.0 contains a discussion of the experimental plan including a description of the equipment used and the procedures followed. The results of the experimental work and discussion of their meaning can be found in Chapter 4.0. Addressing economic feasibility, Chapter 5.0 presents cost comparisons of packed bed generated microbubble foam and spinning disk generated CGA in various applications. Finally, Chapter 6.0 will give conclusions, recommendations, and future directions regarding microbubble foam generation.

2.0 Background

2.1 Aqueous Foams

An aqueous foam is an impermanent form of matter in which a gas, often air, is dispersed in a conglomeration of bubbles that are separated from each other by films of a liquid that is almost but not entirely water. The liquid films, part of a continuous aqueous phase, contain minute amounts of surfactant, sometimes as low as 20 ppm in the bulk, which act to stabilize the foam. Without the surfactant, mixing air into water will produce highly unstable air cavities or holes whose size, shape, and distribution will depend on the turbulence of the mixing process. When surfactant is present, the initial air hole provides an interface at which the surfactant can concentrate, thereby forming a film. The phenomena known as the Gibbs-Marangoni effect describes that this film will stabilize the bubble.

Although the bubbles are stabilized, and thus resist coalescence, they will not persist indefinitely. Due to normal buoyancy forces, the bubbles will rise to meet an air-water interface where the liquid films will begin to drain and, due to evaporation, eventually decay. If the bubbles are prevented or delayed from reaching the air-water interface, e.g. agitated, they will remain stable in suspension for greater lengths of time. Gas diffusion, to a lower degree, also contributes to the

destruction of the bubbles. The surface tension of a bubble is balanced by the pressure of the air trapped within. Because the pressure is higher in the smaller bubbles (LaPlace equation), the air will diffuse from these to the larger ones, thus bringing about the demise of all the small bubbles. In forming a foam it is possible that all the air introduced is not incorporated into the foam [3]. When this situation occurs, it necessarily follows that large voids, indeed a separate gas phase, will coexist with the liquid medium. When surfactant is not present the air-water system is driven to this two phase regime.

There are generally two classes of foams, "wet" foams and "dry" foams. In a wet foam the air content is low, 75% or less, which allows the bubbles to be far enough apart that none of them are distorted by another. As a result, the bubbles adopt a spherical shape in an attempt to minimize their surface energy. The traditional term for a wet foam is *Kugelschaum* or spherical foam. The diameter of the bubbles of a kugelschaum are not limited to any particular size; however, there are practical differences between foams that are made up of mostly tiny bubbles and those that are made up of mostly large bubbles. The greatest difference rests with the time they stay in suspension. As bubble size decreases, the force driving the bubbles to the surface (buoyancy force minus drag force) is also decreased, thus lengthening the amount of time it takes for the bubbles to rise to the surface, i.e. they will remain in suspension longer. Kugelschaums with bubble diameters less than 250 μ are termed microbubble foams and, due to their size, are more stable than the larger (up to several millimeters) kugelschaums.

The more widely known form of foam is the dry foam. Dry or conventional foams are characterized by a high percentage of air, typically 95%, and the presence of distorted, polyhedral cells. Foams with even lower amounts of water, called high-expansion foams exist, and have very low densities (.05-.002 g/mL) [4]. All wet foams become dry foams upon draining. The traditional term for dry foam is *Polyederschaum* or polyhedral foam. As the foam drains, the film between the bubbles becomes so thin that the spherical bubbles begin to influence one another distorting themselves into polyhedral shapes. Polyederschaums are also different from kugelshaums in terms of their mechanical properties, the former behave like psuedoplastic fluids, while the later flow like water.

It should be noted that mere generation of bubbles is not necessarily the precursor to foam generation. Bubbles, large or small, can be generated and exist widely dispersed in a continuous medium. These formulations of dispersed bubbles have very low concentrations of air and are usually transitory in nature. Bubbles formed by electrolysis or dissolved air techniques generally fall into this class. For ease of understanding, any collection of large numbers of bubbles, micron sized or not, will be categorically termed foam. Foams will generally have an air fraction greater than 45%. Formulations where bubbles are formed in a widely dispersed fashion will be referred to as a collection of bubbles.

2.1.1 Colloidal Gas Aphrons

As the size of the bubbles in a kugelschaum is reduced to below 50 μ with few greater than 100 μ, colloidal properties, such as the ability to remain dispersed in liquid without significant coalescence, become apparent. These microbubble foams contain a dispersion of small stabilized air bubbles in an aqueous medium, and have a viscosity approaching that of water. First investigated by Sebba under the name of microfoams [1], their behavior was significantly different from other foams so that in order to prevent confusion the name "colloidal gas aphron" (CGA) was introduced [5]. The name "aphron" comes from the Greek "αφρος", a foam, and has been coined to mean any fluid encapsulated in a thin aqueous shell, or, a true bubble. Like microbubble kugelschaums, CGA consist of gas spheres enclosed in a soap film of dilute surfactant solution, the major difference in the two lies with the stabilized encapsulating soap shell characteristic of CGA. CGA of practical interest typically contain 50 to 65 % air by volume. For future reference, the percentage of air by volume in a foam will also be referred to as quality. As the concentration of air is increased above or below this range, this stabilized microbubble foam demonstrates reduced effectiveness in most applications. Although Sebba lists the size range of CGA at 25 to 50 μ [6], samples taken by the improved technique developed in this work indicate that the range is broader,

15 to 120 μ, with an average of 50.7 ± 22.7 μ. Further technical aspects of CGA structure and properties are discussed in greater detail elsewhere [6].

Gas aphrons were first produced in the laboratory by Sebba using the venturi method. This method essentially depends upon the fast flow of a dilute surfactant solution past a venturi throat, at which point there is a provision for entry of the gas, under about one atmosphere excess pressure, through a very narrow channel [1]. Several years later, in 1984, Sebba developed an improved technique for producing CGA: the spinning disk. This method involves the use of a small disk rotating in excess of 4000 RPM between two carefully positioned baffles in a container filled with dilute surfactant solution [2]. Since the introduction of the spinning disk technique and its ability to generate 4 L/min of CGA, no other generating techniques have been tested. The advent of this colloidal system and the ways of generating it opened up new avenues for separation techniques as well as providing new solutions to old problems. Sebba [7] has identified the following applications:

1. Stripping of dissolved gases from water.
2. Removing finely dispersed oils from water.
3. Ion and precipitate flotation.
4. Removal of ash forming materials from coal.
5. Removal of oil from sands.
6. Flotation of microorganisms such as algae and bacteria.
7. Oxygen transport to subsurface matrices.

Unfortunately, generation techniques have been limited to producing only small amounts of CGA, yet all of these applications, if commercialized, would require much greater quantities of a microdispersion of air bubbles in water. Because of this demand, a technique for generating "commercial" amounts of CGA is needed in order for the work to be applied in the field. Scaled-up versions of the venturi and spinning disk methods would meet the requirements; however, only preliminary tests have been conducted. Sebba, in several papers, rules out the possibility of scaling-up the venturi technique [2,7]; however, Barnett, another pioneer in microfoam work, has claimed that proprietary work on large scale venturi devices has been completed with a high degree

of success [8]. Because of possible patents pending, Barnett is unwilling to disclose detailed evidence to ascertain that his venturi devices are indeed generating CGA. In regard to a larger version of the spinning disk, little work has been accomplished. On first appearance, however, it would seem that the spinning disk can not be used cost effectively, if at all, on a large scale. Spinning disk generation relies on very high shear supplied by baffling and a fast rotating disk. To achieve similar shear rates in a larger vessel much higher RPMs would be required and it is unknown whether the critical baffling could be replicated in a larger vessel. On the other hand, many, many of the small two liter vessels could be operated in parallel in a continuous batch mode; however, this idea is simply not practical from a plumbing, power, and maintenance point of view. Fundamentally new techniques for producing these microbubble foams in larger quantities would find immediate use for large scale field testing for a number of applications.

2.2 *Review of Foam Making Capabilities*

In industry, interest in foams comes from several different areas. In coal processing, conventional foams are used to reduce fugitive coal dust transmission [3]. In the mining industry essential flotation separation processes are carried out using microbubbles [9,10]. High-expansion foams are used in fire fighting, and there are more uses for conventional foam in drilling applications and petroleum production [11-13]. As a result of these varied applications, foam generation techniques differ and are often designed with emphasis on a particular foam characteristic. Since this work deals with microbubble foams, discussion will be limited to techniques generating bubbles less than 250 μ.

A review of the literature reveals that there are essentially five fundamental ways to generate a foam [14]: bubbling gas into the liquid phase; co-injecting or separately injecting gas and liquid through nozzles; mixing in high shear devices; dispersal by splashing or shaking; and reducing pressure on a liquid that initially contains a dissolved gas. Essentially, each of these methods pro-

vides a means of creating air pockets that can be stabilized in an encapsulating soap shell. The methods are different in that the each create a particular environment that the bubbles will be formed in, as well as how the foam is to be delivered or used. However, the kind of foam that is produced and its attendant characteristics are widely varied and depend upon technique and liquid phase formulation. To quote a recent U.S. patent, September 1986, "the selection of surfactants and conditions for optimum formation and stabilization of foams is one mainly of art [14]."

Of the fundamental techniques, gas sparging and high shear generation techniques, including co-injection, are the most popular. Dispersal by splashing or shaking and reducing pressure on a liquid containing dissolved air produces a widely dispersed collection of bubbles of low air concentration. While dissolved air generation techniques are known to produce bubbles of 40 to 150 μ size, their use is limited to flotation.

Though popular, gas sparging [15-17] tends to produce large bubbles in a conventional foam, with some sources simply mentioning that a foam was formed. A literature source presents a novel idea for obtaining microbubble foam by using a hydrocyclone to separate it from conventional foam [18].

The high shear devices can be divided into two groups, those using co-injection, and those using a chamber with some sort of packing. Examples of co-injection devices follow. One device that may produce microbubble foams comes from a 1970 U.S. Patent issued to General Dynamics [19]. This device takes advantage of the laminar sublayer that exists near a surface in turbulent flow. Bubbles of five to ten micron size are made by passing gas into a sparger that is inside a pipe. The clearance between the sparger and pipe is such that a laminar sublayer less than ten microns is formed. At this sublayer, pressure perturbations snap off the bubbles before they can grow larger than ten microns. Although the patent mentions that the microfoam produced is homogeneous and that there is very little coalescence, nothing is mentioned specifically about quality or stability. The patent does cite an example of operating conditions, referring to a device that runs at 100 gpm or greater solution flow rate and 600 scfh or greater air flow rate at 75 psi. Using these rough numbers, a quality of 43% is calculated.

Another U.S. patent [20] uses a co-injection technique to generate a foam. However, based on the patent's cited examples, this device generates bubbles of up to 500 μ size with a quality between 85% to 95% at a rate of 52 gpm. The patent also mentions operating pressures of air and water, these are 10 - 1000 psig and 20 - 2000 psig respectively. As with most foam or microfoam generation devices found in the literature, this device is producing a conventional foam, not a CGA.

The packed chamber ideas abound and are worth reviewing. Materials for the packing are quite varied: micron sized glass beads [21]; stainless steel shavings, plastic shavings, wire mesh, plastic beads [22]; glass beads [22,23]; stainless steel wool [24]; honeycombed metal strips [25]; and even ceramic Rasching rings and Beryl saddles [26]. Only three of these sources mention bubble size. The first [21] claims that a cell filled with glass beads of diameter 200 - 250 μ produces bubbles with diameter 100 - 150 μ, yet gives no mention of quality, stability, or throughput. The second one [3], a report from BETZ Laboratories, produces bubbles of 100 - 200 μ size at throughputs of up to 115 gpm and 50% to 99% quality. The BETZ report is very helpful in that they studied the effects of generator configuration on foam production. Unfortunately, they based the effectiveness of the generator on the quality of foam it was able to produce, not the bubble size or stability. In their study they used a column packed with a honeycombed strip and a commercially available in-line static mixer, as well as two other techniques. The last source uses 1.0 mm sized glass beads in a packed column to produce bubbles whose size can be controlled from "less than 0.1 mm to over 3 mm average bubble diameter [23]." None of the other sources disclose information on the size of the bubbles produced, but some do provide throughput information, e.g. 2 - 5 gpm with a device using steel shavings [22], and 35 gpm for ceramic Rasching rings [26].

In general, in the applications of conventional foams for fire suppression and dust retardation, bubble size is not emphasized but rather formulations used and percent air in the foam is highlighted. On the other hand, all microbubble foam applications--dissolved air flotation, new biodiffusers, and subtle sulfur removal techniques for coal, are concerned with bubble size and effectiveness. However, the bubble size distribution is rarely disclosed partly because bubble sampling and measurement techniques are not well accepted but also for proprietary reasons. When interest has been expressed in bubble size, for example, in coal floatation, the smallest bubble size

reported is 100 μ [3,23], with no indication of uniformity given. It can thus be concluded that, with regards towards the literature, Sebba's CGA generators, producing microbubble foams, are at the front of very small bubble generation technology.

2.3 *Packed Columns*

One of the main advantages of using a packed column to produce a foam, or here, microbubble foams, is the enormous area for gas-liquid contacting provided by the packing. The packing can be viewed as a means of enhancing the turbulence in the column in order to provide greater shearing. This shearing process can be visualized as follows. Air enters the column in a continuous stream, in essence, in the form of an elongated bubble. As this bubble encounters the packing, it is forced to twist, bend, and break up, in order to pass through. The result of the tortuous path is that the stream of air is now broken into many smaller components, each having a diameter not larger than the diameter of the path they followed through the column. While a shear phenomenon forms the bubbles, the mixing effect of the packing allows for the uniform dispersion of the bubbles that are formed.

Packed columns are found throughout industry, and so there is a considerable amount of information about their operating parameters. Two of these parameters, Reynolds number (N_{re}) and pressure drop across the column (ΔP), are important to bubble generation, scale-up, and cost effectiveness. The Reynolds number is a dimensionless quantity that relates to the flow regime in the column. For a single phase fluid [27]:

$$N_{re} = \frac{4D_p \rho V}{\pi \mu D_t^2 (1 - \varepsilon)} \tag{1}$$

For packed columns, the laminar flow regime is given by $N_{re} < 10$, the transition region is given by $10 < N_{re} < 1000$, and the highly turbulent flow regime is given by $N_{re} > 1000$. The void fraction, ε,

has a marked effect on both N_{re} and ΔP. The void fraction is a function of how the column is packed, the ratio of the tube diameter to the packing diameter (α), and of the size uniformity of the packing material. Assuming the packing material is uniform, and the column is packed the same way, e.g. simple dumping followed by tapping, then ε depends entirely upon α. The factor α also indicates the degree to which wall effects will cause the flow pattern to deviate from ideality. When α is greater than eight, flow through the column may be considered ideal [28]. Being a dimensionless quantity, the Reynolds number is used in scale-up. To emulate the flow regime of a small column in a new larger one assuming the packing is the same, the new flow capacity and new column diameter are calculated such that N_{re} does not change. In a large column with the same packing size, α will increase, favoring ideal flow; however, ε may also vary, affecting the pressure drop.

To see how the void fraction can affect ΔP, a correlation can be examined.

$$\Delta P = \frac{600\mu V}{\pi(D_t D_p)^2}\frac{(1-\varepsilon)^2}{\varepsilon^3} + \frac{28\rho V^2}{\pi^2 D_p D_t^4}\frac{(1-\varepsilon)}{\varepsilon^3} \qquad (2)$$

This equation is the Ergun equation [27] and is applicable to single phase fluid flow through packed columns. Note that for high flowrates, $N_{re} > 1000$, the first term on the right side drops out, and at low rates of flow, $N_{re} < 10$, the second term on the right drops out. The Ergun equation is but one of many that have been proposed for describing pressure drop across packed beds. The pressure drop relates directly to economic feasibility since a higher pressure drop requires a more powerful pump to maintain a given throughput. Both higher rates of flow and smaller packing size increase the pressure drop, thus an optimum configuration exists which remains within the confines of cost effectiveness. Further treatments of these parameters as well as flow through packed columns can be found elsewhere [28].

In applying the Reynolds number and Ergun equations to foam/microbubble flow two problems arise. First, the bubbles are being continuously generated beginning at the bottom of the column. This situation creates a poorly mixed, non-uniform flow region which cannot be modeled accurately with any pressure drop equation. The problem also raises the question of bed length.

clearly there is a minimum bed length required to generate microbubbles, but there may also be a bed length at which the packing is no longer generating microbubbles, but merely adding to the pressure drop.

The second problem concerns a flow model. Two phases exist in foam flow, yet the Ergun equation is valid only for single phase flow. Observation of microbubble foam does, however, lend support to the idea that this special foam can be though of, and modeled as, a single phase. Marsden [29], studying foam flow through porous media, notes that "[s]ince the gas and liquid are so intimately mixed that each strongly affects the flow of the other, we hesitate to consider them as separate, independent fluids . . . ." There is a considerable body of information on gas-liquid flow, yet this information is based on surfactant free systems. Perry's Handbook [28], discussing particle dynamics, indicates that much of the published information on bubble dynamics is conflicting, and, that it is believed that these published discrepancies are due to the presence of surface active agents.

Effective use of a packed column to control the size and uniformity of the bubbles requires variations in the physical parameters of the bed. These parameters include the bed length, the size and uniformity of the packing, the factor α, shape of packing, void fraction, velocity of fluid, fluid input configurations, and nature of the fluids. These parameters can be condensed down to simpler forms using dimensionless quantities. For example, the shape, size, and uniformity of the packing can be combined by introducing the definition of mean particle diameter, Dp. This definition is most convenient for spheres, since the mean particle diameter is just the mean diameter of the spheres. The nature of the fluids and the velocity of the fluid through the bed have already been combined via the Reynolds number. As mentioned previously, ε is a function of α given uniformity of packing and packing procedure. Simpler still is the fact that α is directly proportional to the packing diameter when the tube diameter is held constant. Thus, the physical parameters of a packed bed can be summarized into four key parameters:

- Length, L
- Mean particle diameter, D_p

- Reynolds number, N_{re}
- Geometry of input streams.

For this work, only two of these parameters are examined: particle diameter and Reynolds number. The other two, length and geometry of input streams, do not directly relate to the flow conditions in the column. The other parameters chosen for study are not particular to the generator used. These variables are concentration of surfactant, solution flowrate, quality, and recycle ratio.

3.0 Experimental

3.1 Goals

The objectives of this thesis are:

1. To review microbubble foam generation techniques and select a promising direction to pursue.
2. To develop a method to rapidly and quantitatively characterize microbubble foams.
3. To design and fabricate a portable microbubble foam generation pilot unit for testing various generation techniques.
4. To design and fabricate a packed bed generation device.
5. To produce microbubble foam continuously using a packed bed generation device in greater amounts than currently available.
6. To determine what variables significantly influence the character of microbubble foam produced with a packed bed device.
7. To evaluate the economic feasibility of using a packed bed generation device, especially in terms of future applications.

Confronted with the problem of generating microbubble foam, hundreds of ideas can be conjured up from the exotic to the simple. A review of the literature did not uncover any high shearing commercial techniques that specifically generated foams with bubbles less than 100 μ in diameter. Of the methods for producing foams with small bubbles, each used high shear phenomena. One exception is pressure reduction of water containing dissolved air. This technique is capable of producing bubbles in the 40 to 150 μ range, however the technique produces a collection of bubbles or, at best, a low quality foam. CGA generation techniques including the venturi idea work well in the laboratory, but as mentioned, do not lend themselves to scale-up. The packed bed idea, one of the high shear techniques, attracted particular attention--it was cited often, it was simple, and it offered an operation that has been frequently and exhaustively studied by the chemical engineer. As the packed bed idea had the most information associated with it, it was selected as a starting point in new microbubble foam generation techniques. A program of study, including fabrication of a testing network, was established that would ask and answer the questions necessary to decide which microbubble foam generation device offers the greatest promise at commercialization.

3.2 Characterization

Microbubble foams are characterized by three properties: quality, stability, and bubble size distribution. Quality and stability information is provided by taking 250mL samples, while bubble size distribution is found by image analysis of photomicrographs of the foam produced. Specifically, the quality, which is defined as the volume percent of air in the product, is found by dividing the tared weight of a filled sample container by the volume of microbubble foam taken (nominally 250 mL). As samples are taken at atmospheric pressure, the quality value calculated will only apply at atmospheric pressure. Stability, a function of how long microbubbles remain in suspension, is measured by plotting bubble rise versus time. When the sample is first taken, there will be no

microbubble/water interface. Within 60 seconds, an interface will form that slowly rises as the microbubbles collapse into a conventional foam. Eventually, the foam will disintegrate leaving only the original surfactant solution. The rate at which the interface rises, i.e., the slope of a plot of bubble rise versus time, can be used as an indicator of stability (see Section 4.3 Characterization). Another indicator of stability is the position of the interface at a given time. Here, the lower the interface at a given time, the more stable the microbubble foam is. In order to compare the interface heights for each test, a normalized value is required. If the microbubble foam is allowed to sit indefinitely, the foam will completely break down. At this point, the height of the liquid is the highest it will ever reach for that sample. Calling this height 100%, any previous interface height can be viewed as a fraction of this height. That fraction, a value from 0 to 100%, represents the normalized interface height. The 100% level can be derived from the quality of the sample, and is equivalent to the volume fraction of water in the microbubble foam.

Most critical is size and uniformity of the microbubbles produced. Analysis of these properties primarily involves photography and image analysis. Photomicrographs are made with the aid of a Nikon microscope fitted with a small video camera and a specially fabricated view cell. The video camera connects to the top of the microscope, and sends its signal to a small (14″ diagonal) black and white monitor. Originally, it was intended that photomicrographs would be taken directly from the microscope for image analysis; however, the opaque quality of the microbubble foam and the mechanics of mounting a camera did not allow sufficient light to pass for these direct photographs. Instead, pictures were taken by photographing the monitor directly. Photomicrographs suitable for image analysis were produced using the 10x setting of the microscope and placing the camera in front of the monitor such that the screen filled the entire viewing field of the camera. The monitor was marked with a calibration scale one centimeter long which was equivalent to 32 μ. Using the automatic shutter speed setting of the Minolta camera and setting the aperture to f/5.6, good black and white pictures can be made using Kodak Panatomic-X 32 film.

Image analysis is really a computer analysis of a photograph based on grey levels, levels that the human eye and mind can disregard when attempting to identify a shape. However, while the human eye see bubbles in a photograph, the computer sees patches of grey which may not even

be spherical. In order to solve this problem, the background needs to be a uniform level of grey, while the outline of the bubbles needs to be a different uniform level of grey (black). This effect could not be achieved, therefore, analysis was done semi-automatically, that is, the computer enhanced an image, and an operator used a computer "mouse" to mark the diameter of each bubble. From this point, the computer provided the statistical information on the bubble size distribution; namely, average size, standard deviation, maximum and minimum diameters, and the number of bubbles in the sample. The image analysis work on this project was done using a Kontron image analyzer. A picture of the image analyzer can be found in Figure 1. The department of Mining and Minerals engineering provided use of the image analyzer at a rate of $36/hr. Image analysis work using the same "diameter marking" procedure performed by Keyser [30] included a calibration of the technique. Using Latex spheres of a given diameter, the image analyzed diameters were determined. The results appear in Appendix C.

As a final note, in characterizing microbubble foams, it is important that a representative sample be taken. Therefore, for each test run, three 250 mL samples were collected, and three photomicrographs were taken.

3.3 Equipment and Procedure

3.3.1 Microscope Viewing Cell

In order to be able to detect the shape, size, and size distribution of microbubbles, a means of microscopically viewing the bubbles immediately after they are produced is required. A specially designed view cell was fabricated that allows continuous samples of the microbubble foam to be viewed in such a manner. The view cell is made out of a small block of Lexan 1" high by 3" long by 1 1/2" wide (see Figure 2). The viewing chamber is a 1/2" diameter hole bored 7/16" into the

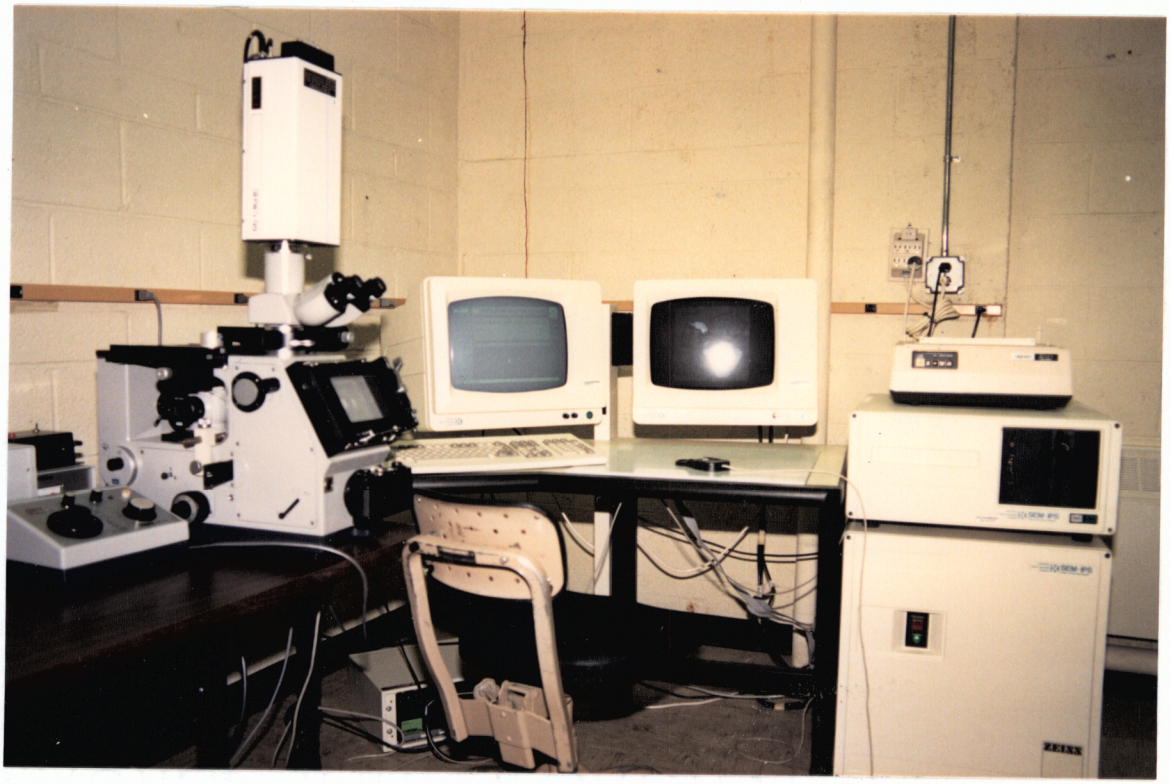

Figure 1. Picture of Kontron image analyzer.

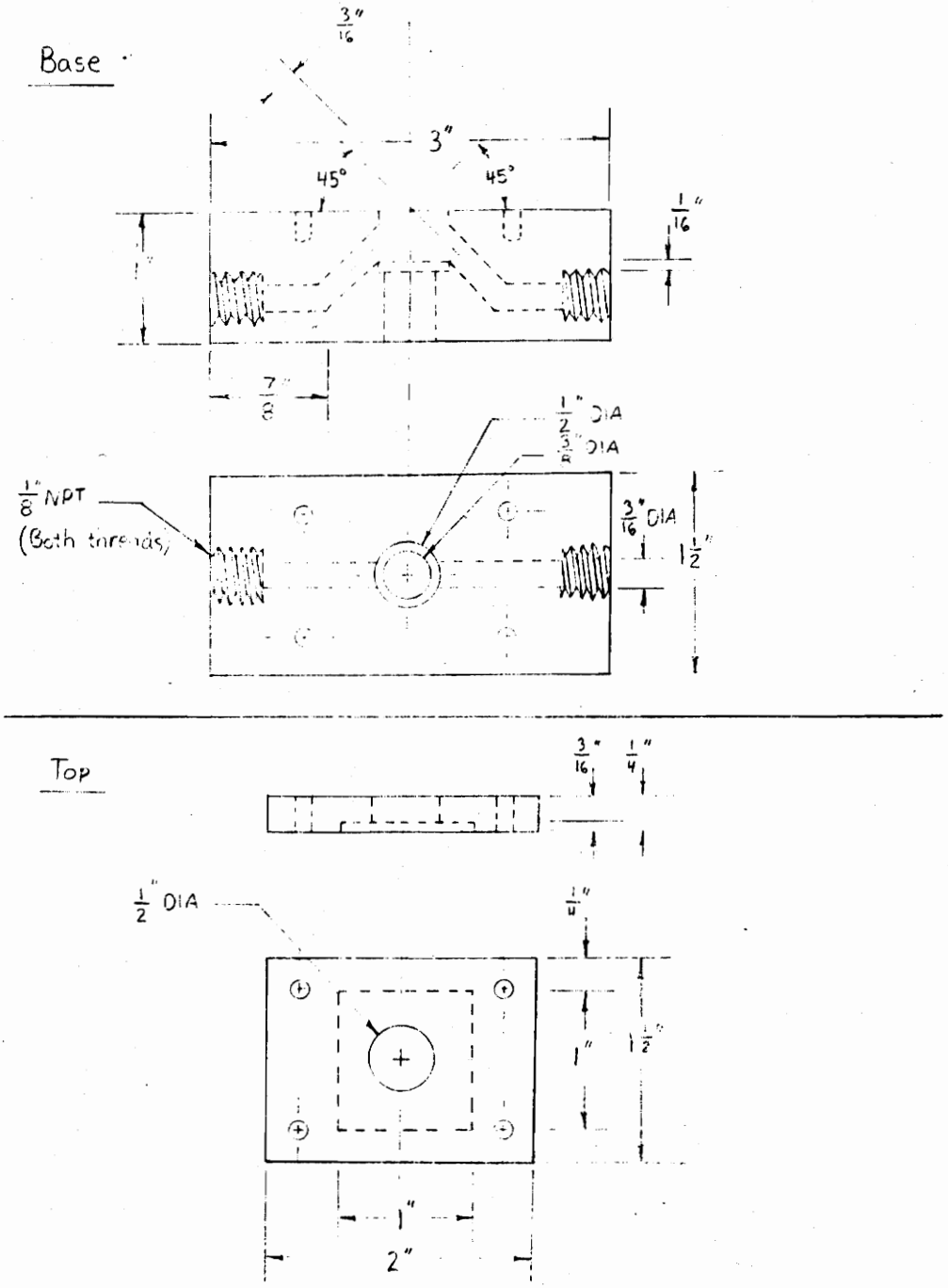

Figure 2. Schematic diagram of microscope viewing cell.

top of the block, which is in communication with a delivery line and a discharge line. Illumination of the chamber is provided through a smaller hole, 3/8″ diameter, bored through the bottom of the block to a height of 1/2″. The described arrangement thus leaves an inherent chamber bottom of 1/16″ thickness.

The delivery and discharge lines, 3/16″ in diameter, are horizontal from the side of the block to 7/8″ into the block, at which point each turns upward toward the viewing chamber at a 45 degree angle. The bend forces the passing fluid to strike the glass slide covering the viewing chamber, thus continually washing it in order to give a fresh sample. The ends of the cell are fitted with 1/4″ Swagelok male connects for quick universal interchangability. The top of the viewing chamber as mentioned is a glass microscope slide cut into a one inch square which rests in the recession of a 1/4″ thick Lexan top. This top, which has a 1/2″ hole in the center to allow for viewing, is bolted into place on the body. A gasket, made from such a material as Silicone Form-a-Gasket, rests between the top and the body. The size of the view cell has been designed to be compatible with a Nikon Optiphot biological microscope (see Figure 3).

3.3.2 Portable Microbubble Foam Generation Pilot Unit

In compliance with the goals, a testing apparatus and a packed bed generation device were designed and fabricated. The pilot unit was designed for a microbubble foam production rate of 40 L/min at 60% quality, a rate which represents ten times the capacity currently available using the spinning disk. The pilot unit was also designed with flexibility and ease of operation in mind, which corresponds to its portability. Being skid mounted, transportation of the device, via trailer, to a field test site is facilitated.

The pilot unit consist of 3/4″ CPVC (chlorinated polyvinyl chloride) piping, and 1 1/4″ galvanized steel piping, several gauges and flowmeters, a sampling line, a centrifugal pump used for feed, a positive displacement screw-type pump used for recycle, an air supply, and two large tanks (field testing will not require the tanks). A schematic diagram of the test loop is shown in Figure

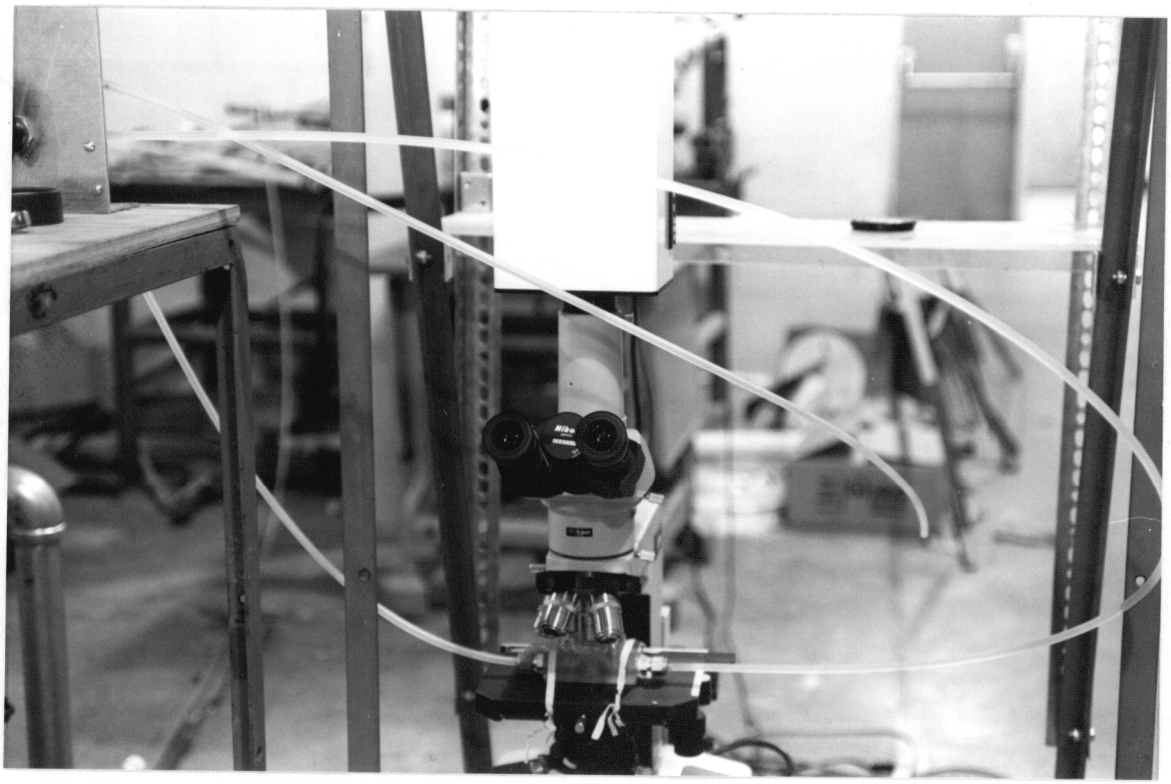

Figure 3. Picture of microscope set-up.

4, and a picture is shown in Figure 5. The sampling line incorporates a microscope and viewport as well as an exit valve leading to a graduated cylinder. Only the recycle line and the screw pump's bypass control line use galvanized pipe; the delivery and transfer lines of the network use CPVC pipe. The feed pump is a 3/4 HP centrifugal pump with all wetted parts made of brass or noryl plastic. The recycle pump is a 3 HP rotary screw pump using cast iron in all wetted parts. Air is delivered from an air cylinder at 60 psig. For field work, the option to use a portable air compressor exists. The surfactant solution feed uses the surfactant sodium dodecylbenzenesulfonate (NaDBS) at very low concentration levels.

Overall, the system is designed to handle foam flows up to 190 L/min and pressures up to 80 psig. The tank capacity, 380 Litres for feed and 1040 Litres for holding, allows for 24 minutes of continuous operation at 40 L/min of 60% quality microbubble foam. Naturally, however, lower and higher rates of flow and pressures are attainable, and owing to the CPVC piping, great flexibility exists in the system for modification.

3.3.3 Packed Bed

The packed bed microbubble foam generator is made of a 1/8″ walled 3″ outside diameter Lexan tube (see Figure 6). The length of available packing is 12″. The ends of the tube are capped by flanged Lexan plates, the top end having one plate, and the bottom end having two plates. The bottom plates make up a "premixing" chamber 1/4″ thick. The plate closest to the tube retains the packing support, while the plate away from the tube contains a 3/4″ diameter water entrance port and six air entrance ports surrounding the water port. The six ports have 1/4″ diameter Swagelok male connects allowing for air lines or caps, thus making many air-in configurations possible. Between these two plates is a rubber/cork gasket to ensure an air tight fit. The top plate has a 3/4″ diameter exit port. The plates nearest the tube each have a rubber O-ring between the plate and the tube end. Two support plates each with a pattern of 3/8″ diameter holes and completely covered by a 12-mesh plastic screen are used. One packing support will rest atop the actual packing,

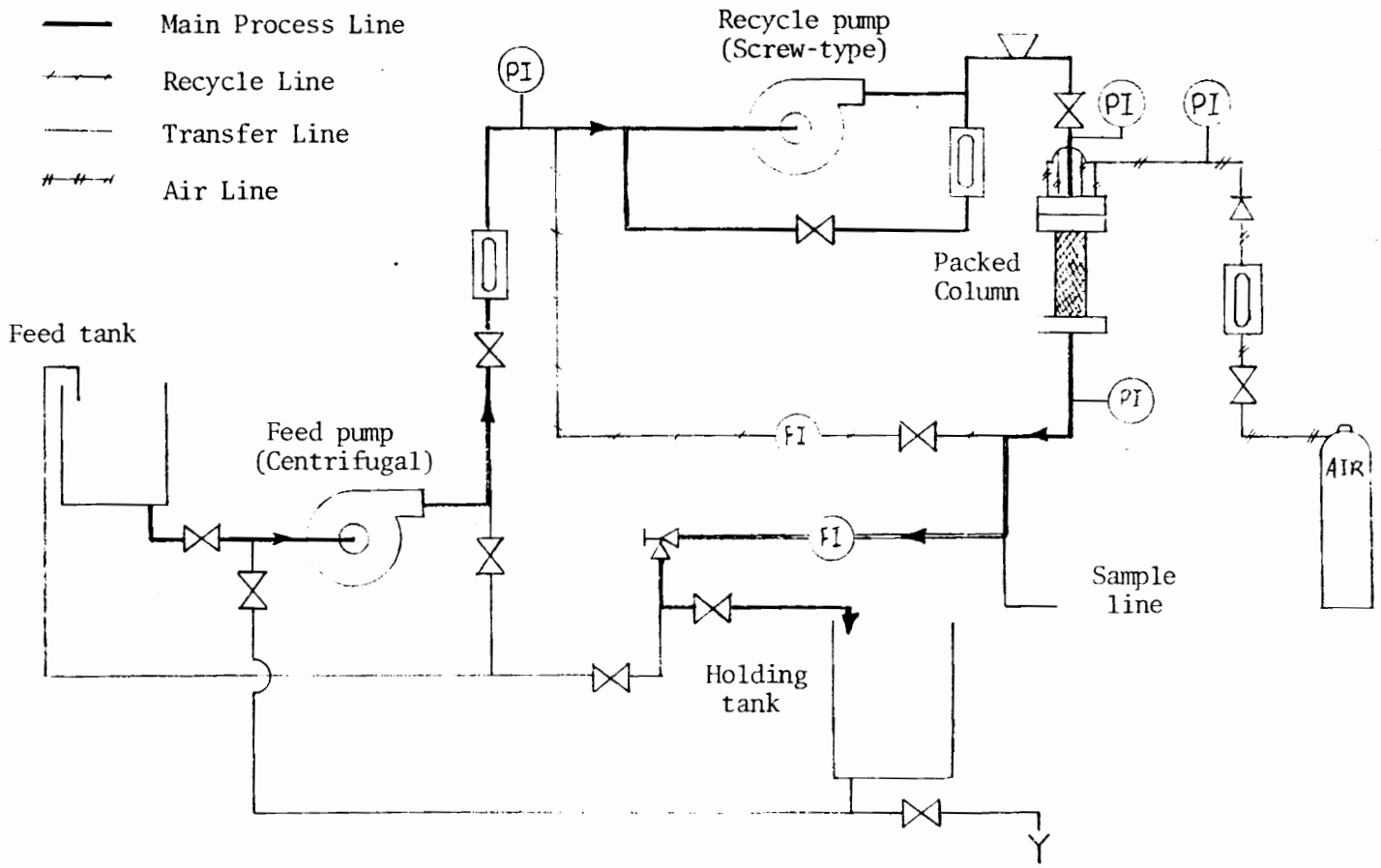

Figure 4. Schematic diagram of the portable microbubble foam generation pilot unit.

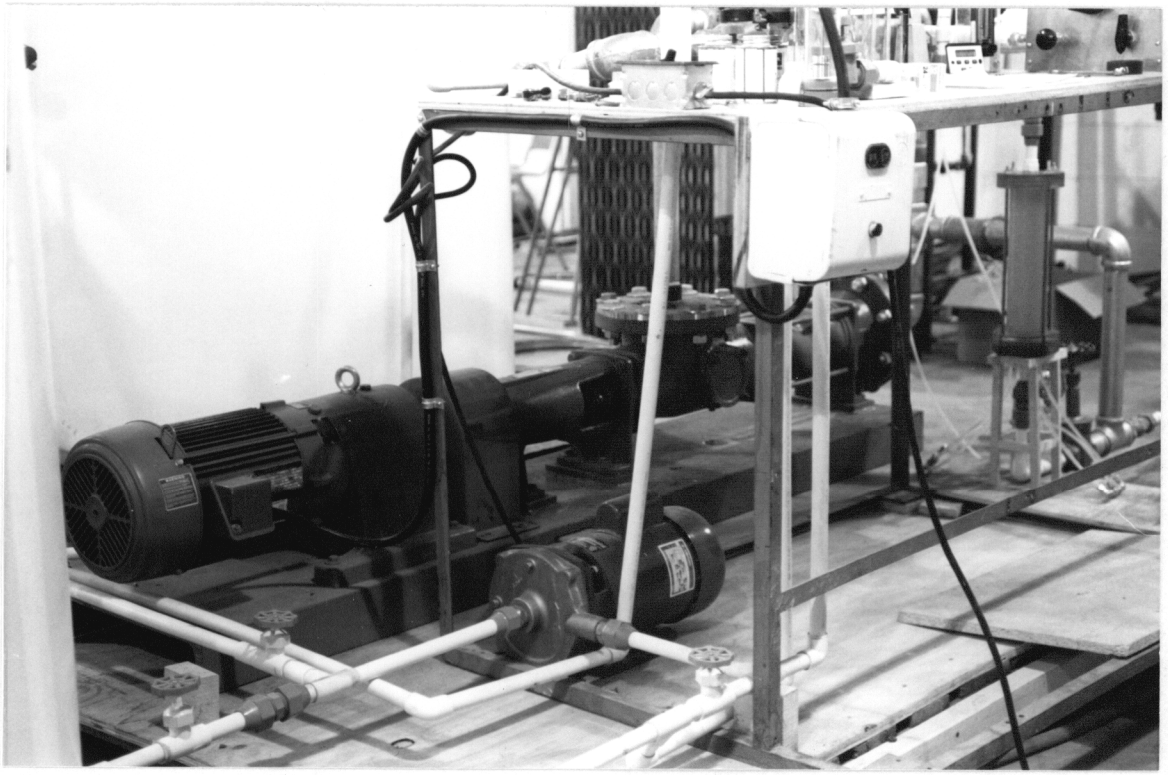

Figure 5. Picture of the portable microbubble foam generation pilot unit.

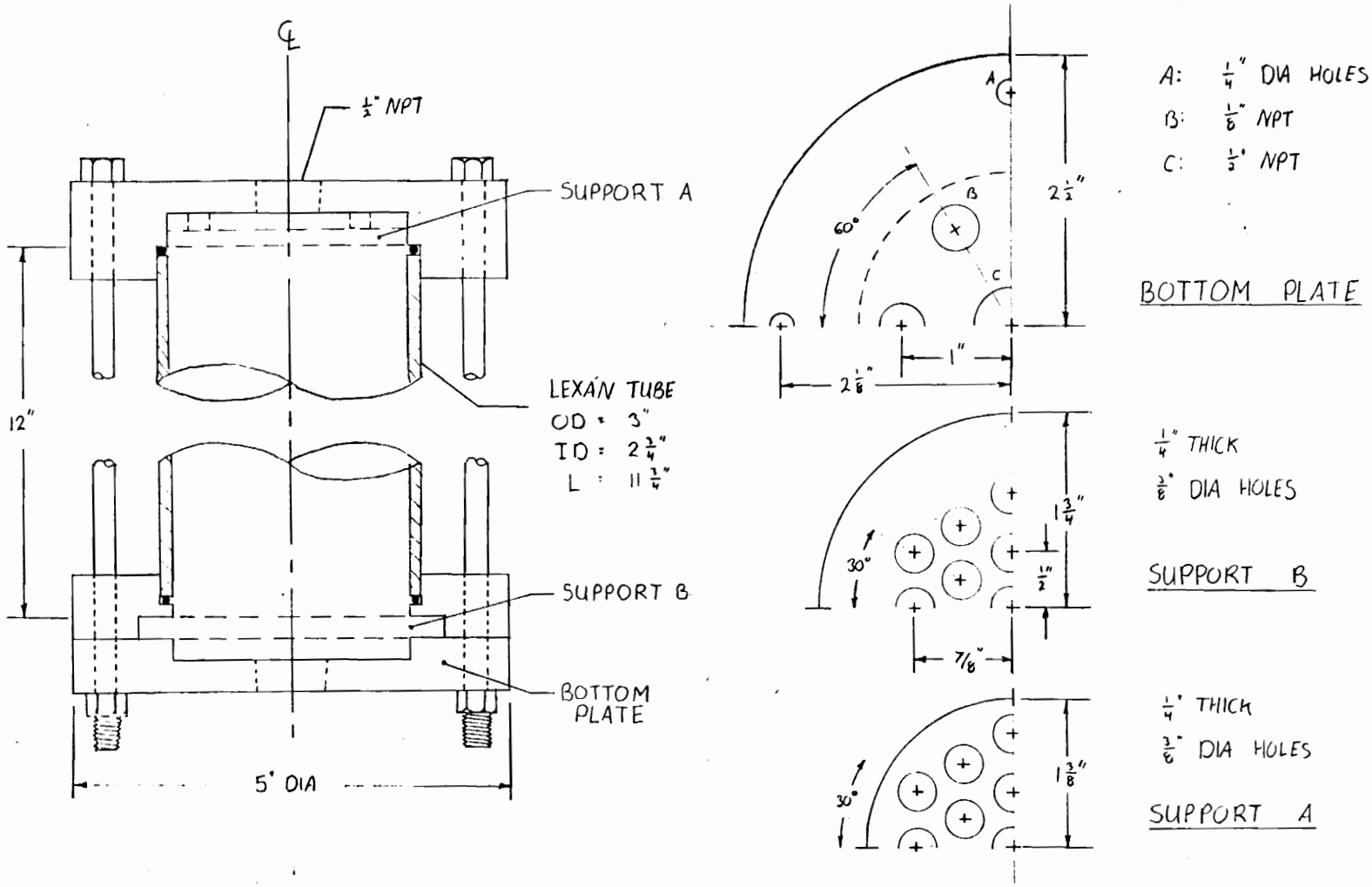

Figure 6. Schematic diagram of the packed column: (a) Packed bed. (b) Support plates.

effectively wedged against the top plate; the location of the other packing support has already been mentioned. The packing is technical grade glass spheres. For testing, four mean diameters are used. These diameters are 3.4 mm, 3.0 mm, 2.0 mm, and 1.5 mm. A picture of the packed bed is displayed in Figure 7.

3.3.4 Plan of Investigation

After the pilot unit and packed bed had been built, all calibrations completed, and preliminary trials finished, the actual testing program could begin. This program targeted studying the effects of surfactant concentration, packing size, Reynolds number, and recycle ratio on microbubble character and production. Soon after experimentation was begun, it was discovered that Reynolds number, as defined, was not indicative of the flow conditions required to produce microbubbles; however, for a fixed bead size, Reynolds number is directly proportional to solution feed flowrate (mass flowrate). For experimentation, solution feed flowrate was incorporated as a study variable. It was also soon discovered that the quality (percentage air) also greatly influenced the character of the microbubbles produced. The effects of quality on microbubble foam generation were consequently added to the investigation. Table 1 lists the values at which each variable is to be tested. An outlined detailed procedure of operation of the pilot equipment can be found in Appendix B.

3.3.5 Testing Procedure

To evaluate the effect of each of the selected variables, factorial testing was used. This method of testing involves changing one variable at a time, testing, then moving on to test a new variable, keeping the value of the just tested variable that gave the most favorable results. As an example, the first set of experiments varied the diameter of the particles in the packed bed while surfactant concentration, feed flowrate, quality, and recycle rate were set constant. At the end of this series

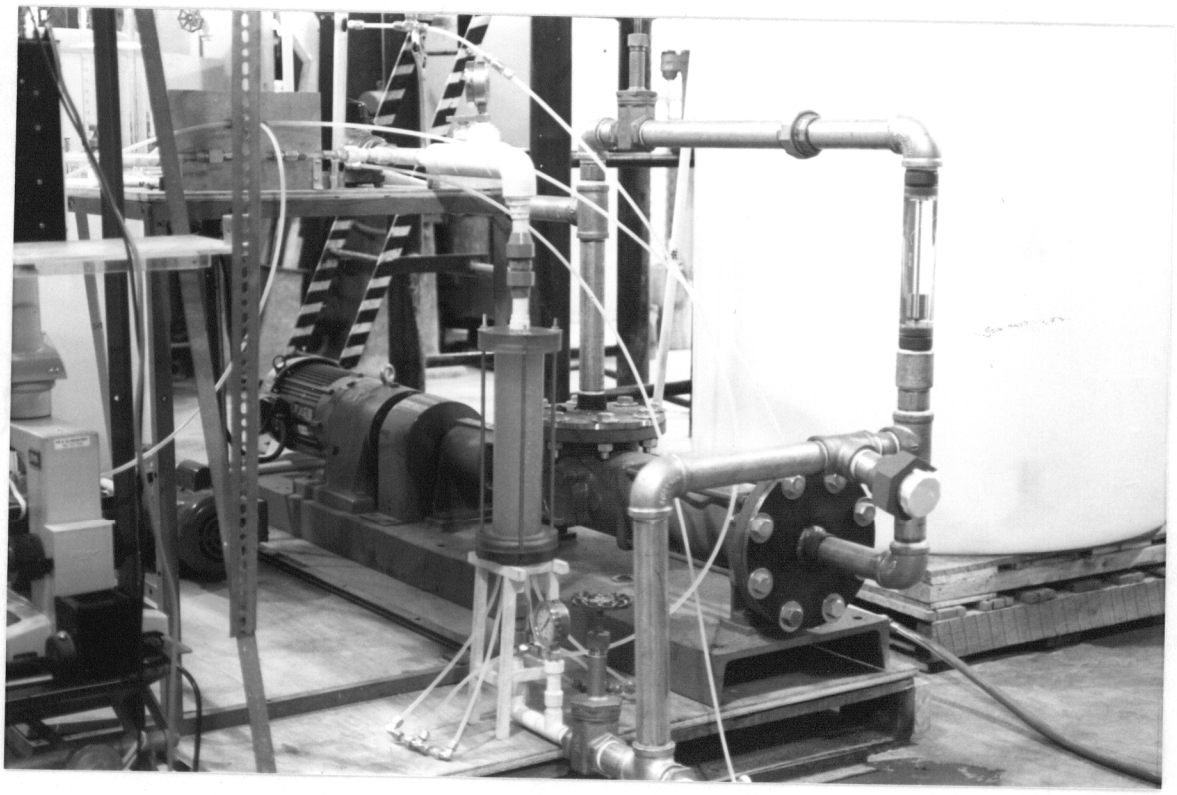

Figure 7. Picture of the packed column.

Table 1. Values to be tested.

Variable	Values
Packing diameter, Dp (mm)	3.4, 3.0, 2.0, 1.5
Quality,Q (%)	50, 60, 70
Feed flowrate, Fw (L/min)	12, 16, 20, 24
Reynolds Number, Nre	100, 150, 200, 250, 300, 350
Surfactant concentration (ppm)	50, 70, 100, 300, 500
Recycle ratio, RR	0.01, 0.1, 0.5, 1.0

of tests, runs with the 1.5 mm diameter packing gave the most promising results; thus, when testing the effect of concentration on microbubble production, particle size was kept constant at 1.5 mm. There were two exceptions to this procedure: one, when recycle was engaged, 3.0 mm diameter packing was used (allowed higher throughputs); and, two, although recycle produced favorable results, when the recycle rate was called to be constant, the rate was set at zero, i.e. no recycle. When recycle is operated, the system is not pure, that is, the packed bed no longer becomes the sole source of bubble generation.

Before testing could proceed, several minor obstacles required clearing. First, both the feed water rotometer and the air rotometer required calibration. The water rotometer's calibration revealed that the markings on the rotometer were accurate within the desired limits. The air rotometer calibration is included in Appendix C. The turbine meters in the discharge and recycle lines were used to measure the recycle rate of particular tests. By marking a beginning reading of each meter and a final reading after two minutes, the flowrate through each can be calculated. The ratio of these two flowrates, recycle line over process line, is the recycle ratio. This relative measuring technique was chosen since it required no calibration. A method of calibrating absolute microbubble flowrates could be used but would yield only fair results due to the changing pressures in the system, and the fact that foams are compressible fluids. Another area of special interest regards loading the packed bed. Each time a new bead size is required, the bed must be filled with packing. The pellets are weighed and dumped, via a funnel, into the empty chamber. Knowing both the density of the pellets and the volume of the bed, the void fraction can be calculated. After filling, the end plates are secured and the column is shaken to insure that the packing is tight. The density of the beads was found by measuring the amount of water that a particular mass of beads displaced. This value is 2.46 g/cm^3. The last special area involves feed solution preparation. When the surfactant was dissolved in tap water, the water assumed a cloudy appearance. Investigation revealed that the surfactant, Sodium Dodecylbenzensulfonate (NaDBS) provided by Pfaltz and Bauer, was only 90% pure. The impurities of the surfactant were reacting with the calcium ions in the hard tap water. To remedy the situation, a chelating agent was added to the water. Ethylenedinitrilo tetraacetic acid disodium salt (EDTA) at 90 ppm was used to effectively remove

the calcium from solution. This action was necessary to preserve the integrity of the experimentation.

4.0 Results and Discussion

4.1 Presentation of Results

The experimental results are divided into six sections, each addressing the effect of a different variable. Two new variables quality and feed flowrate, were added to the testing roster when, during the course of experimentation, it was discovered that each affected the character of the bubbles produced. Although microbubble foams are characterized by quality, stability, and size information, the quality of the bubbles, as mentioned was included as a variable, thereby leaving differences in the bubbles to be judged by stability and size information.

Tables 2 through 9 present the results of the investigation of the effect of different variables on microbubble foam generation. A brief description of how the data in the tables is interpreted is given, followed by short remarks addressing the content of each table. Each table gives pertinent stability and bubble size data for the tests that were used to determine the effect of a given variable. The important data from all test runs showing this information as well as bubble size histograms can be found in Appendix D. The stability portion of each table is divided into three parts, quality, normalized height at a given time and pseudo slope. Although the quality is a study variable, difficulty was encountered keeping it constant during different tests. Since the quality was found to

Table 2. Effect of quality (A)

Stability (500 mL cylinders)

Run	Quality(%)	Interface height at: 1 min	2 min	Slope
9	52.0	..... No stability		
5	65.6	80	88	8
10	70.7	64	80	16

Size and Distribution

Run	Peaks (μ)	Bubbles < 30μ	Bubbles > 210μ	Fraction < 90μ (%)	Number of Bubbles
9	75	0	11	34.5	29
5	105, 45	0	8	31.8	44
10	45, 135	2	3	54.2	72

Concentration = 500 ppm of NaDBS
Feed Flowrate = 12 L/min
Recycle Rate = 0
Packing Diam. = 1.5 mm

Peaks : Midrange value of size range, e.g. 45μ = 31-60μ. Listed from largest to smallest.

Fraction < 90 : (Σ bubbles < 90) / all bubbles

Table 3. Effect of quality (B)

Stability (500 mL cylinders)

Run	Quality(%)	Interface height at: 1 min	2 min	Slope
11	53.6	83	92	9
7	61.7	70	82	12
12	72.3	46	67	21

Size and Distribution

Run	Peaks (μ)	Bubbles < 30μ	Bubbles > 210μ	Fraction < 90μ (%)	Number of Bubbles
11	45, 105	4	7	40.3	62
7	45, 165	6	6	50.9	53
12	15, 135, 205	38	0	68.9	122

Concentration = 500 ppm of NaDBS
Feed Flowrate = 20 L/min
Recycle Rate = 0
Packing Diam. = 1.5 mm

Peaks : Midrange value of size range, e.g. 45μ = 31-60μ. Listed from largest to smallest.

Fraction < 90 : (Σ bubbles < 90) / all bubbles

Table 4. Effect of water flowrate

Stability (500 mL cylinders)

Run	Water Flowrate (L/min)	Quality	Interface height at: 1 min	2 min	Slope
5	12	65.6	80	88	8
6	16	62.8	77	87	10
7	20	61.7	70	82	12
8	24	62.2	63	78	15

Size and Distribution

Run	Peaks (μ)	Bubbles < 30μ	Bubbles > 210μ	Fraction < 90μ (%)	Number of Bubbles
5	45, 105	0	8	31.8	44
6	105, 195, 45	0	6	26.2	42
7	45, 165	6	6	50.9	53
8	45, 105, 195	3	3	46.2	52

Concentration = 500 ppm of NaDBS
Packing Diam. = 1.5 mm
Recycle Rate = 0

Peaks : Midrange value of size range, e.g. 45μ = 31-60μ. Listed from largest to smallest.

Fraction < 90 : (Σ bubbles < 90) / all bubbles

Table 5. Effect of packing diameter (A)

Stability (500 mL cylinders)

Run	Glass Packing Diam. (mm)	Quality	Interface height at: 1 min	2 min	Slope
1	3.4	59.0	..... No stability		
2	3.0	59.7	..... No stability		
22	2.0	64.1	76	88	12
6	1.5	62.8	77	87	10

Size and Distribution

Run	Peaks (μ)	Bubbles < 30μ	Bubbles > 210μ	Fraction < 90μ (%)	Number of Bubbles
1	75	2	7	52.4	42
2	45, 135	0	9	58.3	48
22	45, 105, 165	7	5	53.2	47
6	105, 195, 45	0	6	26.2	44

Concentration = 500 ppm of NaDBS
Feed Flowrate = 16 L/min
Recycle Rate = 0

Peaks : Midrange value of size range, e.g. 45μ = 31-60μ. Listed from largest to smallest.

Fraction < 90 : (Σ bubbles < 90) / all bubbles

Table 6. Effect of packing diameter (B)

Stability (250 mL cylinders)

Run	Glass Packing Diam. (mm)	Quality	Interface height at: 1 min	2 min	Slope
3	3.0	60.9	..... No stability		
25	2.0	67.7	62	76	14
7	1.5	61.7	52	70	18

Size and Distribution

Run	Peaks (μ)	Bubbles < 30μ	Bubbles > 210μ	Fraction < 90μ (%)	Number of Bubbles
3	135	0	7	21.1	19
25	45, 195	13	7	60.3	63
7	45, 165	6	6	50.9	53

Concentration = 500 ppm of NaDBS
Feed Flowrate = 20 L/min
Recycle Rate = 0

Peaks : Midrange value of size range, e.g. 45μ = 31-60μ. Listed from largest to smallest.

Fraction < 90 : (Σ bubbles < 90) / all bubbles

Table 7. Effect of surfactant concentration

Stability (500 mL cylinders)

Run	Conc. (ppm)	Quality	Interface height at: 1 min	2 min	Slope
17	50	66.5	..... No stability		
16	70	65.8	82	92	10
14	100	67.2	70	83	13
15	300	68.9	67	81	14
13	500	67.9	66	81	15

Size and Distribution

Run	Peaks (μ)	Bubbles < 30μ	Bubbles > 210μ	Fraction < 90μ (%)	Number of Bubbles
17	45, 135	20	4	73.5	98
16	45	21	3	76.4	123
14	45	31	2	77.5	129
15	45, 195	6	4	61.4	70
13	45, 195	5	1	46.3	82

Packing Diam. = 1.5 mm
Feed Flowrate = 16 L/min
Recycle Rate = 0

Peaks : Midrange value of size range, e.g. 45μ = 31-60μ. Listed from largest to smallest.

Fraction < 90 : (Σ bubbles < 90) / all bubbles

Table 8. Effect of recycle ratio

Stability (250 mL cylinders)

Run	Recycle Ratio	Quality	Interface height at: 1 min	2 min	Slope
3	0.00	60.9	..... No stability		
18	0.08	71.3	53	72	19
19	0.17	68.4	(37)	68	31
21	0.90	61.1	25	43	18

Height at one minute on run 19 is an estimate.

Size and Distribution

Run	Peaks (μ)	Bubbles < 30μ	Bubbles > 210μ	Fraction < 90μ (%)	Number of Bubbles
3	135	0	7	21.1	19
18	45	16	5	83.9	118
19	45	31	5	81.9	138
21	45	56	0	96.4	137*

Data for run 21 comes from one picture.

Concentration = 500 ppm of NaDBS
Feed Flowrate = 20 L/min
Packing Diam. = 3.0 mm

Peaks : Midrange value of size range, e.g. 45μ = 31-60μ. Listed from largest to smallest.

Fraction < 90 : (Σ bubbles < 90) / all bubbles

Table 9. Effect of Reynolds number

Stability (500 mL cylinders)

Run	Reynolds Number	Quality	Interface height at: 1 min	2 min	Slope
5	107	65.6	80	88	8
6	143	62.8	77	87	10
7	179	61.7	70	82	12
22	199	64.1	76	88	12
8	215	62.2	63	78	15
2	285	59.7	..... No stability		
1	319	59.0	..... No stability		
3	357	60.9	..... No stability		

Size and Distribution

Run	Peaks (μ)	Bubbles < 30μ	Bubbles > 210μ	Fraction < 90μ (%)	Number of Bubbles
5	45, 105	0	8	31.8	44
6	105, 195, 45	0	6	26.2	42
7	45, 165	6	6	50.9	53
22	45, 105, 165	7	5	53.2	47
8	45, 105, 195	3	3	46.2	52
2	45, 135	0	9	58.3	48
1	75	2	7	52.4	42
3	135	0	7	21.1	19

Concentration = 500 ppm of NaDBS
Recycle Rate = 0

Peaks : Midrange value of size range, e.g. 45μ = 31-60μ. Listed from largest to smallest.

Fraction < 90 : (Σ bubbles < 90) / all bubbles

have a pronounced effect on microbubble generation, it is included in the table. The values listed for each run in the first part represent the normalized height of the interface between liquid and microbubbles (see Section 3.2 Characterization) at one minute and two minutes after the sampling graduated cylinder was filled to the 250 mL mark. The size of the cylinder is also listed. Many of the values represent an average of three samples; however, some values come from only one sample because different sizes of graduated cylinders were errantly used for sampling. The pseudo slope represents the difference in normalized interface height at one and two minutes. The last column gives the average quality for that run. This value was included when it was discovered that the quality has a marked effect on microbubble production.

The bubble size and distribution portion of the tables derives its information from the collective histograms of each pertinent test run. For each test, three photomicrographs were taken and image analysis produced three histograms. Each histogram divides the bubbles in to size groups of 30 μ range beginning at zero. Thus, the ranges are 0 - 30 μ, 30 - 60 μ, 60 - 90 μ, and so on up to the last group, 240+ μ. Each of these individual plots was, in turn, combined to make a cumulative histogram for each test. Five columns of values are listed in the bubble size and distribution portion of the results tables. The first column gives the average size of the high concentrations of bubbles in the sample. These values are the size groups where peaks are found on the histogram (thus the heading "peaks"). The peaks are listed in decreasing size, e.g., the first peak listed is larger than the next. The second column provides an indication of the number of very small bubbles in the sample. This value is the absolute number of bubbles less than 30 μ found in the sample. The third column supplies information on very large bubbles. This column lists the number of bubbles over 210 μ that appear in the histograms. The fraction of bubbles less than 90 μ is given in column four, while the total number of bubbles found in the sample, N, is given in the last column. The number of bubbles in a sample provides input on data reliability. For low values of N, less than 30, either poor pictures were taken making analysis difficult, or there were extremely large, 500+ μ, bubbles in the sample excluding many small ones. In either case, a low value of N equates with low reliability of the sample representing the bulk.

In each study of the effect of the variables, when one variable is being changed, the others are held constant. The values at which the non-study variable were held also appears in the table. Finally, both the packing diameter variable and the quality variable have two tables. This situation comes about as the result of the various factorial testing that occurred and is helpful in that the variable in question can have its effects checked twice.

4.1.1 Effect of the Variables

It is overwhelmingly clear from the quality data shown in Tables 2 and 3 that bubble size decreases with increasing quality. At both the low flowrate and the high flowrate tested, this statement is true. Especially noticeable is the lack of small bubbles and the presence of big bubbles at the low flowrate, intimating that higher rates of flow produce smaller bubbles.

The trend that showed itself in the quality data, bubble size decreasing with increasing flowrate of feed solution, is confirmed by the tests which varied flowrate (Table 4). Higher flowrates create more shearing action, thus the bubbles will tend to break into smaller bubbles.

A trend is apparent that shows that as packing diameter decreases, bubble size decreases (Table 5 and 6). An anomaly in the trend occurs at the 2.0 mm sized beads. At first appearance, this bead size seems to produce smaller and more uniform bubbles than the 1.5 mm beads; however, a closer look must be taken. First, in both runs 22 and 25, higher qualities were used, 64.1% verses 67.8% for group "A", Table 5, and 61.7% verses 67.7% for group "B", Table 6. As discussed previously, higher quality produces smaller bubbles. Fortunately, an opportunity exists to compare another 1.5 mm bead test at a higher quality. Comparing run 13, at 67% quality, to run 22, we see that fewer large bubbles were formed in run 13, as well as a lower interface height at one minute. On the other hand, the proportion of very small bubbles is still greater for run 22. Nonetheless, there is no theoretical indication that an optimum particle size should appear. In light of the small diameter difference between the two bead sizes, and the stability data indicating greater stability for the 1.5 mm bead runs, the anomaly may be attributed to experimental deviation.

Table 7 indicates that surfactant concentration has a curious effect on microbubble production. Clearly, stability, as interpreted by interface height at one minute, increases with increasing concentration; however, a change in bubble distribution also occurs with increasing concentration. At 100 ppm and below, only one grouping of bubbles exists (the second peak of run 17 appears to be a result of statistical variation). As the concentration increase above 100 ppm, a second peak appears at 195 μ which increases in size as the concentration increases from 300 ppm to 500 ppm. Throughout the other tests, this double peak phenomenon also is evident. Regarding very small bubbles, lower concentrations appear to produce proportionately more smaller bubbles. The discrepancy in run 16 is most likely due to statistical error.

The parameter that introduced the greatest visual effect on microbubble production is the recycle. Table 8 shows that even at recycle ratios of 17%, very small stable bubbles are produced. The trend with recycle is that as the recycle ratio increases, the bubble size decreases, and, regardless of concentration, a high degree of uniformity exists.

Finally, the data in Table 9 show that, as anticipated, there is no trend to be found in the tests which vary the Reynolds number. First, from the equation for Reynolds number, it can be seen that the value increases as flowrate increases and decreases as bead size decreases. Thus, if an increase in Reynolds number were to be indicative of the production of smaller bubbles, then as the bead size increases, all other variables held constant, then more very small bubbles should form. The observed effect, however, is the opposite, small microbubbles form at smaller bead sizes, not larger ones.

4.2 Discussion

4.2.1 Characterization

Since the performance of any particular variable upon the character of the microbubbles produced hinges on the stability and size distribution of the bubbles, these properties and the meaning of the recorded data should be scrutinized. First, stability. Stability really means two things, the ability of the bubbles to resist coalescence, and, the bubble settling time, that is, the time it takes for the bubbles to rise to the top of their containing vessel and transform into polyedershaum. As mentioned in the background, kugelshaums naturally resist coalescence, so in order to distinguish between two kugelshaums, the latter definition of stability must be used. Examination of the forces at play reveals that this rise time is a function of the bubble size and size distribution, and can be analyzed by Stokes law. Examples from the testing do not all adhere to this claim, suggesting that some coalescence is occurring (See Figure 8). The Figure illustrates that three different relationships between stability and bubble size exist. The main relationship is the expected one, bubble size decreasing with increasing stability. This is displayed by the tests which only varied Q′ and Fw. The relationship when recycle is employed is reflective of the fact that the number of large bubbles is decreasing, thereby lending increased stability without changing the fraction of small bubbles. The last relationship involves the concentration of surfactant. As the concentration goes down, small bubbles of a much lower stability are formed. Here, the small bubbles that are formed are not resisting coalescence.

Interpretation of the stability data thus falls along the following lines. When the interface height at a given time is low, then there are many small bubbles resisting coalescence in the sample, and thus the sample may be called stable. This ideas holds best for the height at one minute. The slope is inversely proportional to the interface height. For example, in Table 4 from runs 5 through 8, the slope increases from 8 to 15 while the interface height at one minute is decreasing from 80

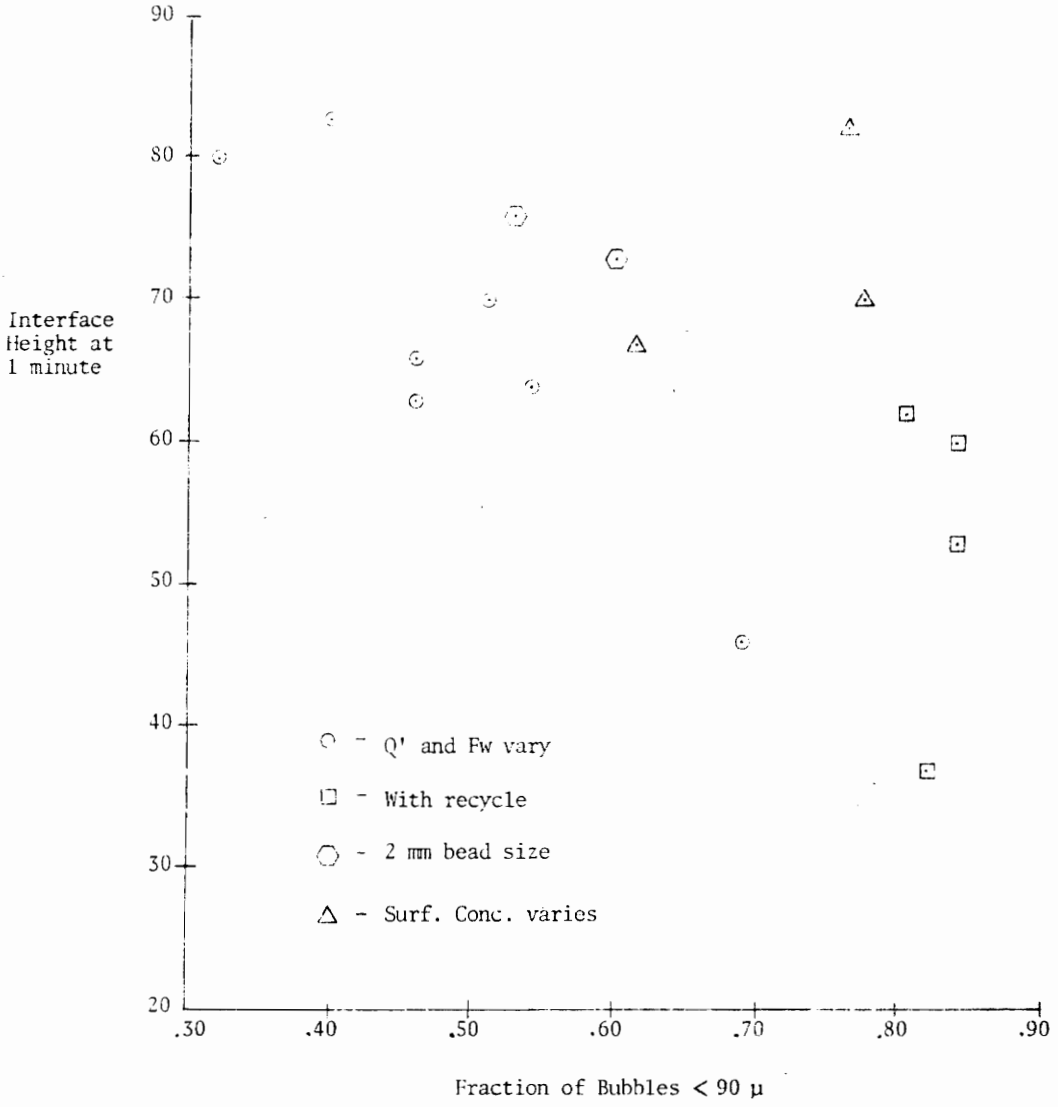

Figure 8. Bubble stability as a function of microbubbles less than 90 μ

to 63. At low interface heights, the slope is high--the bubbles are in the process of breaking down, yet remain dispersed and stable. When the slope is low, the bubbles have broken down early as represented by a high interface.

Size distribution data serves as a necessary supplement to the stability information. In order to fully appreciate the second group of data, consideration of the sampling technique and the analytical technique must be taken into account. Two problems are encountered in the technique used to sample bubble size: representativeness of the samples and stratification. As only three pictures of the microbubbles were taken in each test it is not guaranteed that each picture, or a sum of the three, gives the proper image of the microbubbles generated in that particular test. In one test six pictures were made. Visually, the collection of six all appear to be from the same test. It is not until four of the six are taken away that doubt enters the viewers mind that the remaining two are of the same test. The case of having one picture has a trivial interpretation. Thus, based on this one example, three pictures seems sufficient. The second problem in sampling involves stratification. Even as the microbubble foam is flowing through the sampling line, larger bubbles, because of their size and greater buoyance force, work their way to the top of the tube or viewing chamber. The design of the microscope view cell minimizes this effect by providing a means of washing the microscope slide; nonetheless, when the flow stops the driving force that brings the larger bubbles to the top is still in effect. The experimenter notes that when the flow was stopped, large bubbles could be seen rising in the viewing chamber. This problem has been addressed by Cheng and Lemlich [31].

Regarding analysis, problems also exist. First, size sensitivity is lost by grouping the bubbles into 30 micron size ranges. This loss of sensitivity is, however, not entirely damaging. Indeed, much random "noise" can be filtered out with this procedure. The second problem involves combining the three pictures' histograms into one. Combination certainly increased the sample base (number of bubbles), but the question remains as to whether this action is justified. Finally, image analysis provided mean diameters and standard deviations, but with multiple peaks (high frequency of one size range) and the inclusion of bubbles with diameters two orders of magnitude greater than others, these statistics become meaningless.

Size distribution data essentially answers three questions: are small bubbles made, are big bubbles made, and are the bubbles uniform in size. The desired microbubble foam product will have large numbers of small, less than 60 μ, bubbles, and uniformity about this small diameter range. The peak information gives a good idea of where large numbers of bubbles are, while the fraction of bubbles less than 90 μ provides an indication of whether small bubbles were made. Both the number of large and small bubbles in the sample relate to the quality of production. Before the data con be correctly interpreted, adjustment for quality and sample size must be incorporated. As Tables 2 and 3 show, the number of small stable bubbles produced increases as the quality increases, thus runs with higher than average qualities will tend to produce smaller bubbles. In reference to sample size, as previously mentioned, when N is less than 30, that run may be suspect.

4.2.2 Explanations

Generation of microbubble foam in a packed column can be attributed to shearing forces and surface chemistry phenomena. When the surface tension of the liquid medium is reduced, less energy is required to form bubbles. As the shearing force that forms the bubbles increases, the bubble size will tend to decrease. Therefore, one can expect to find that smaller bubbles are formed at higher flowrate through the column due to the increase in the shearing force. On the other hand, the role of the surfactant, beyond that of reducing surface energy, is not entirely understood.

In determining flowrate through the column, the question arises as to which flowrate to consider: mass flowrate or volumetric flowrate. In the experimentation mass flowrate, i.e. feed solution flowrate, was the considered variable that was either held constant when testing other variables, or varied when it was being studied. Using mass flowrate in this manner was preferred since microbubble foam is a compressible fluid. However, in order to have a firm understanding of how the packed column is affecting microbubble foam generation, the volumetric flowrate must be used. In terms of the bubbles produced, the volumetric flowrate will follow the same trend as mass flowrate.

Tied in with the volumetric flowrate is the quality. As the quality increases, the flowrate increases. Because of this connection, and the fact that during experimentation the quality could not be finely controlled, it will be prudent to examine the effects of quality and flowrate together. Table 10 presents the volumetric flowrate, V, and the quality of the microbubble foam under pressure, Q′, for all the tests which held bead size and surfactant concentration constant (1.5mm and 500 ppm respectively). An in-column volume of air was calculated based on an average of the inlet and outlet pressures of the bed. From this volume of air, V and Q′ were calculated.

The results indicate that as the quality increases, smaller, more stable bubbles are generated, and that an increase in mass flowrate also produces more smaller bubbles. At this point, a model can be introduced that depicts stability (interface height at one minute) as a function of volumetric flowrate and quality:

$$H = a\,V + b\,Q' + c$$

Multiple linear regression permits determination of the coefficients and the suitability of the model (See Table 11). A high correlation coefficient, 0.9672, is found indicating that the model predicts well. Examination of the sequential sum of squares (type II SS) for both the flow and quality variable in an F-test indicate that each variable is necessary for accurate prediction. Table 12 shows each run with pertinent stability and size distribution data ranked according to its predicted interface height value. Undoubtedly, volumetric flowrate and quality enhance microbubble foam generation, yet a trade-off exists. As flowrate increases, the pressure drop across the column increases, compressing the entrained air and thus lowering the quality in the bed. Eventually a point will be reached where the effect of decreasing quality counters the advantage of increasing flowrate.

Table 10. Volumetric flowrate and adjusted quality for runs with Dp = 1.5mm and concentration = 500 ppm

Run	Water Flowrate (L/min)	Quality Q (%)	Average Column Pressure (psia)	Volumetric Flowrate (L/min)	Quality in Column Q′ (%)	Interface Height at One minute
5	12	65.6	16.5	22.4	46.4	80
6	16	62.8	18.0	27.7	42.2	77
7	20	61.7	20.5	32.9	39.2	70
8	24	62.2	24.5	38.2	37.2	63
9	12	52.0	15.0	18.2	34.1	--
10	12	70.7	18.0	24.5	51.0	64
11	20	53.6	18.5	29.8	32.9	83
12	20	72.3	25.0	38.5	48.1	46
13	16	67.9	19.0	30.2	47.0	66

Table 11. Multiple linear regression analysis of stability prediction model.

DEP VARIABLE: HEIGHT

ANALYSIS OF VARIANCE

SOURCE	DF	SUM OF SQUARES	MEAN SQUARE	F VALUE	PROB>F
MODEL	2	947.74006	473.87003	73.731	0.0002
ERROR	5	32.13494356	6.42698871		
C TOTAL	7	979.87500			

ROOT MSE	2.535151	R-SQUARE	0.9672
DEP MEAN	68.625	ADJ R-SQ	0.9541
C.V.	3.694209		

PARAMETER ESTIMATES

VARIABLE	DF	PARAMETER ESTIMATE	STANDARD ERROR	T FOR H0: PARAMETER=0	PROB > |T|
INTERCEP	1	187.77754	10.07165939	18.644	0.0001
FLOW	1	-1.82653360	0.17290550	-10.564	0.0001
QUAL	1	-1.47436290	0.16321706	-9.033	0.0003

VARIABLE	DF	TYPE I SS	TYPE II SS
INTERCEP	1	37675.12500	2234.04945
FLOW	1	423.31283	717.20823
QUAL	1	524.42722	524.42722

OBS	ACTUAL	PREDICT VALUE	RESIDUAL
1	46.0000	46.5391	-0.5391
2	63.0000	63.1577	-0.1577
3	66.0000	63.3212	2.6788
4	64.0000	67.8350	-3.8350
5	70.0000	69.8896	0.1104
6	77.0000	74.9644	2.0356
7	80.0000	78.4528	1.5472
8	83.0000	84.8403	-1.8403

SUM OF RESIDUALS	7.81597E-14
SUM OF SQUARED RESIDUALS	32.13494

Table 12. Stability and size distribution data of runs ranked according to predicted interface height.

Predicted Height	Run	Interface Height	Bubbles < 30μ	Bubbles > 210μ	Fraction < 90μ	Largest Peak (μ)
46.5	12	46	38	0	68.9	15
63.2	8	63	3	3	46.2	45
63.3	13	66	5	1	46.3	45
67.8	10	64	2	3	54.2	45
69.9	7	70	6	6	50.9	45
75.0	6	77	0	6	26.2	105
78.5	5	80	0	8	31.8	45
84.8	11	83	4	7	40.3	45
----	9	--	0	11	34.5	75

$$H = 187.8 - 1.827\ V - 1.474\ Q'$$

4.2.3 Effect of Packing Diameter

The data in Tables 4 and 5 suggest that as packing diameter decreases, bubble size decreases. Although the mass flowrate was held constant for the tests listed in these tables, changing bead size causes pressure drop changes ultimately affecting the volumetric flowrate. An examination of the pressure drops for these runs reveals a dramatic change. In run 1, for instance, the pressure drop is eight psia compared to a 21 psia pressure drop for run 6. Since the bead size and pressure drop are linked, to which is attributed the increase in small bubble generation?

As mentioned before, bubble generation is derived from shearing forces, and a key indicator of shear is pressure drop. One is inclined to assume then, that the poor performance of the larger bead size is due to low shearing forces. From this assumption, it can be suggested that, even with larger packing, generation of microbubble foam is possible at rates of flow higher than those attempted in the tests. It is further suggested that at the higher flow condition, the effects of volumetric flowrate and bed quality will apply as described previously. Effectively bead size only affects microbubble foam generation in terms of the limits it places on flow through the bed. Just as a smaller diameter tube will increase the pressure drop, thus enhancing microbubble foam generation, so too will smaller packing have the same effect.

Another consideration is that as the beads become smaller, the interstitial pathways through the bed also become smaller. A restriction on the opening that a bubble must pass through limits the size that a passing bubble can be. For a perfect packing where each bead touches eight others (body centered cubic), analysis of the geometry involved shows that the largest sphere with radius R, that could pass through a bed packed with spheres of radius r, is given by:

$$R = 0.1516r$$

Confirmation of the above assertions was not possible with the pilot unit due to the small piping diameters used. It is recommended that corrections be made that allow testing at flowrates

sufficiently high to provide pressure drops with the large bead size equivalent to the pressure drops encountered with the 1.5 mm beads. This testing should provide insight to whether microbubble formation is shear controlling or bead size controlling.

4.2.4 Effect of Surfactant Concentration

Not enough is known about the microscopic details of how microbubbles are formed to fully explain the effects of surfactant concentration. It would seem that at higher concentrations the bubbles formed become tenacious and resist tearing apart (both large and small bubbles are found); however, it is the surfactant, by reducing the surface tension of the water, that allows the bubbles to tear and be readily formed in the first place. The results show that as surfactant concentration decreases, the bubbles formed become smaller but less stabilized. In terms of applications, above a critical stabilization point, surfactant concentration may be employed as a control on bubble size and distribution. Further work should be undertaken to determine how different shear rates and pressure drops, influence the bubble size and distributions found.

4.2.5 Effect of Recycle

The effect of the recycle was so drastic that a special test was run to see what effects the recycle pump alone had on microbubble foam generation (see Table 13). The test showed that the recycle pump indeed generated microbubble foam, yet the packed bed was necessary to produce the very small bubbles as well as the increased stability found in the recycle runs.

Recycle produces smaller bubbles because there is more opportunity to shear the bigger bubbles. With a single pass through the bed, big bubbles may escape, but if the big bubbles were made to return to the shearing of the packed bed, they would be subject to another attempt at break down. The extremely low recycle rates required to make an effect is more due to the configuration

Table 13. Effect of recycle pump alone

Stability (250 mL cylinders)

Run	Recycle Ratio	Quality	Interface height at: 1 min	2 min	Slope
23*	0.72	63.4	62	73	11
24*	0.85	64.4	60	74	14
21	0.90	61.1	25	43	18

* Run without packed bed.

Size and Distribution

Run	Peaks (μ)	Bubbles < 30μ	Bubbles > 210μ	Fraction < 90μ (%)	Number of Bubbles
23	45,75	18	3	80.6	98
24	45	36	3	84.2	164
21	45	56	0	96.4	137*

* Data for run 21 comes from one picture.

Concentration = 500 ppm of NaDBS
Feed Flowrate = 20 L/min
Packing Diam. = 3.0 mm

Peaks : Midrange value of size range, e.g. 45μ = 31-60μ. Listed from largest to smallest.

Fraction < 90 : (Σ bubbles < 90) / all bubbles

of the pilot unit. For research, an oversized positive displacement pump was used. As positive displacement pumps must have a place to send their discharge, a bypass loop was installed (standard practice for positive displacement pumps). At a steady state condition, there is a considerable percentage of air in the bypass line regardless of the quality selected for production. This air is continually sent through the screw pump which, as noted earlier, produces microbubble foam. At low recycle rates the bypass recycle rate is high, thus the pump and its bypass emulate a stirred tank where many smaller bubbles can be continually generated. It follows then that when a small amount of recycle is employed, the small bubbles from the bypass line will show up in a sample.

The ability of the screw pump alone to produce microbubble foams may lead to further developments in microbubble foam generation. These avenues should be pursued with examination of the effects of rotor RPM, amount of recycle, and air introduction location in mind. Care should be exercised when using the screw pump in a field application due to the low tolerances found within the pump--solid particulates should not be pumped. In terms of its use as a recycle pump in the pilot unit, testing was limited due to the pipe size of the system and poor controllability of recycle rates. Because of the drastic impact the recycle had on the microbubbles produced, more testing and testing at higher recycle rates should be explored.

4.2.6 Microbubble Foam Flow Characteristics

For this thesis, an investigation was carried out to determine if microbubble foam flow through a packed column could be modeled as a single phase fluid. Using the experimental equipment, pressures and pressure drop measurements were taken for a variety of liquid flow rates. (For these tests, percent air, bead size, and surfactant concentration were held constant at 49.5%, 1.5 mm, and 500 ppm, respectively). Since the column is pressurized, the volume of air in the column will be different from the volume of air exiting at atmospheric pressure. Using Q′ for the new quality, the density of the foam in the column can be derived.

$$\rho_f = (1 - Q)\rho_w \tag{5}$$

With this value and assuming the viscosity of the foam to be that of water, substitution can be made into the Ergun equation. The result is a predicted pressure drop for given flowrates and is shown in Figure 9.

The shapes of the curves are nearly identical; however, the predicted ΔP's are offset below the experimental ΔP's. Examination of the Ergun equation reveals that by increasing the value of the viscosity, the offset can be corrected. Relaxing the assumption that the foam viscosity is equal to that of water is also logical. Surfactant alone increases the water's viscosity, and it is known that the viscosity of foam also increases with increasing quality [25]. An arbitrary viscosity 2.35 times that of water was substituted into the prediction model to produce the third curve in Figure 9. Above 20 L/min, the correlation to the experimental data is excellent. Discrepancies below 20 L/min may be due to bubble size and distribution. Predominantly large ($>210\ \mu$) bubbles were found to form at low rates of flow. Figure 10 shows a graph of pressure drop predicted by the Ergun equation versus the actual pressure drop measured for all applicable test runs. For the predicted values, a viscosity of 1.7 cP was assumed. A trend for predicting actual pressure drops exists, however, the predicted values are higher than the actual pressures, especially at higher pressure.

Further investigation and verification is recommended. Particularly helpful would be viscometric measurements of surfactant laden water and low quality foams. Preliminary viscometric measurements of CGA at 60% quality indicate a viscosity between 5 and 9 cP. The measurement technique needs improvement as readings exhibited time dependant properties. Also, different air qualities and shear rates need to be examined.

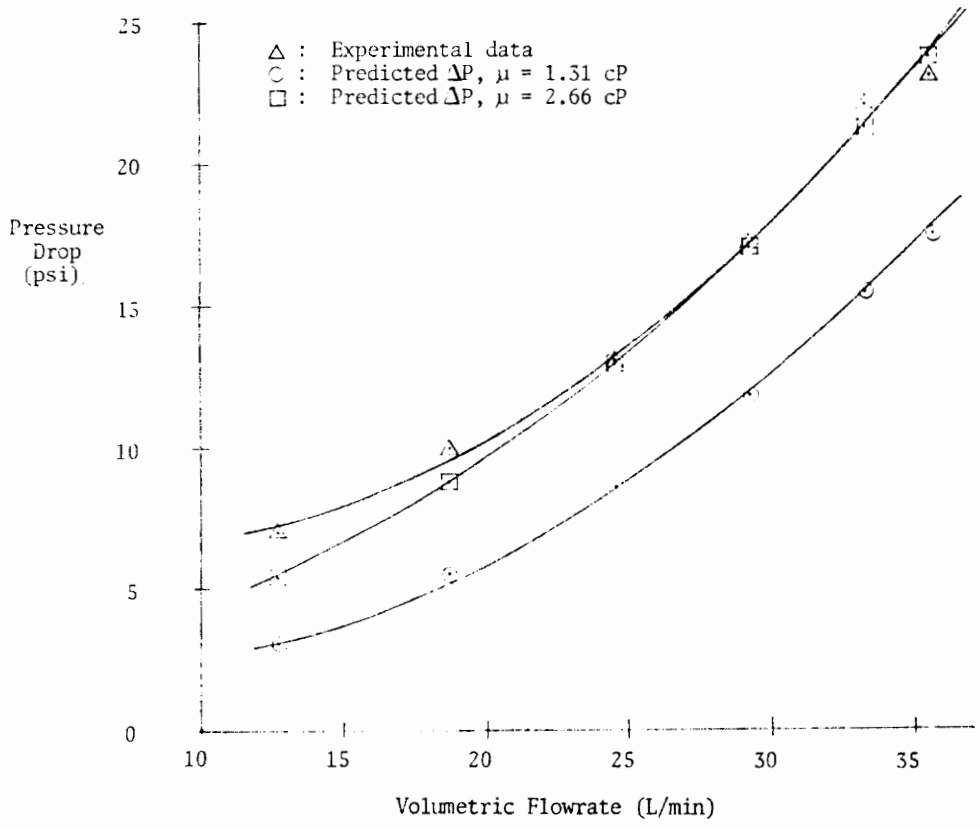

Figure 9. Pressure drop versus flowrate.

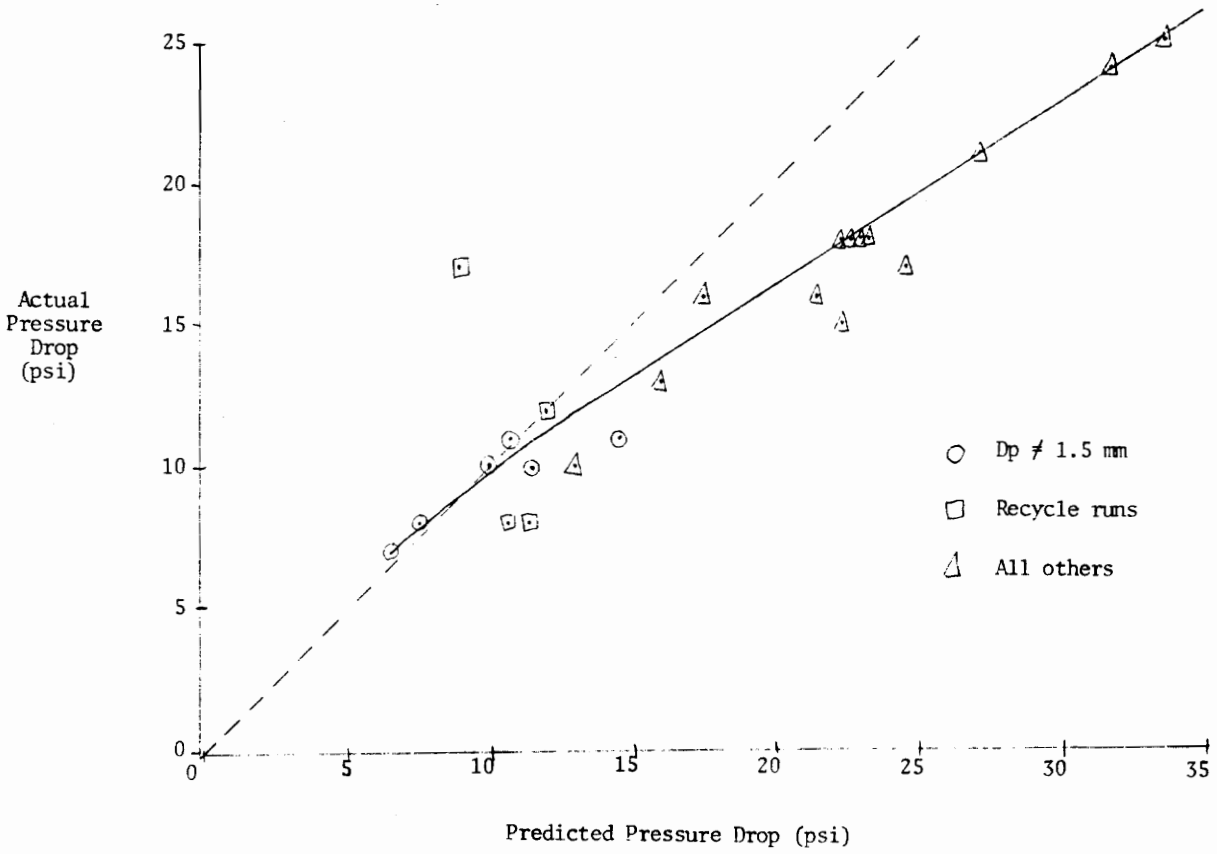

Figure 10. Predicted pressure drop versus actual pressure drop for all applicable experimental runs.

5.0 Economic Feasibility

A preliminary cost comparison for microbubble foam generation using the spinning disk and packed bed techniques is examined (see Table 14). One application of these foams is in direct subsoil air sparging. The cost of air sparging alone is also listed for the same flowrate of air. In the comparison, the following bases and assumptions are used (calculations of these costs are found in Appendix C):

- 30 L/min standard air delivered at 10 psig.
- 250 ppm surfactant to produce 60% quality microfoams.
- Hourly operation.
- No capital cost or labor included.

A comparison of dissolved air flotation (DAF) using conventional means versus using a packed bed foam generator is also made. These calculations and supporting assumptions are also in Appendix C. The calculations show that conventional DAF costs $ 0.5825/hr while the packed bed method costs $ 0.3483/hr. If the flotation process stream contains natural surfactants, the need to add surfactant no longer exists thus making the packed bed technique even more economical.

Table 14. Production cost of microbubble foams and sparged air

Packed bed:	**Usage**	**Unit Cost**	**Total Cost**
Solution feed:	0.01344 kWhr	$ 0.0706 /kWhr	= $ 0.00095
Generation:	0.2475 kWhr	$ 0.0706 /kWhr	= $ 0.01747
Surfactant:	0.661 lb	$ 0.50 /lb	= $ 0.3308
Total hourly utility and chemical cost for 50 L/min (30 L/min air)			$ 0.349
Spinning disk:			
Solution feed:	0.01344 kWhr	$ 0.0706 /kWhr	= $ 0.00095
Generation:	0.8745 kWhr	$ 0.0706 /kWhr	= $ 0.06174
Surfactant:	0.661 lb	$ 0.50 /lb	= $ 0.3308
Total hourly utility and chemical cost for 50 L/min (30 L/min air)			$ 0.3935
Direct air:			
Air costs:	0.0567 kWhr	$ 0.0706 /kWhr	= $ 0.00400
Total hourly utility cost for 30 L/min of air			$ 0.004

6.0 Conclusions and Recommendations

6.1 Conclusions

A review of microbubble foam generation techniques revealed that packed column devices, with their large area for gas-liquid contacting, their simple construction, as well as their ability to be readily scaled to different sizes offered great promise for producing microbubble foam. To study the packed column in this role, a pilot unit and prototype packed bed generator was designed and built. Operation of the pilot equipment was highly successful as judged by the equipments' ability to control microbubble production. In addition to the excellent performance of the pilot unit, considerable gains were made in the area of microbubble foam characterization. The use of a microscope viewing cell to observe and to photograph microbubble foam immediately after it is produced has led to the use of image analysis to determine bubble size distributions. The bubble size distributions and the standard bubble rise versus time data provide a quantitative picture of the microbubble foam produced. In regard to the effect of the variable parameters associated with the packed column generation device on the character of the microbubble foam produced, the following conclusions based on the results and discussion in Chapter 4.0 are offered.

1. As expected, high shear forces in the bed resulting from high volumetric flowrates and increased air quality enhanced the production of micron sized bubbles. The size of the packing also contributed to the shearing effect. With small bead sizes, 1.5 mm, lower flowrates are required to produce the shear necessary to form microbubbles. The larger bead size, 3.0 mm, was not able to enhance microbubble foam production at the flowrates tested.
2. An increase in the quality of the foam produced a decrease in the size of the microbubbles formed.
3. Surfactant concentration affected the microbubble foam in two ways. First, as the concentration decreased, smaller, but less stable, bubbles were formed. Second, at higher concentrations, the distribution of bubbles by size became binodal.
4. The use of recycle promoted the production of very uniform, very small bubbles. However, it was discovered that the recycle pump itself and the configuration of the test equipment was contributing greatly to this effect.
5. Microbubble foam flow can be considered a pseudo single phase fluid for use in pressure drop equations.

In summary, a column packed with millimeter sized glass beads is able to produce an effective microbubble foam that contains a majority of bubbles less than 90 μ, and few greater than 150 μ The ideal operating conditions for producing these microbubbles are as follows: any feed flowrate from 12 to 24 L/min; air quality of 65% (34 - 68 L/min of microbubble foam); surfactant solution of 200 ppm NaDBS; bead size of 3.0 mm: and, a recycle ratio of 1.0. If the inclusion of a few large, 200 to 300 μ, bubbles does not affect the application for which the product will be used, operation without recycle is recommended. For this case, operating conditions require 20 L/min or more feed flowrate, 65% air quality (57+ L/min of microbubble foam), 200 ppm NaDBS, and a bead size of 1.5 mm.

From an economic stand point, microbubble foam generation with a packed column is superior to a series of spinning disk CGA generators. In terms of application, any microbubble foam generator will encounter higher operating expenses if surfactant needs to be added. Indeed,

surfactant costs make up 95% of the total operating costs. In a comparison with existing microbubble foam applications, dissolved air flotation and direct air sparging, the packed bed is able to compete economically with dissolved air, however, unless there is a significant advantage to using the packed bed, direct air sparging is more economically sound.

6.2 *Recommendations*

In light of the discussion of the experimental work, the following recommendations are suggested:

1. As a matter of procedure, all bubble rise stability data should be standardized for future work with microbubble foams. A standard 23.5 cm high 250 mL graduated cylinder is recommended.
2. Physico-chemical properties of microbubble foams should be examined and recorded in detail so that predictions of behavior in different applications may be made, as well as providing further insight to other possible generation techniques.
3. The recycle pump should be tested at greater lengths, especially in its role as a microbubble foam generator.
4. The pilot unit should be modified to accommodate higher flowrates to allow for the study of the effects of large bead sizes at high shear on microbubble generation.
5. The ability of the Ergun equation to predict pressure drops in other flow regimes should be examined to verify that microbubble foam flow can be modeled as a single phase. Other testing along this line includes accurate viscosity measurements of microbubble foam at low qualities and high shear rates.
6. Surface chemistry theory should be probed to uncover the microscopic phenomena occurring in microbubble generation. This work should also be supported by high powered microscopy.

References

1. Sebba, F., "Microfoams--an unexploited colloid system," **J. Coll. Interface. Sci.**, 35(4), pp. 643-6, 1971.

2. Sebba, F., "An improved generator for micron-sized bubbles," **Chem. Ind.**, pp. 91-2, Feb., 1985.

3. Jordan, S. T. and Termine, F., "Production of high quality dust control foam to minimize moisture addition to coal," **Coal Technol.** (Houston), 8th(1-2), pp. 207-20, 1985.

4. Aubert, J. H., Kraynik, A. M. and Rand, P. B., "Aqueous foams," **Sci. Amer.**, 254(5), pp. 74-82, 1986.

5. Sebba, F. and Barnett, S. M., "Separations using Colloidal gas aphrons," **Proc. 2nd Int. Congress of Chem. Eng.**, Vol IV, p. 27, 1981.

6. Sebba, F., "Investigation of the modes of contaminant capture in CGA (MGD) foams," U.S. Department of the Interior, Office of Water Research and Technology, OWRT/RU-82/10, 1981.

7. Sebba, F., "Separations using aphrons," **Sep. Purif. Methods** , 14(1), pp. 127-48, 1985.

8. Personal communication with Dr. S. M. Barnett, Dept. of Chem Eng, Univ. of R. I., Apr. 6, 1987.

9. Klassen, V. I., "Theoretical basis of flotation by gas precipitation," Internationsl Mineral Processing Congress, The Institution of Mining and Metallurgy, London, pp 309-22, 1960.

10. Fuerstein, D. W., "Fine particle flotation," **Fine particles Processing** 1st ed., vol 1, Port City Press, Baltimore, MD, pp. 669-705, 1960.

11. Goins, W. C., Jr., and Magner, H. G.,"How to use foaming agents in air and gas drilling," **World Oil**, 152(4), pp 59-64, 1961.

12. Fried, A. N., "The foam-drive process for increasing the recovery of oil," RI 5866, USBM, 1961.

13. Raza, S. H., "Foam in porous media: characteristics and potential applications," **Soc. Pet. Eng. J.**, Trans. AIME 249, pp. 328-36, 1970.

14. Bock, J., Downs, H. H., Siano, D. B. and Pace, S. J., US Patent 4612332 (Sept. 1986).

15. Mathieu, G. I., "Comparison of flotation column with conventional flotation for concentration of a molybdenum ore," **CIM Bulletin**, pp. 41-5, 1972.

16. Thondavadi, N. N. and Lemlich, R., "Flow properties of foam with and without solid particles," **Ind. Eng. Chem. Process Des. Dev.**, 24(3), pp. 748-53, 1985.

17. Datye, A. K. and Lemlich, R., " Liquid distribution and electrical conductivity in foam," **Int. J. Multiphase Flow**, 9(6), pp. 627-36, 1983.

18. Shea, P. T. and Barnett, S. M., "Flotation using microgas dispersions," **Sep. Sci. Tech.** 14(9), pp. 757-767, 1979.

19. McManus, D. S., US Patent 3545731 (Dec. 1970).

20. Wright, F. C., US Patent 4328107 (May 1982).

21. Minssieux, L., "Oil displacement by foams in relation to their physical properties in porous media," **J. Petrol. Technol.** (Jan.), pp. 100-8, 1974.

22. Brown, L. W. and Bartenfield, J. E., US Patent 4394289 (July 1983).

23. Foot, D. G., Jr., McKay, J. D., and Huiatt, J. L., "Column flotation of chromite and fluorite ores," 24th CIM Conf., Vancover, August 19, 1985.

24. Rand, P. B. and Kraynik, A. M., "Drainage of aqueous foams: generation-pressure and cell-size effects," **Soc. Pet. Eng. J.**, 23(1), pp. 152-4, 1983.

25. Cole, H. W., Jr., Canadian Patent 1170253 (July 1984).

26. Johnson, R. M., Canadian Patent 1187776 (May 1985).

27. Bird, R. B., Stewart, W. E., and Lightfoot, E. N., **Transport Phenomena**, John Wiley & Sons, New York, p. 200, 1960.

28. Green, D. W., ed., **Perry's Chemical Engineers' Handbook**, sixth edition, McGraw-Hill, New York, NY, 1984.

29. Marsden, S. S. and Khan, S. A., "The flow of foam through short porous media and apparent viscosity measurements," **Soc. Pet. Eng. J.** (March), pp. 17-25, AIME 237, 1966.

30. Keyser, P. M. "Continuous column flotation of ultrafine coal using microbubbles," Masters Thesis, Department of Mining and Minerals Engineering, Va. Poly. Inst. & S. U., p.44, March 1987.

31. Cheng, H. C. and Lemlich, R., "Errors in the measurement of bubble size distribution in foams," **Ind. Eng. Chem. Fundam.** 22(1), pp. 105-9, 1983.

Appendix A. Equipment List

The following is a list of the equipment used in the project.

- Feed tank -- American Scientific Products, 100 gal, 28″ x 42″, polyethylene, with cover.
- Holding tank -- American Scientific Products, 275 gal, 42″ x 48″, polyethylene, with cover.
- Water rotometer -- McMaster 4350K43, 8-40 L/min, ss float.
- Pressure gauges (4) -- McMaster 4083K33, 0-160 psig, ANSI grade A.
- Flow meters (2) -- Berkness Control & Equipment MVR-B-S-150, 1 1/2″ turbine flow meter/accumulator.
- Back pressure regulator -- Grainger 2P072, 5-300 psi, 25 gpm max.
- Air rotometer -- Cole Parmer J3217-34, 4-43 L/min, ss ball float.
- Recycle rotometer -- Cole Parmer J3248-72, 4-40 gpm, ss float.
- Rupture disk -- Cavalier Controls, 1 1/2″, 89 psi.
- Plumbing -- CPVC for 1/2″ and 3/4″ piping, PVC for 1 1/4″ piping, and galvanized steel for 1 1/2″ piping.
- Feed pump -- Price Pump Co. HP-75-75, high pressure single stage brass volute centrifugal pump. (50.7 psi @ 0 L/min; 46.7 psi @ 22.7 L/min, 23% eff; 44.1 psi @ 56.8 L/min, 44% eff)

- Recycle pump -- Allweiler Pump Co. SEP380.1H31P13G13PP3207MO, 3 hp, 50.7 gpm, 79 psi, 280 rpm, screw-type positive displacement pump.
- Microscope -- Nikon, Optiphot biological microscope.
- Video camera -- Dage-MTI, Inc., 66 series camera.
- Video monitor -- Dage-MTI, Inc., 66 series camera.
- Image analysis --Kontron SEM-IPS.

- Glass beads -- Potters Industries and Ferro, 3.4 mm (avg), 3.0 mm, 2.0 mm, 1.5mm.
- Surfactant -- Sodium Dodecybenzenesulfonate, Pfalz & Bauer, 85-90 %.
- EDTA -- Fischer Scientific.
- SLR camera -- Minolta X-700.

Appendix B. Procedure

The following is a detailed procedure on the operation of the portable microbubble generation pilot unit. An accompanying keyed figure is located at the end of this section.

I. Preparation of feed solution

A. Weigh out the appropriate amount of surfactant and transfer it to a ten gallon container. (Example: To make 400 L of 0.5 g/L surfactant concentration, add 222.2 g of 90% pure surfactant.)

B. Slowly add hot tap water to the container, stirring gently to prevent excessive foaming.

C. With a garden hose attached to a water faucet, open the water faucet and allow tap water to run for several minutes to drain.

D. Add appropriate amount of EDTA to the feed tank, T1. (Example: For a 400 L solution add 36 g of EDTA.)

E. Turn off water and transfer hose outlet to T1.

F. Turn on water and fill T1 to the 50 L level.

G. Slowly add the concentrated surfactant solution to T1.

H. With the end of the hose under the surface of the feed solution, turn on the water and fill T1 to the desired level.

I. If foaming occurs, allow the solution to settle for two hours.

II. Operation

A. Preparation

1. Plug the feed pump's, P1, electrical cord into the wall power outlet.
2. Check to see that all valves are closed except VP1 and VB1, which should be open.
3. Connect drain attachment to line B.
4. Attach hose to drain outlet and position hose outlet to an open drain.
5. Prime pump P1. [Note: The pump only needs to be primed when the potential to have air in the feed lines exists. This problem usually occurs when the pump has accidentally drained a tank dry, or during plumbing changes.]
   a. Remove top volute screw allowing air to escape.
   b. Replace volute screw when water issues from the volute.
   c. Open VP2 slightly.
   d. Turn on pump for ten seconds.
   e. Repeat steps a thru d until all air in the feed lines has escaped.
6. Turn on P1, then the recycle pump, P2, for five minutes.
7. Replace drain attachment with plug.
8. Open VP5.

9. Replace feed tank return line with drain attachment. [Note: This and the following three steps are needed only for the first operation after the system has been flushed.]

10. Attach hose to drain outlet and position hose outlet to an open drain.

11. Turn on P1 for two minutes.

12. Replace drain attachment with feed return line.

13. Open VP3 and close VP4.

14. Open air cylinder valve.

15. Regulate air to 60 psig.

B. Without recycle pump.

1. Prepare for operation.

2. Turn on feed pump, P1.

3. Adjust VP2 to give desired flow rate of feed.

4. Adjust VA1 to give desired flow rate of air.

5. Make final adjustments on VP2.

6. Take samples. (See sampling procedure)

7. As often as needed, readjust flows to meet next sampling condition and take samples.

C. With recycle pump.

1. Prepare for operation.

2. Turn on feed pump, P1 and open VP2.

3. Check that recycle rotometer is completely filled with water.

4. Adjust VP2 to give desired flow rate of feed.

5. Adjust VA1 to give desired flow rate of air.

6. Open VR1.

7. Turn on recycle pump, P2.

8. Adjust VR1 to desired recycle rate. [Note: Do not allow pressure in P1 to drop below 5 psig.]

9. Make final adjustments on VP2 and VA1.

10. Take samples. (See sampling procedure)

11. As often as needed, readjust flows to meet next sampling condition and take samples.

III. Sampling procedure.

A. Record the weights of several empty 250 mL or 500 mL graduated cylinders. (Caution: do not mix different types.)

B. Open VS1.

C. Turn VS3 to the 'd' position.

D. Open VS2 for ten seconds.

E. Take picture, and advance film.

F. Repeat steps D and E twice.

G. Turn VS3 to the 's' position.

H. Samples and discards are made by turning VS2 on and off.

1. Discard current contents of sample line.

2. Fill first graduated cylinder to the 250 mL mark.

3. Immediately after filling, start timer.

4. Fill next graduated cylinder to the 250 mL mark, and immediately after filling, record the time displayed on the timer.

5. Repeat step 4.

I. Record the position of the foam/water interface in the three cylinders every minute for six minutes.

IV. Transfer from holding tank to feed tank.

A. Allow foam in holding tank, T2, to collapse; approximately 4-5 hours.

B. Close the following valves: VP1, VP2, VP4.

C. Open the following valves: VT1, VT2.

D. Prime the feed pump, P1. (See step II.3 above)

E. Turn on P1.

F. Turn off P1 just before the holding tank is empty.

V. Flushing the system

A. Close all valves.

B. Replace feed tank return line with drain attachment.

C. Attach hose to drain outlet and position hose outlet to an open drain.

D. Open the following valves: VP1, VT2, VB1.

E. From the water supply, hose down and scrub the inside walls of the feed tank, T1.

F. If the tank is more than one-half full or when the tank becomes one-half full, turn on the pump P1.

G. Allow T1 to empty making sure not to run the pump dry.

H. Continue this rinsing operation until the liquid in the tank no longer foams.

I. Turn off P1 and fill T1 with fresh water.

J. Close VT2 and open VP4.

K. Turn on P1 and open VP2.

L. After five minutes, open VT2 and close VP4.

M. Exhaust contents of T1, turning off P2 just before the tank is empty.

N. Close the following valves: VP1, VP2, VP4.

O. Open the following valves: VT1, VT2.

P. Repeat steps E-G with the holding tank, T2.

Q. Turn off the water and allow pump P1 to exhaust the contents of T2, turning off the pump just before the tank is empty.

R. Close all valves.

S. Replace drain attachment with feed tank return line.

T. Attach hose to drain on holding tank T2 and place hose outlet to an open drain.

U. Open VT3 and allow T2 to drain dry.

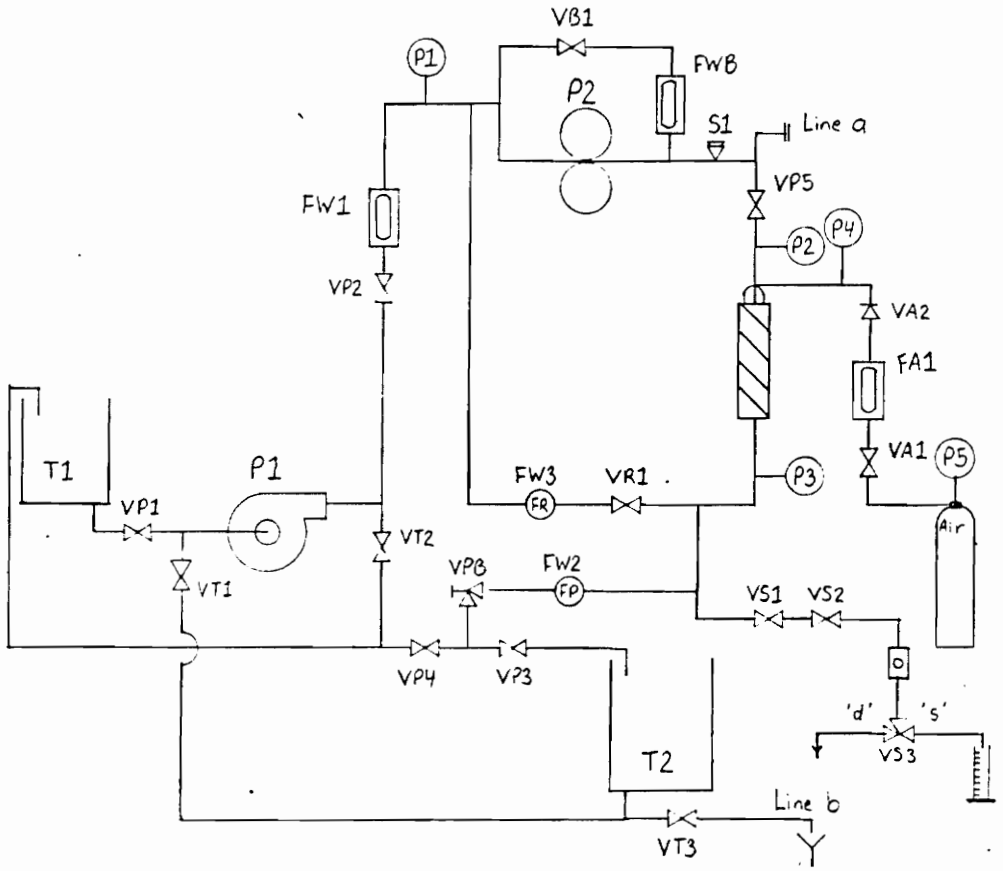

Figure 11. Labeled schematic diagram of pilot unit.

Labeling Key

Process Equipment

T1	Feed tank, 100 gallons.
T2	Holding tank, 275 gallons.
P1	Centrifugal feed pump.
P2	Positive displacement screw-type pump.
S1	Rupture disk safety mechanism (89 psi).

Process Valves

VP1	3/4″ CPVC.
VP2	3/4″ CPVC.
VP3	3/4″ Qest.
VP4	3/4″ Qest.
VP5	1 1/2″ Brass gate.
VPB	Back pressure regulator.

Air Valves

VA1	Built into rotometer.
VA2	Brass check valve.

Sample Valves

VS1 Needle valve, brass, 1/4″.

VS2 Ball valve, brass, 1/4″.

VS3 3-Way ball valve, brass, 1/4″.

Transfer Valves

VT1 3/4″ CPVC.

VT2 3/4″ CPVC.

VT3 3/4″ CPVC.

Miscellaneous Valves

VB1 Bypass valve, brass gate, 1 1/2″.

VR2 Recycle valve, 3/4″ CPVC.

Flowmeters

FW1 Water rotometer, 0-40 L/min.

FW2 Flow accumulator, turbine, 1 1/2″ (process line).

FW3 Flow accumulator, turbine, 1 1/2″ (recycle line).

FWB Water rotometer for bypass line, 0-40 gpm.

FA1 Air rotometer, 0-40 L/min (see calibration, Appendix D).

Appendix C. Miscellaneous

C.1 Comparison of Costs: Packed Bed vs Spinning Disk vs Direct Aeration

Surfactant solution feed system (Packed bed and spinning disk only)

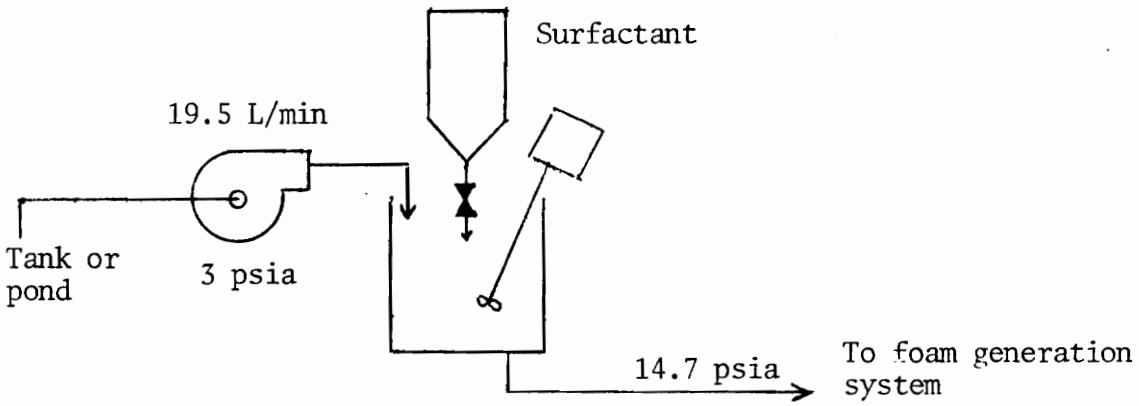

Assumptions: 1. Surfactant solution mixed in tank, energy neglected.

2. Surfactant added to mixing tank by gravity feed.
3. Pump operates at 50% efficiency.

Pump:

$$Ws(kWhr) = 115x10^{-6} F(L/min) P(psia) / Eff$$

$$Ws = 115x10^{-6} * 19.5 * 3.0 / 0.5$$

$$Ws = 0.0135 \text{ kWhr}$$

Surfactant cost:

$$Mass(lb/hr) = 0.1323 F(L/min) C(g/L)$$

$$Mass = 0.1323 * 20 * 0.250$$

$$Mass = 0.661 \text{ lb/hr}$$

Packed bed operating costs

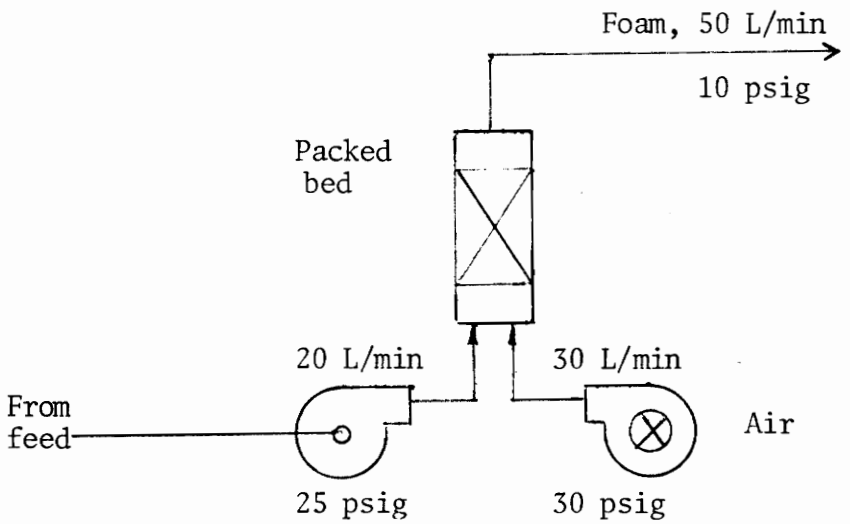

Assumptions:
1. 30 psig air and 25 psig water needed to make good foam.
2. 60% quality refers to foam at 14.7 psia.

3. Compressor operates at 50% efficiency.

Air compressor:

$$W_s = \frac{k}{k-1} P_1 q \left[\frac{P_2}{P_1}^{\frac{k}{k-1}} - 1 \right] \frac{B}{E}$$

k = Cp/Cv = 1.4

P = Pressure at inlet (1) and outlet (2) (psia)

q = Flowrate (L/min)

B = Conversion factor

E = Efficiency

$$W_s = \frac{1.4}{0.4} (14.7) (30.0) \left[\frac{44.7}{14.7}^{\frac{1.4}{0.4}} - 1 \right] 115 \times \frac{10^{-6}}{0.5}$$

$$W_s = 0.1326 \text{kWhr}$$

Feed pump:

Ws(kWhr) = 115 × 10^{-6} F(L/min) P(psia) / Eff

Ws = 115 × 10^{-6} * 20.0 * 25.0 / 0.5

Ws = 0.1150 kWhr

Spinning disk operating costs

Assumptions:

1. Air sucked in, no pressurization.
2. 60% quality refers to foam at 14.7 psia.
3. Each generator produces 4 L/min, 12 generators used.
4. Full load of one generator is 1/12 hp.

Feed pump:

$$Ws(kWhr) = 115 \times 10^{-6} F(L/min) P(psia) / Eff$$

$$Ws = 115 \times 10^{-6} * 20.0 * 3.0 / 0.5$$

$$Ws = 0.0138 \text{ kWhr}$$

Exit pump:

$$Ws(kWhr) = 115 \times 10^{-6} F(L/min) P(psia) / Eff$$

$$Ws = 115 \times 10^{-6} * 50.0 * 10.0 / 0.5$$

$$Ws = 0.1150 \text{ kWhr}$$

Generators:

$$12\ 1/12 = 1 \text{ hp} => \quad Ws = 0.7458 \text{ kWhr}$$

Direct Aeration

Assumptions: Only need to compress air to 10 psig at 30 L/min.

As before:

$$Ws = 0.0567 \text{ kWhr}$$

C.2 Comparison of Flotation costs: Dissolved Air vs Packed Bed

Packed bed:

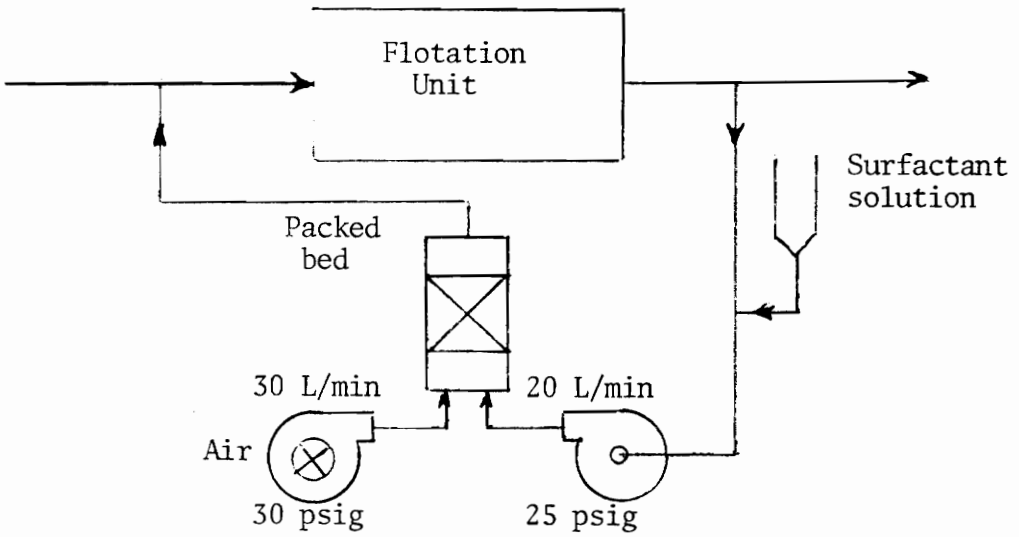

Dissolved air:

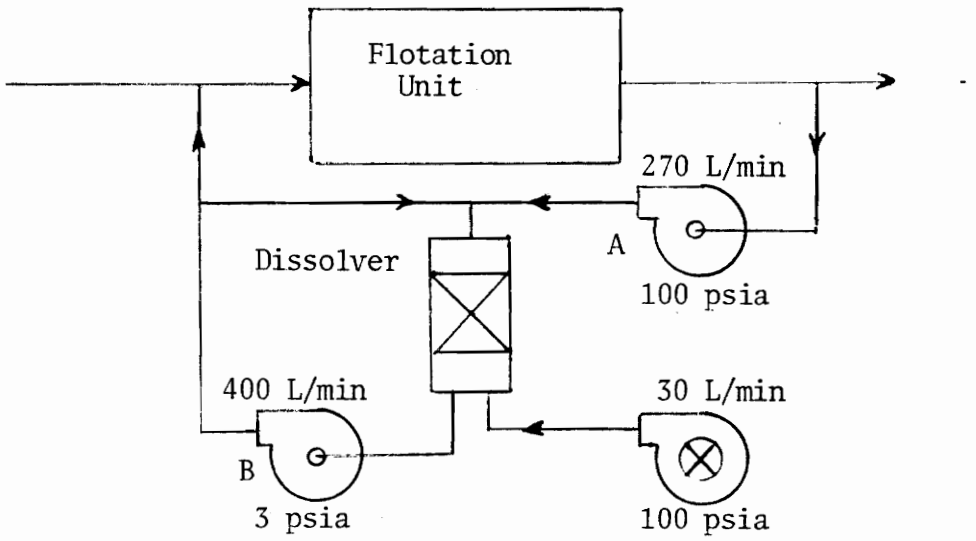

Assumptions:

- 30 L/min standard air delivered to dissolver unit.
- Nine volumes water to one volume air (atmospheric) to dissolve air.
- Air dissolved at 100 psig with recycle.
- Volume of air under pressure is negligible or dissolved.
- Pumps and compressors operate at 50% efficiency.
- Flotation feed stream delivered at 10 psig.
- Hourly operation.
- No capital costs or labor included.

Packed Bed Costs

The packed bed costs are the same as given before minus the solution feed system. Total power is 0.2475 kWhr.

Dissolved Air Costs

Pump A:

$$Ws(kWhr) = 115 \times 10^{-6} F(L/min) P(psia) / Eff$$

$$Ws = 115 \times 10^{-6} * 270. * 100. / 0.5$$

$$Ws = 6.21 \text{ kWhr}$$

Pump B:

$$Ws(kWhr) = 115 \times 10^{-6} F(L/min) P(psia) / Eff$$

$$Ws = 115 \times 10^{-6} * 400. * 3.0 / 0.5$$

$$Ws = 0.276 \text{ kWhr}$$

Air Compressor:

As before, now with 30 L/min at 100 psia.

$$Ws = 1.76 \text{ kWhr}$$

Total power from dissolved air is 8.25 kWhr.

Table 15. Comparison of costs: dissolved air vs packed bed

Packed bed:	Usage	Unit Cost	Total Cost
Power:	0.2475 kWhr	$ 0.0706 /kWhr	= $ 0.01747
Surfactant:	0.661 lb	$ 0.50 /lb	= $ 0.3308
Total hourly utility and chemical cost:			$ 0.3483

Dissolved air:	Usage	Unit Cost	Total Cost
Power:	8.25 kWhr	$ 0.0706 /kWhr	= $ 0.5825
Total hourly utility cost:			$ 0.5825

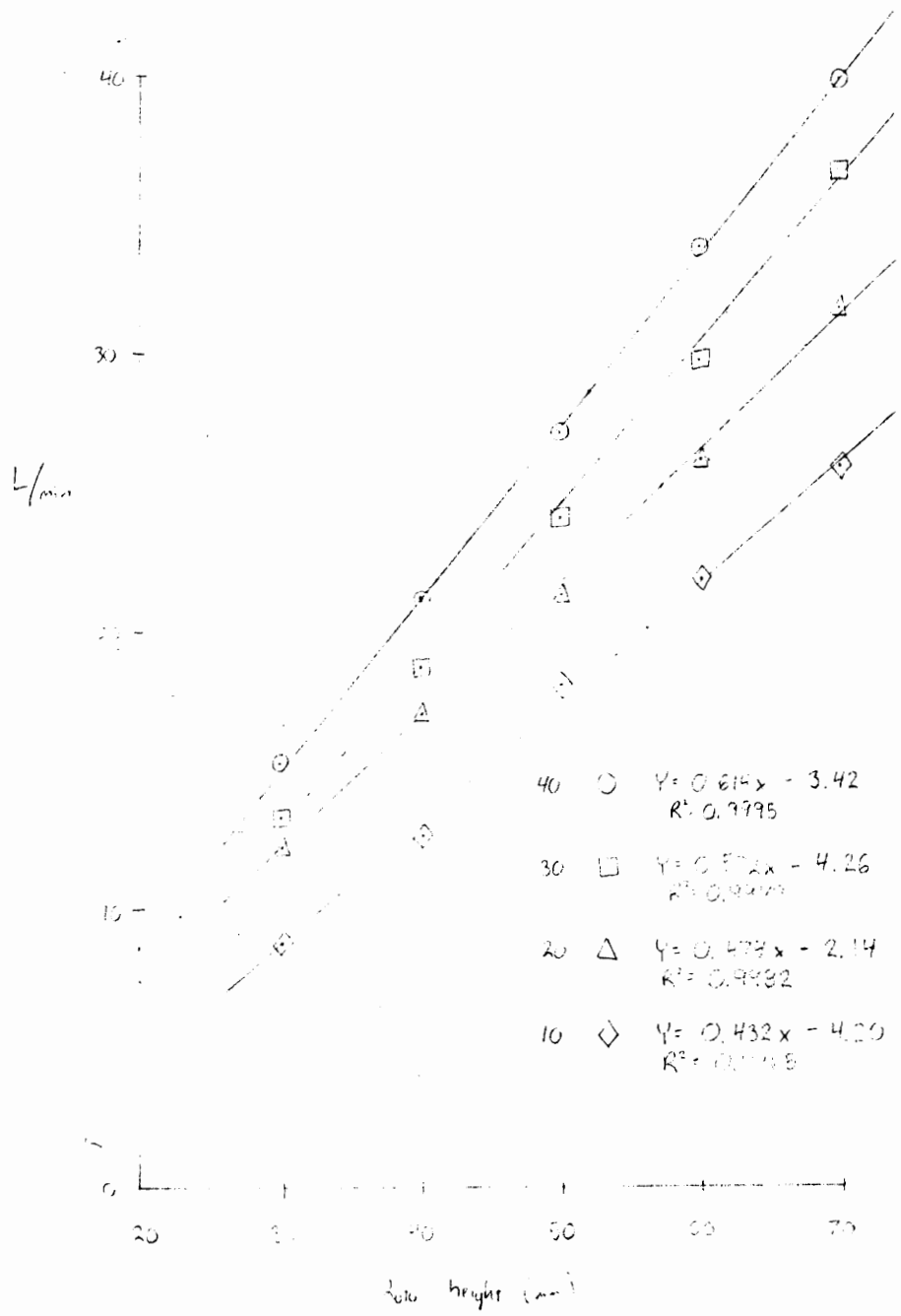

Figure 12. Air rotometer calibration

Table 16. Accuracy of image analysis: calibration of Latex spheres.

Reported Diameter (μ)	Measured Diameter (μ)	Samples
91.2 ± 1	91.5 ± 3.7	54
44.66 ± 0.5	44.78 ± 2.4	88

Image analysis was done by digitizing the photomicrographs,
enhancing the image,
then marking bubble diameters using an interactive two-point technique.

Appendix D. Data

The following contains selected data from 26 test runs.

Data Sheets For Test # 1

Packing Diameter (mm)	: 3.4	Reynolds Number	:
Solution Feed Flowrate (L/min)	: 16	Pressure Drop Across Bed (psia)	:
Average Quality (% air)	: 59.0		
Solution Concentration (ppm)	: 500	(number of reuses: 0)	
Recycle Ratio (rec/dis)	: 0	System Pressure (psig)	: 7

Notes: No stability

Legend: O - Sample A
Δ - Sample B
□ - Sample C

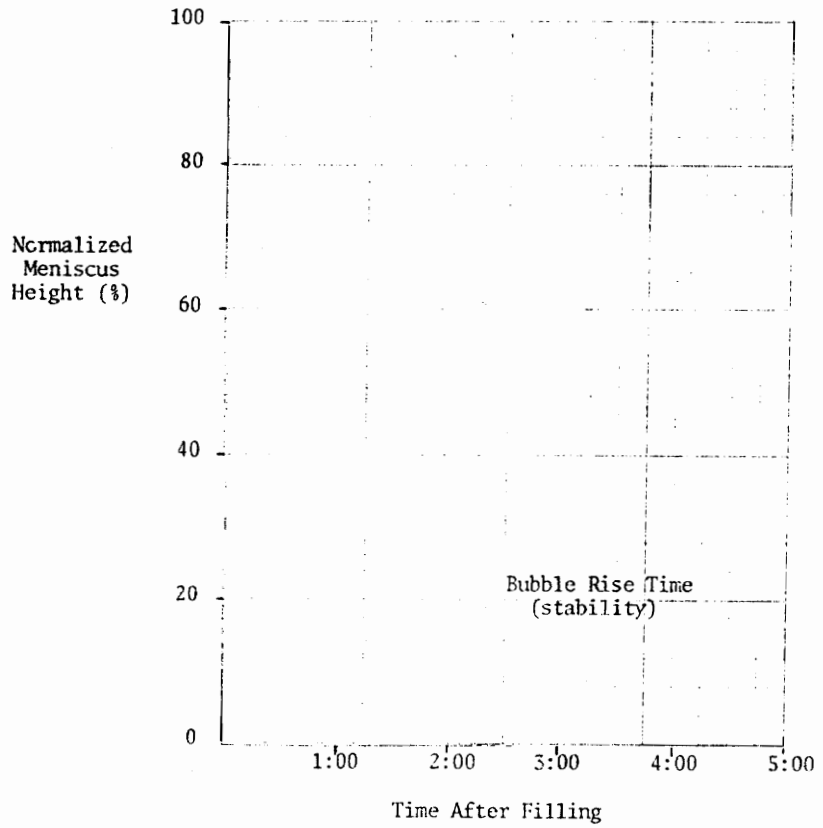

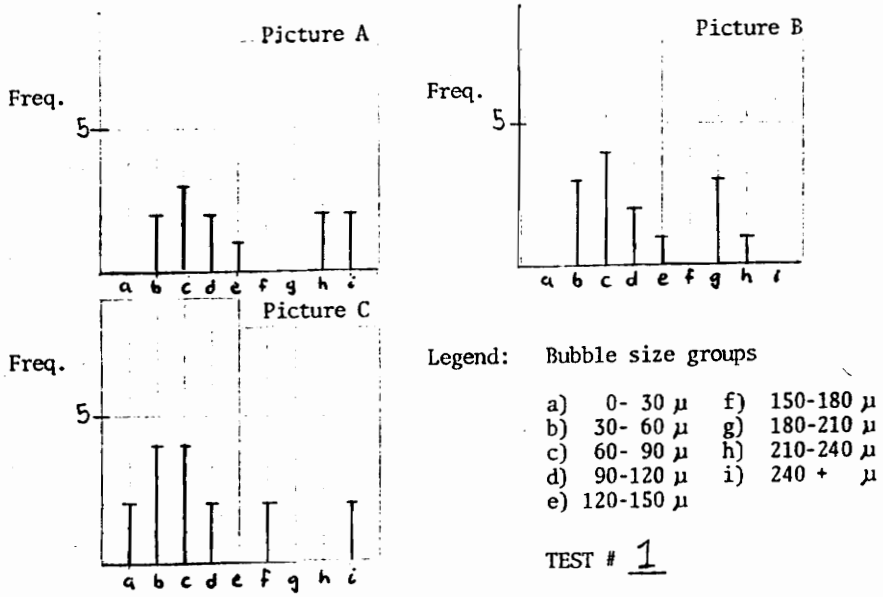

Legend: Bubble size groups

a) 0- 30 μ
b) 30- 60 μ
c) 60- 90 μ
d) 90-120 μ
e) 120-150 μ
f) 150-180 μ
g) 180-210 μ
h) 210-240 μ
i) 240 + μ

TEST # 1

Histograms of Individual Photos

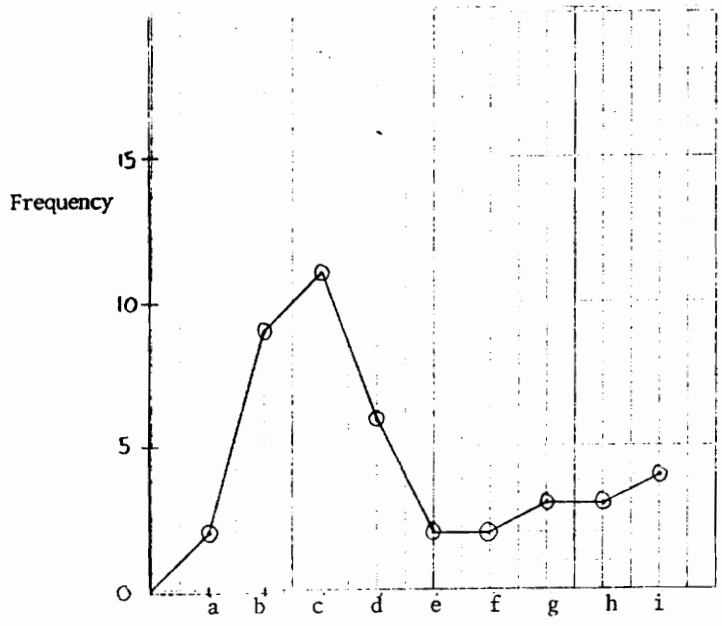

Cumulative Histogram

Data Sheets For Test # 2

Packing Diameter (mm)	: 3.0	Reynolds Number	: 285
Solution Feed Flowrate (L/min)	: 16	Pressure Drop Across Bed (psia)	: 8
Average Quality (% air)	: 59.7		
Solution Concentration (ppm)	: 500	(number of reuses: 0)	
Recycle Ratio (rec/dis)	: 0	System Pressure (psig)	: 7

Notes: No stability

Legend: O - Sample A
Δ - Sample B
□ - Sample C

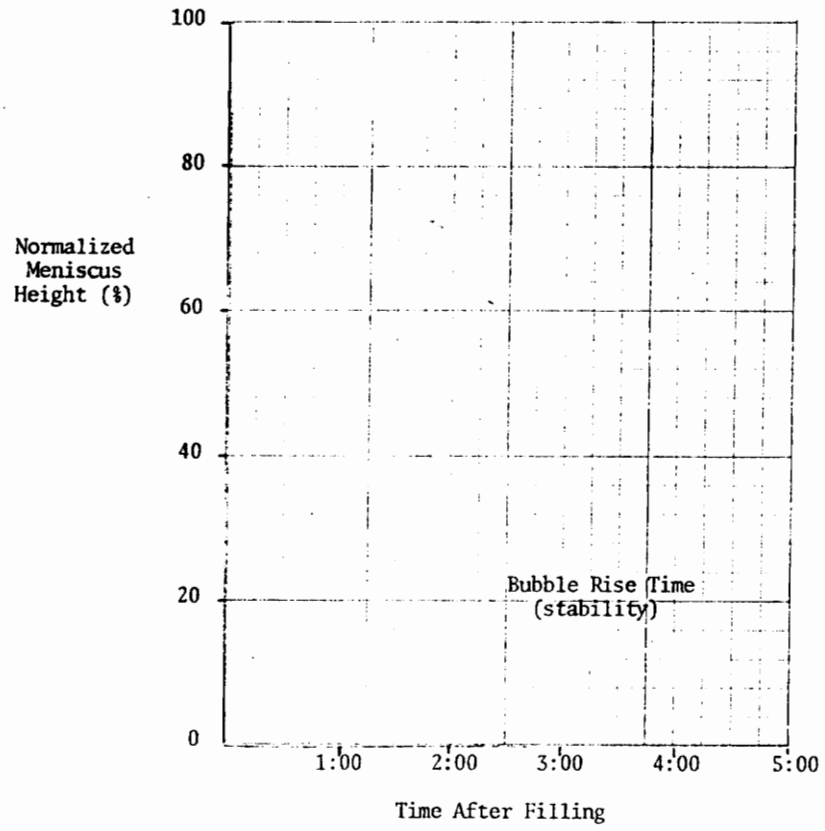

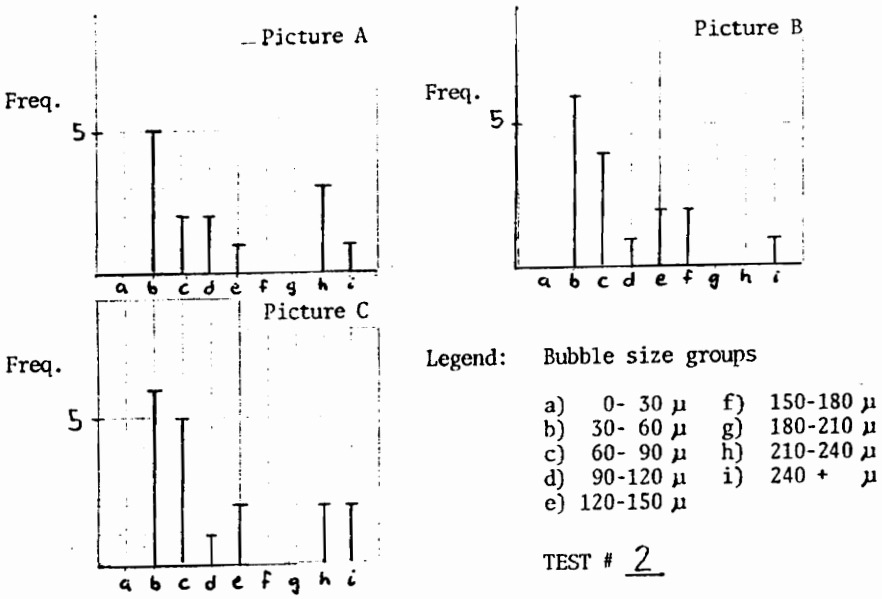

Histograms of Individual Photos

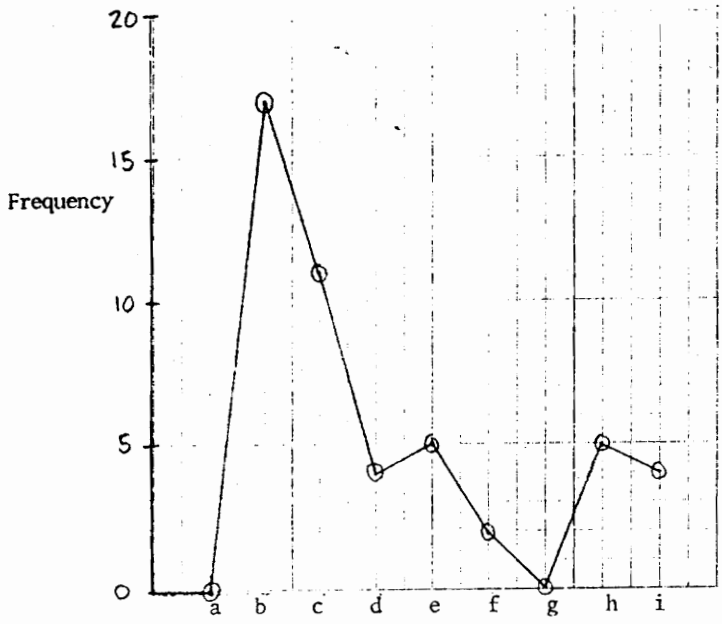

Cumulative Histogram

Data Sheets For Test # 3

Packing Diameter (mm)	: 3.0	Reynolds Number	: 357
Solution Feed Flowrate (L/min)	: 20	Pressure Drop Across Bed (psia)	: 10
Average Quality (% air)	: 60.9		
Solution Concentration (ppm)	: 500	(number of reuses: 1)	
Recycle Ratio (rec/dis)	: 0	System Pressure (psig)	: 10

Notes: No stability

Legend: O - Sample A
Δ - Sample B
□ - Sample C

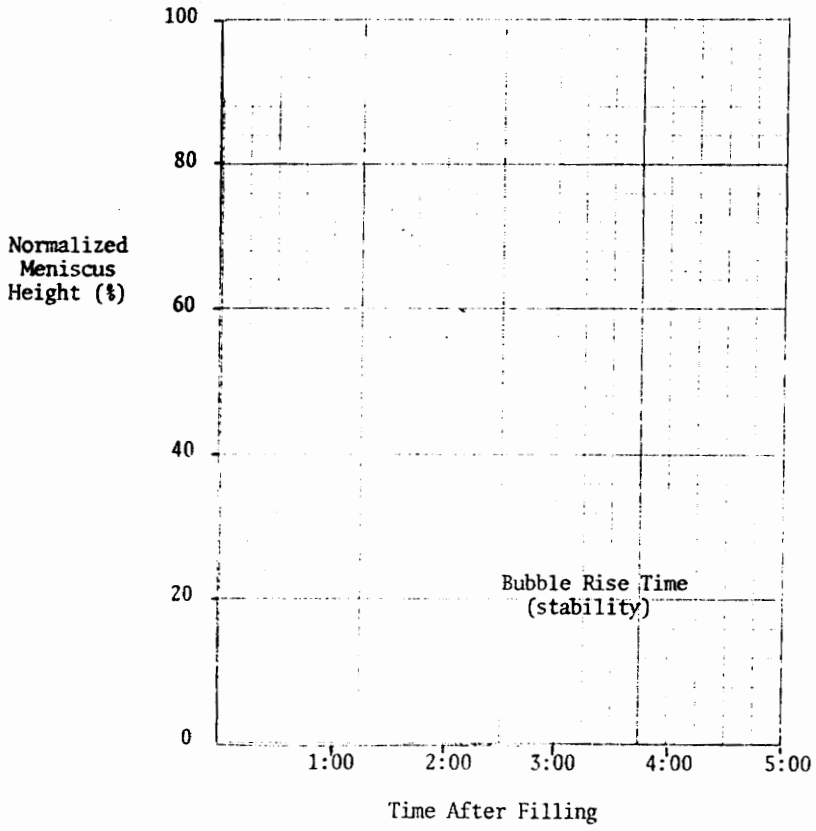

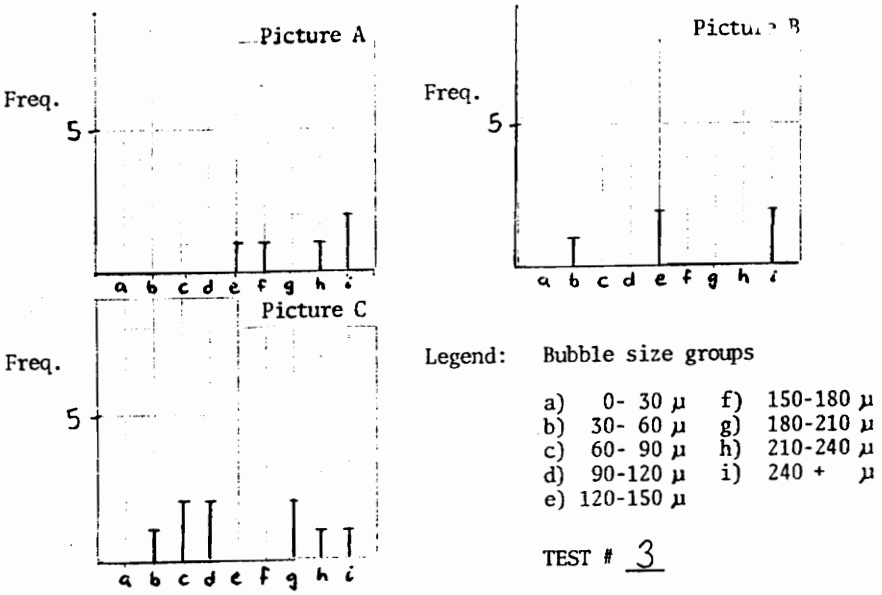

Histograms of Individual Photos

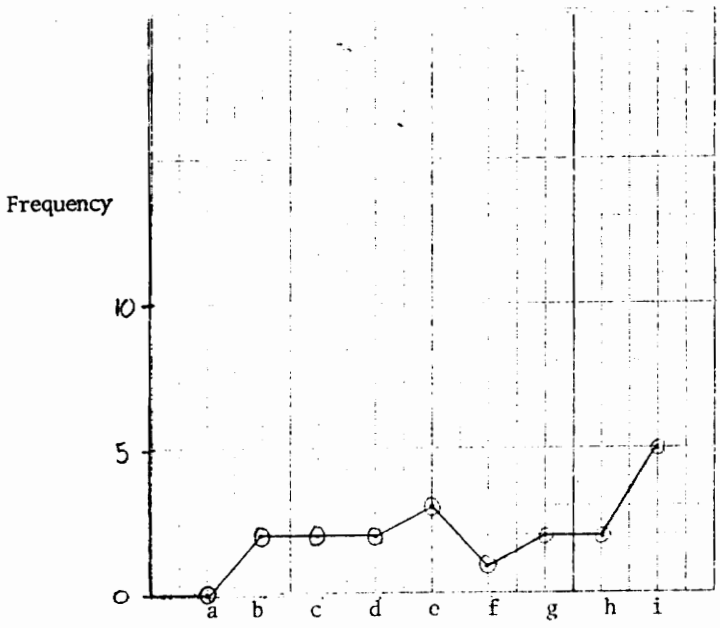

Cumulative Histogram

Data Sheets For Test # 4

Packing Diameter (mm)	: 3.0	Reynolds Number	: 428
Solution Feed Flowrate (L/min)	: 24	Pressure Drop Across Bed (psia)	: 10
Average Quality (% air)	: 53.2		
Solution Concentration (ppm)	: 500	(number of reuses: 1)	
Recycle Ratio (rec/dis)	: 0	System Pressure (psig)	: 11

Notes: No stability

Legend: O - Sample A
Δ - Sample B
□ - Sample C

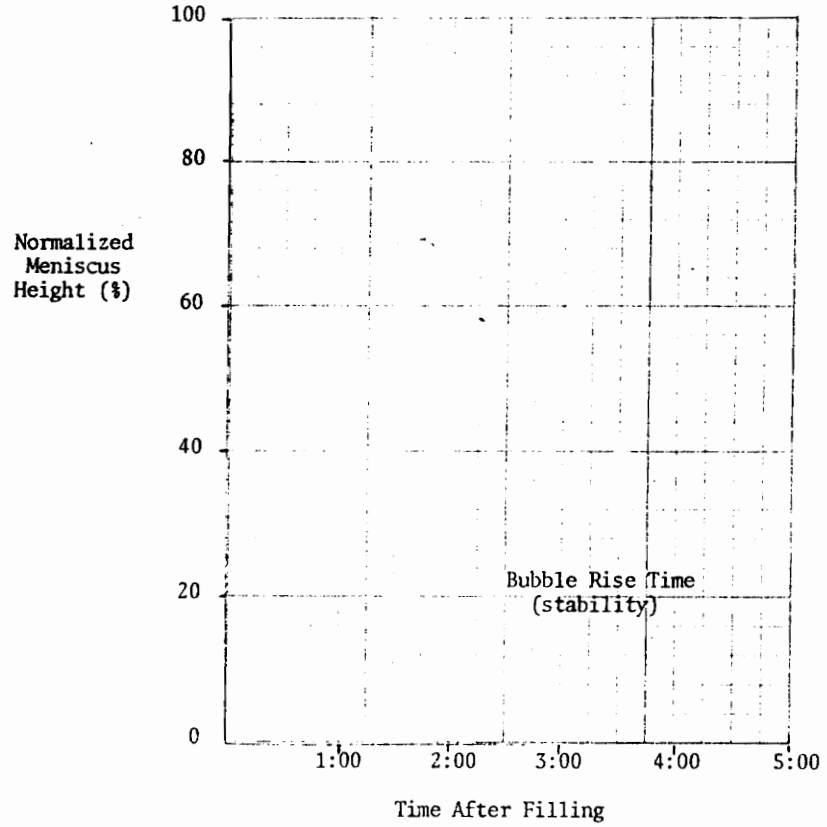

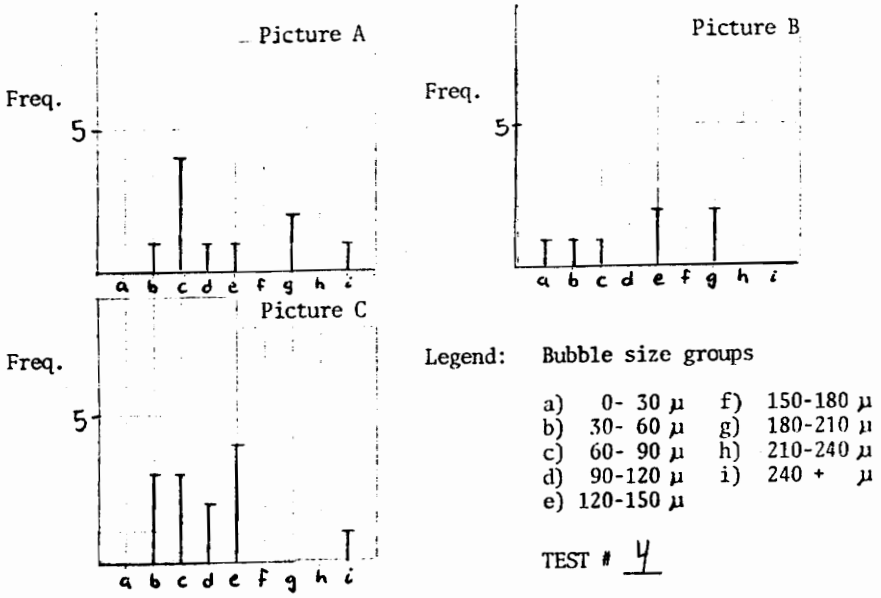

Histograms of Individual Photos

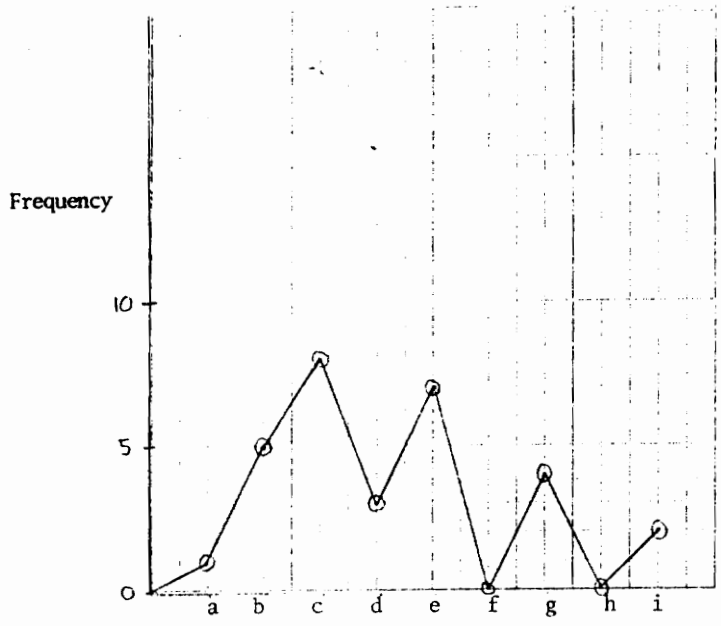

Cumulative Histogram

Data Sheets For Test # 5

Packing Diameter (mm)	:	1.5	Reynolds Number	:	107
Solution Feed Flowrate (L/min)	:	12	Pressure Drop Across Bed (psia)	:	13
Average Quality (% air)	:	65.6			
Solution Concentration (ppm)	:	500	(number of reuses: 0)		
Recycle Ratio (rec/dis)	:	0	System Pressure (psig)	:	10

Notes:

Legend: O - Sample A
Δ - Sample B
□ - Sample C

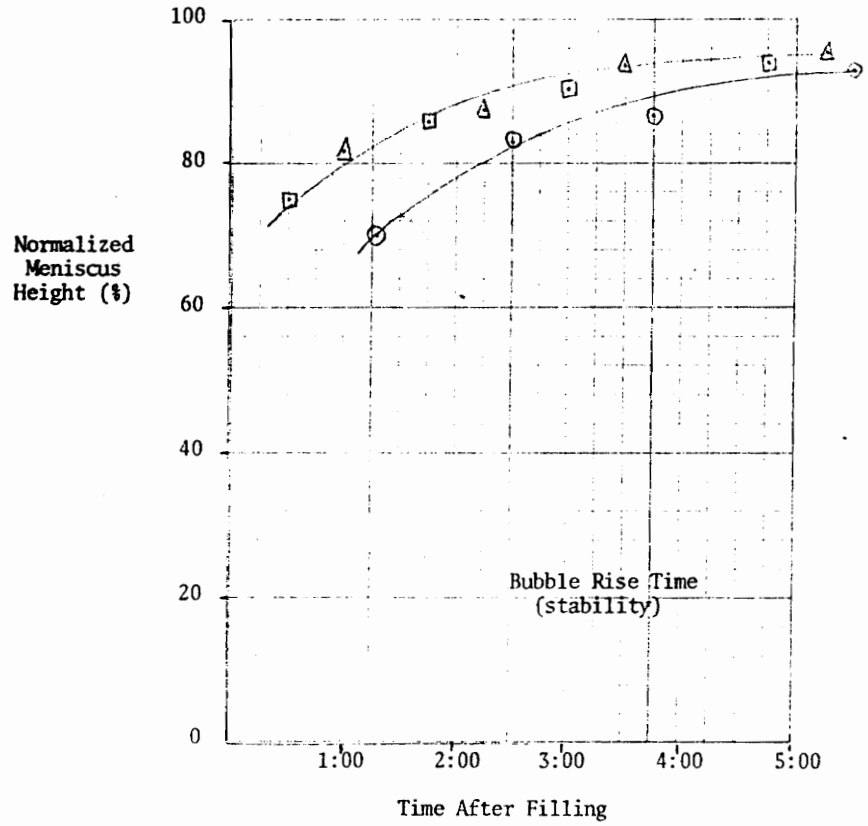

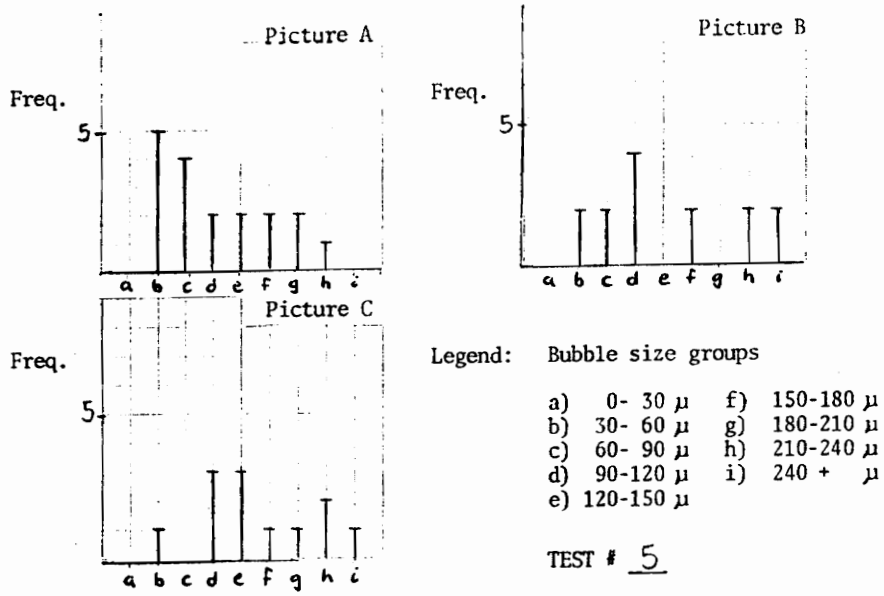

Histograms of Individual Photos

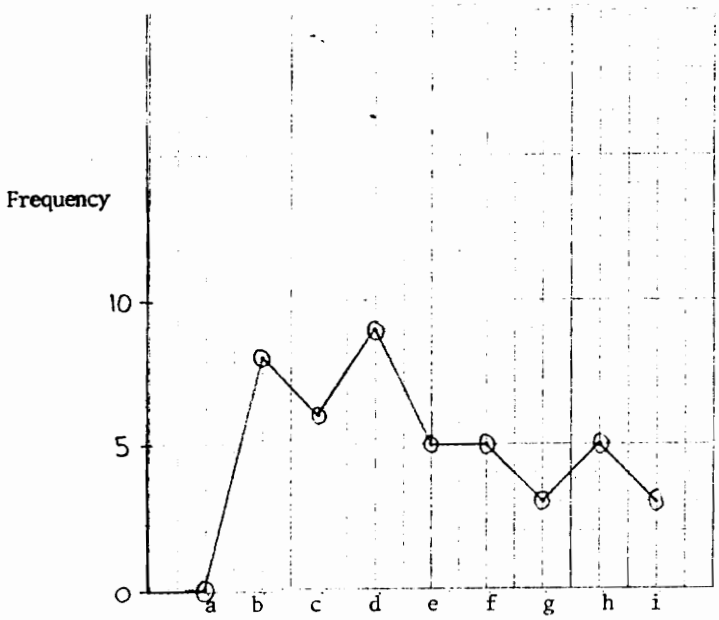

Cumulative Histogram

Data Sheets For Test # 6

Packing Diameter (mm)	:	1.5	Reynolds Number	:	143
Solution Feed Flowrate (L/min)	:	16	Pressure Drop Across Bed (psia)	:	16
Average Quality (% air)	:	62.8			
Solution Concentration (ppm)	:	500	(number of reuses: 0)		
Recycle Ratio (rec/dis)	:	0	System Pressure (psig)	:	10

Notes:

Legend: O - Sample A
Δ - Sample B
□ - Sample C

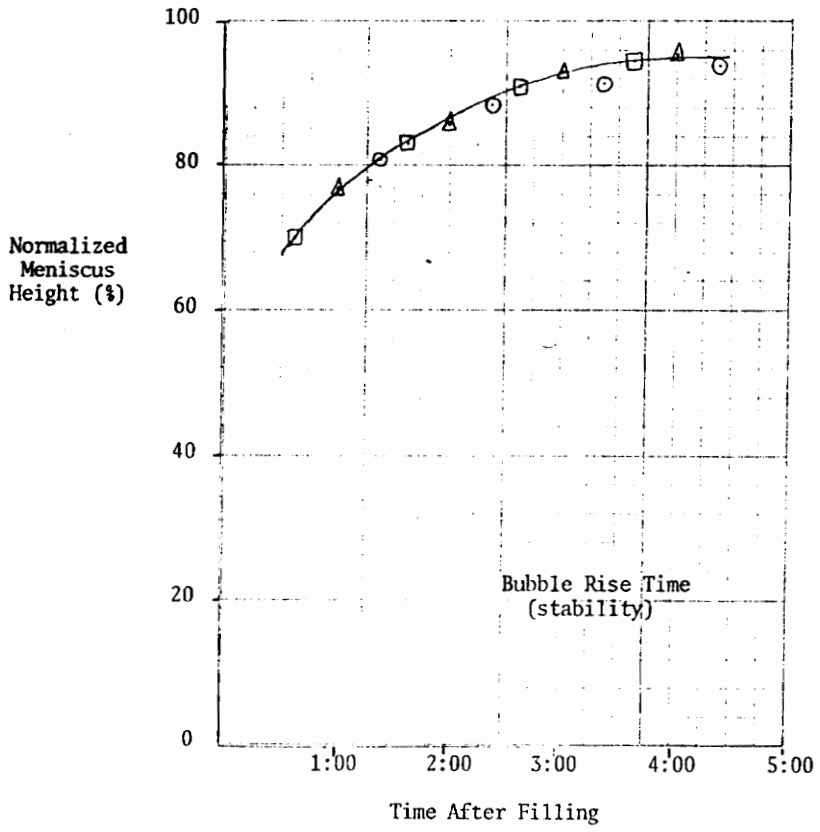

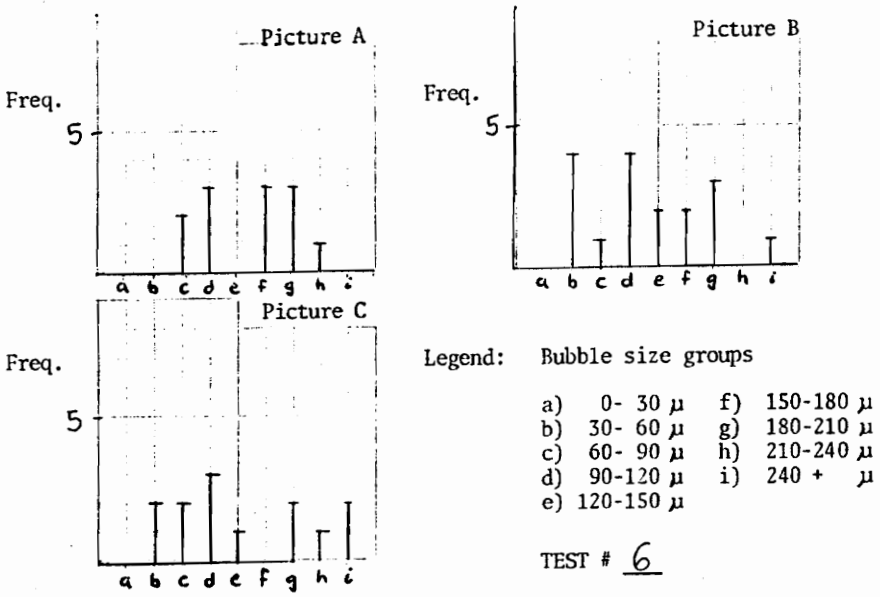

Legend: Bubble size groups

a) 0- 30 μ
b) 30- 60 μ
c) 60- 90 μ
d) 90-120 μ
e) 120-150 μ
f) 150-180 μ
g) 180-210 μ
h) 210-240 μ
i) 240 + μ

TEST # 6

Histograms of Individual Photos

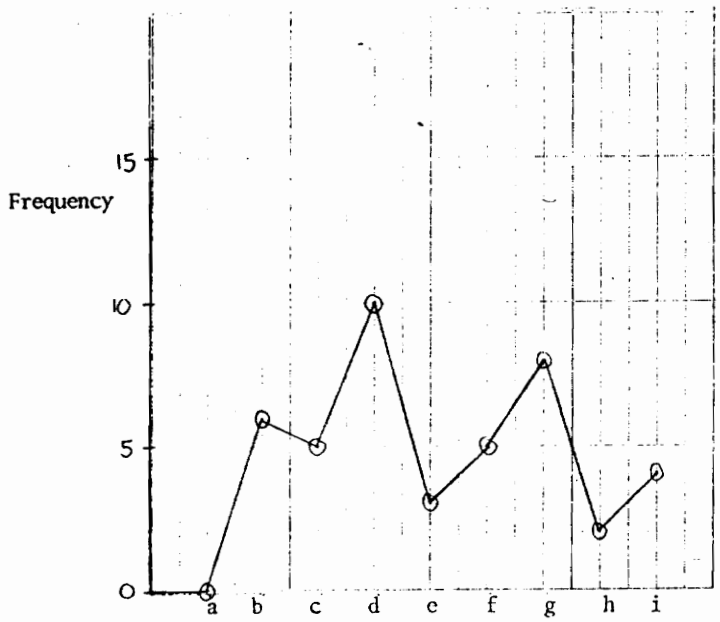

Cumulative Histogram

Data Sheets For Test # 7

Packing Diameter (mm)	: 1.5	Reynolds Number	: 179
Solution Feed Flowrate (L/min)	: 20	Pressure Drop Across Bed (psia)	: 21
Average Quality (% air)	: 61.7		
Solution Concentration (ppm)	: 500	(number of reuses: 0)	
Recycle Ratio (rec/dis)	: 0	System Pressure (psig)	: 10

Notes:

Legend: ○ - Sample A
△ - Sample B
□ - Sample C

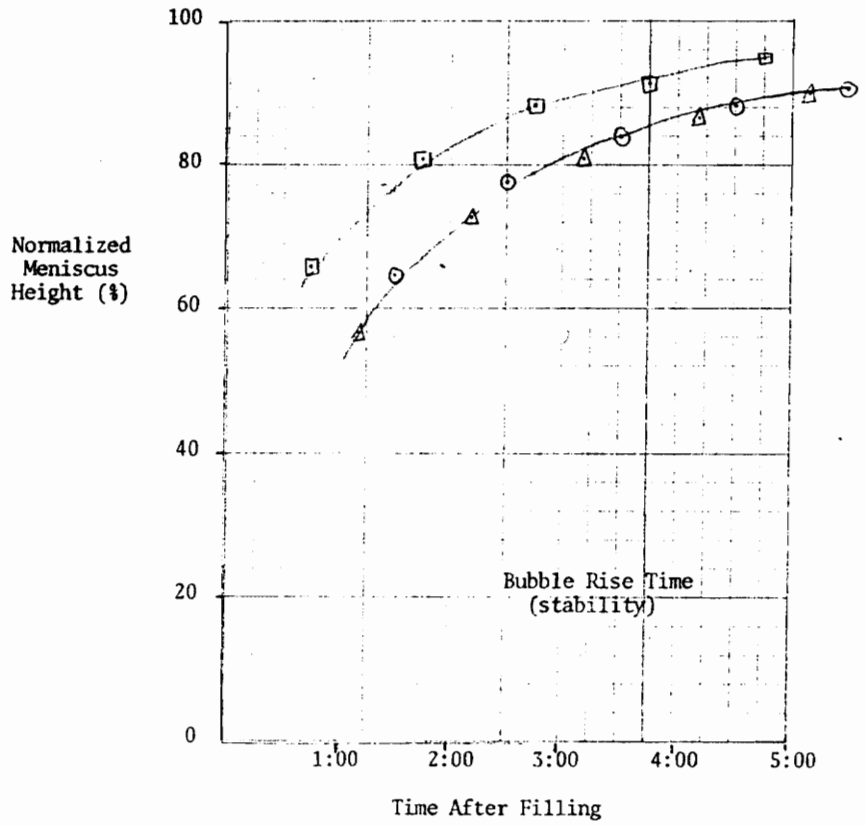

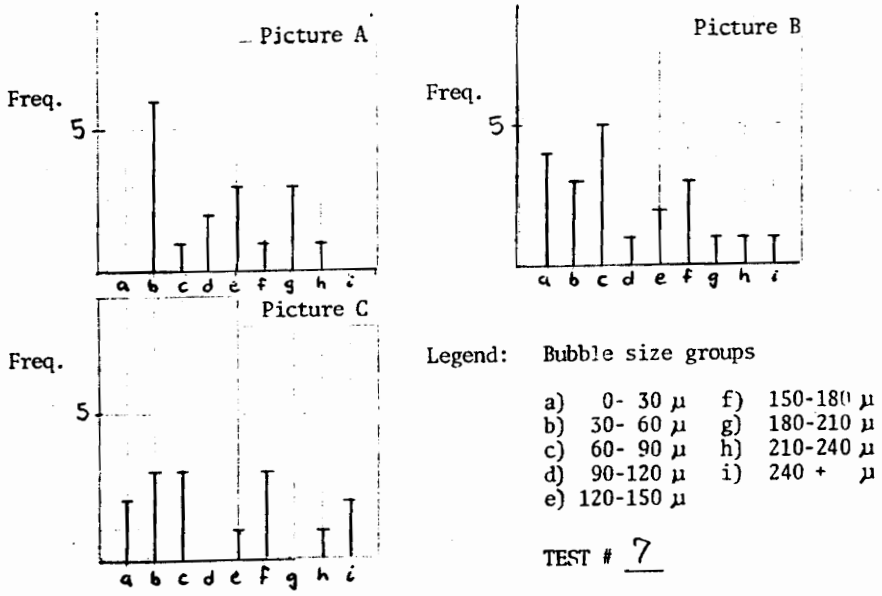

Histograms of Individual Photos

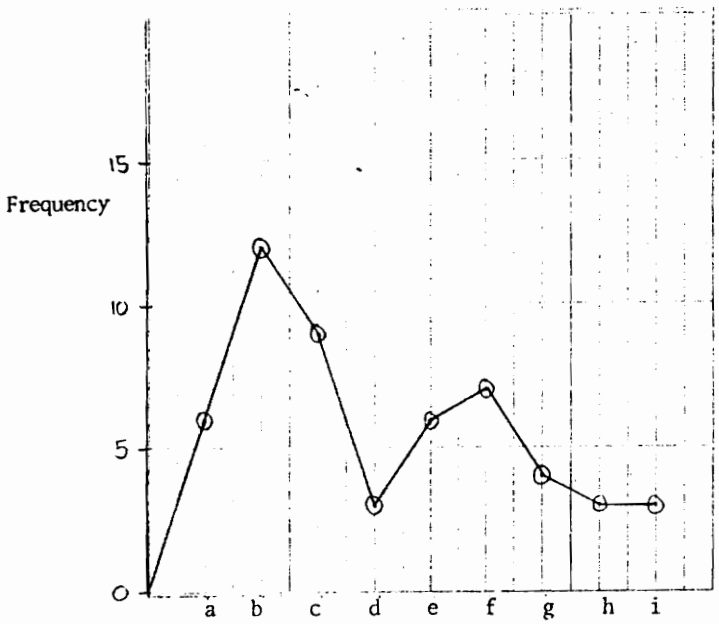

Cumulative Histogram

Data Sheets For Test # 8

Packing Diameter (mm)	: 1.5	Reynolds Number	: 215
Solution Feed Flowrate (L/min)	: 24	Pressure Drop Across Bed (psia)	: 25
Average Quality (% air)	: 62.2		
Solution Concentration (ppm)	: 500	(number of reuses: 0)	
Recycle Ratio (rec/dis)	: 0	System Pressure (psig)	: 12

Notes:

Legend: O - Sample A
△ - Sample B
□ - Sample C

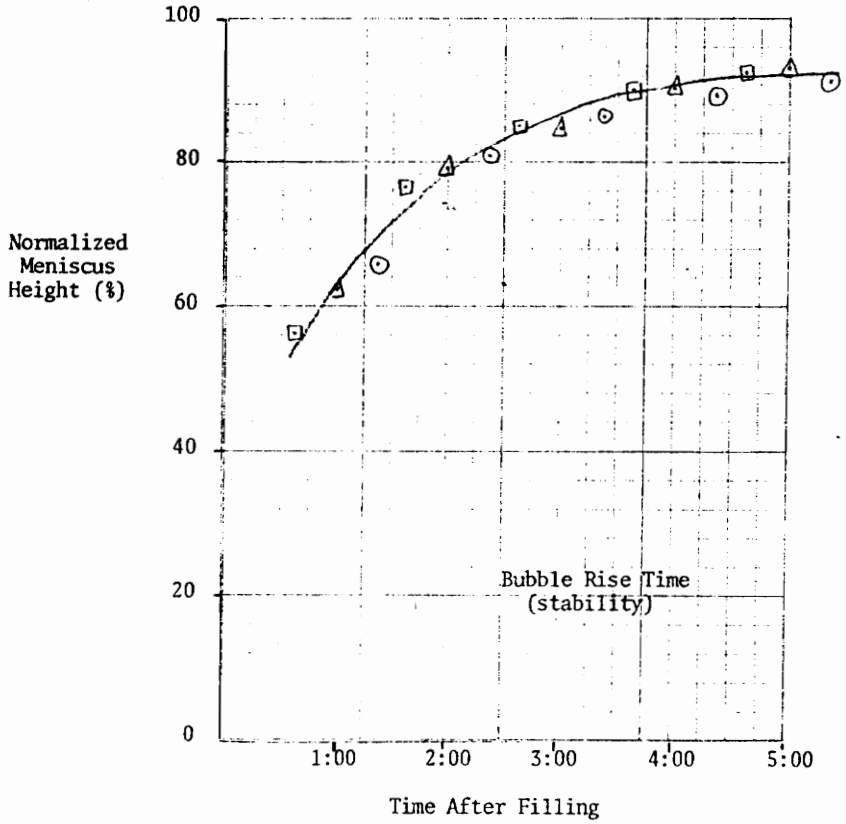

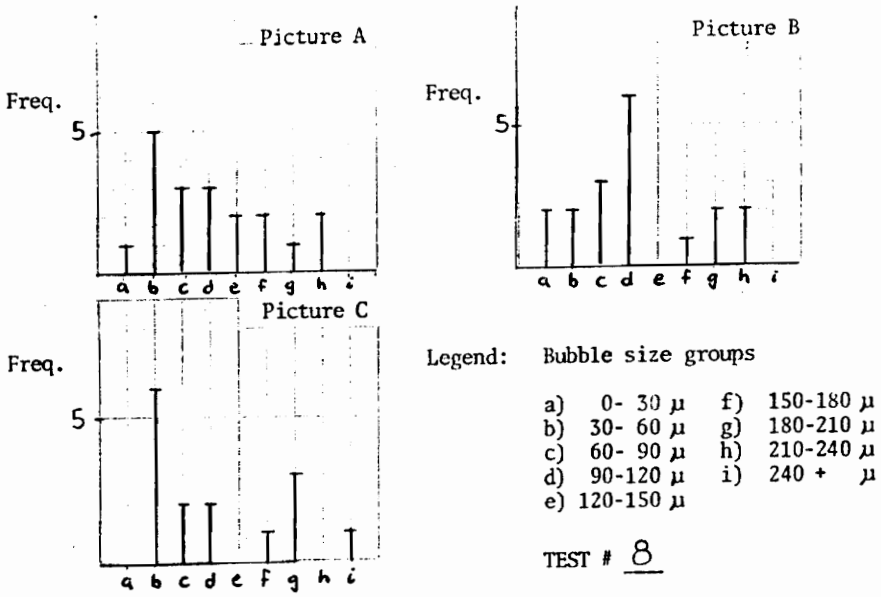

Histograms of Individual Photos

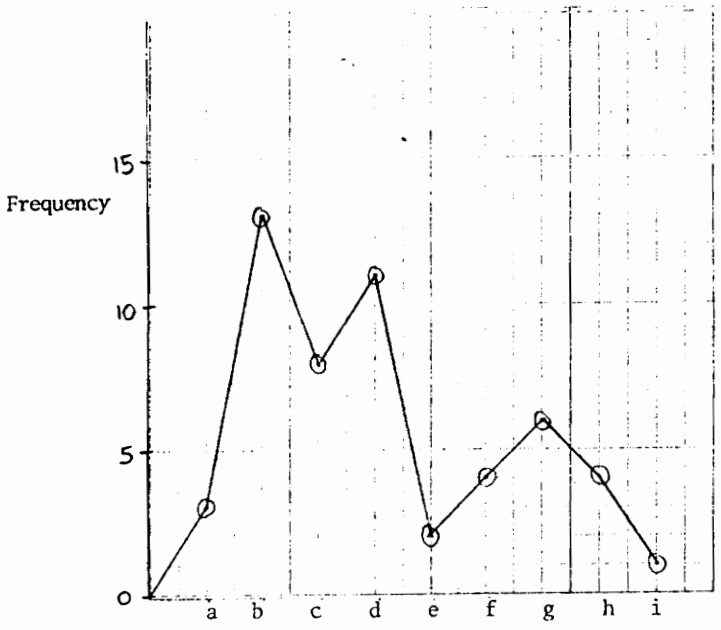

Cumulative Histogram

Data Sheets For Test # 9

Packing Diameter (mm)	:	1.5	Reynolds Number	:	107
Solution Feed Flowrate (L/min)	:	12	Pressure Drop Across Bed (psia)	:	10
Average Quality (% air)	:	52.0			
Solution Concentration (ppm)	:	500	(number of reuses: 0)		
Recycle Ratio (rec/dis)	:	0	System Pressure (psig)	:	10

Notes: No Stability

Legend: O - Sample A
Δ - Sample B
□ - Sample C

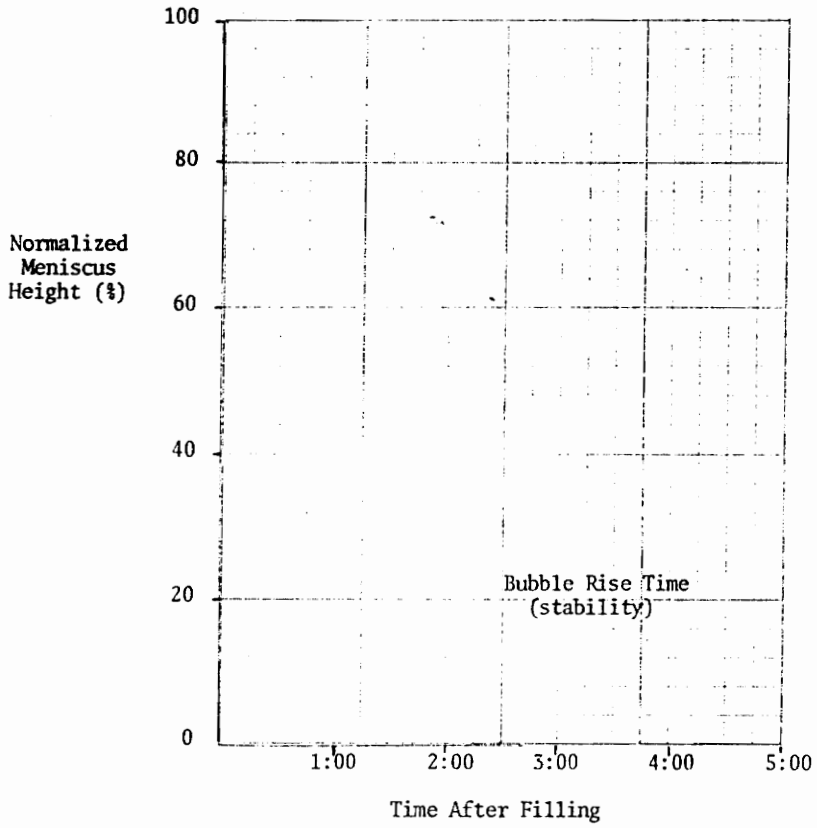

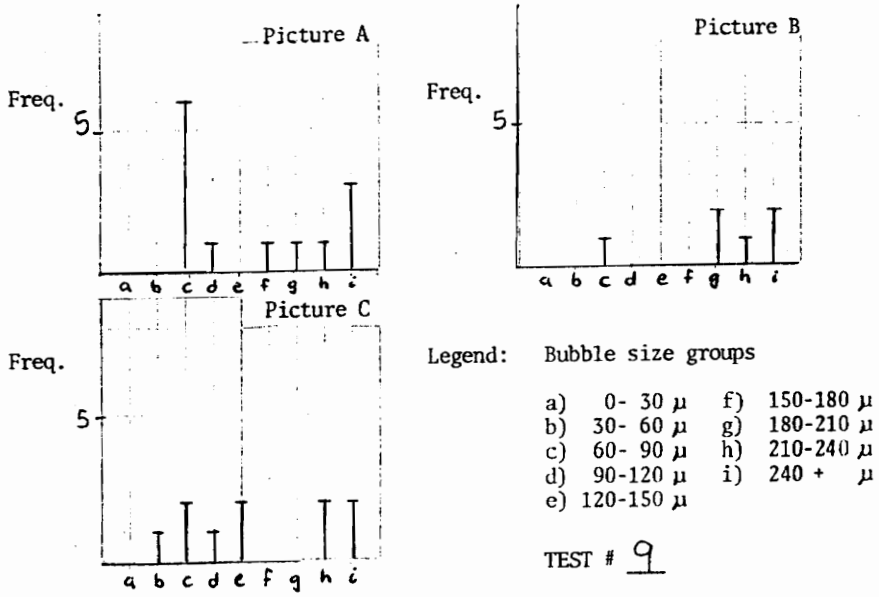

Histograms of Individual Photos

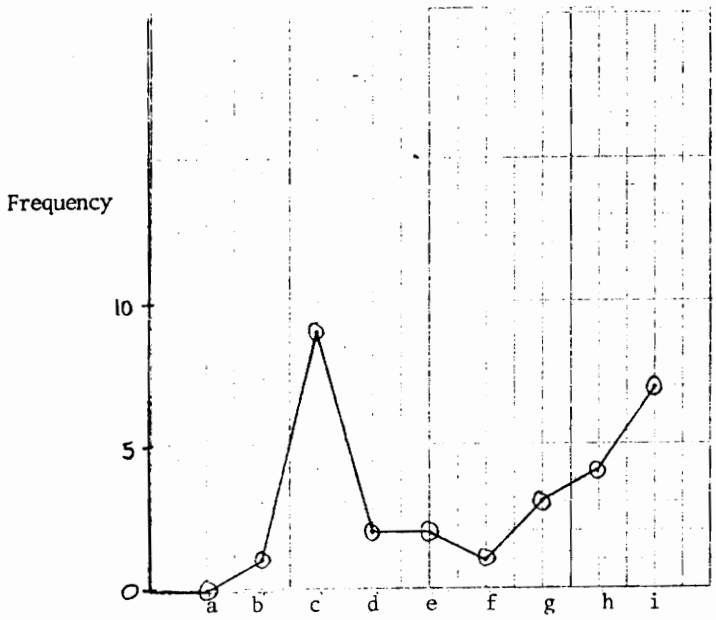

Cumulative Histogram

Data Sheets For Test # 10

Packing Diameter (mm)	:	1.5	Reynolds Number	:	107
Solution Feed Flowrate (L/min)	:	12	Pressure Drop Across Bed (psia)	:	16
Average Quality (% air)	:	70.7			
Solution Concentration (ppm)	:	500	(number of reuses: 1)		
Recycle Ratio (rec/dis)	:	0	System Pressure (psig)	:	10

Notes:

Legend: O - Sample A
Δ - Sample B
□ - Sample C

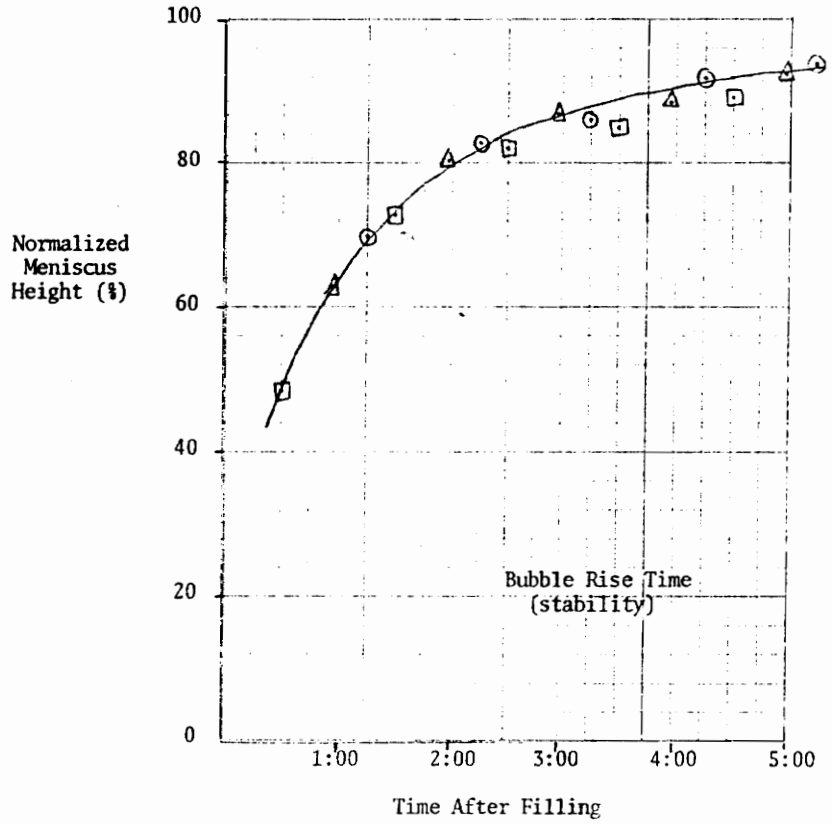

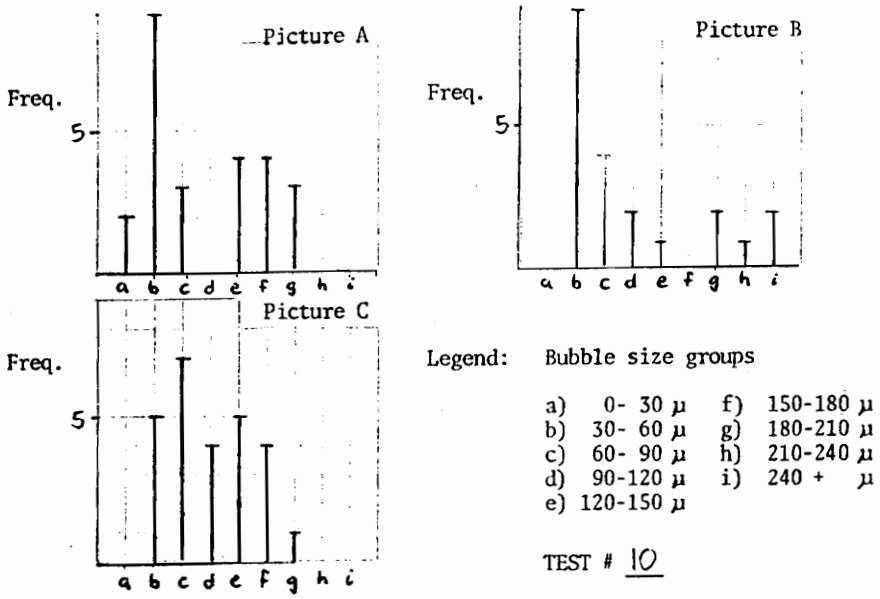

Legend: Bubble size groups

a) 0- 30 μ
b) 30- 60 μ
c) 60- 90 μ
d) 90-120 μ
e) 120-150 μ
f) 150-180 μ
g) 180-210 μ
h) 210-240 μ
i) 240 + μ

TEST # 10

Histograms of Individual Photos

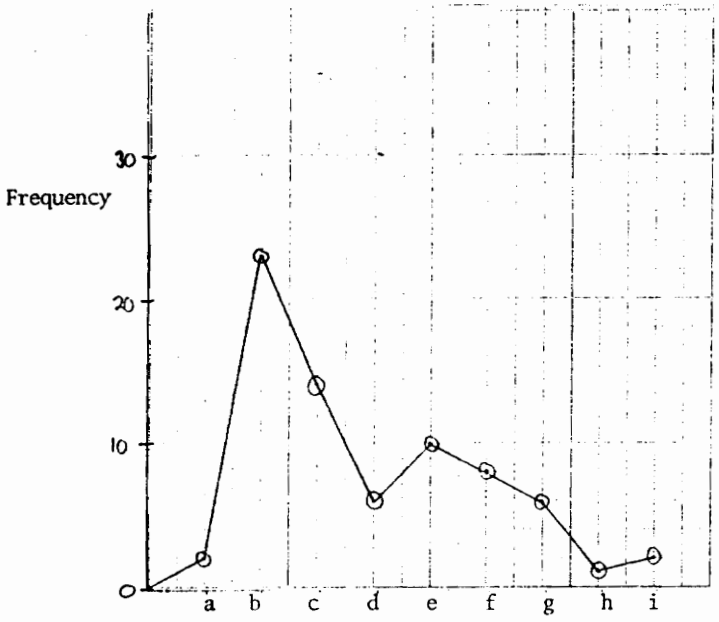

Cumulative Histogram

Data Sheets For Test # 11

Packing Diameter (mm)	:	1.5	Reynolds Number	:	179
Solution Feed Flowrate (L/min)	:	20	Pressure Drop Across Bed (psia)	:	17
Average Quality (% air)	:	53.6			
Solution Concentration (ppm)	:	500	(number of reuses: 1)		
Recycle Ratio (rec/dis)	:	0	System Pressure (psig)	:	10

Notes:

Legend: O - Sample A
Δ - Sample B
□ - Sample C

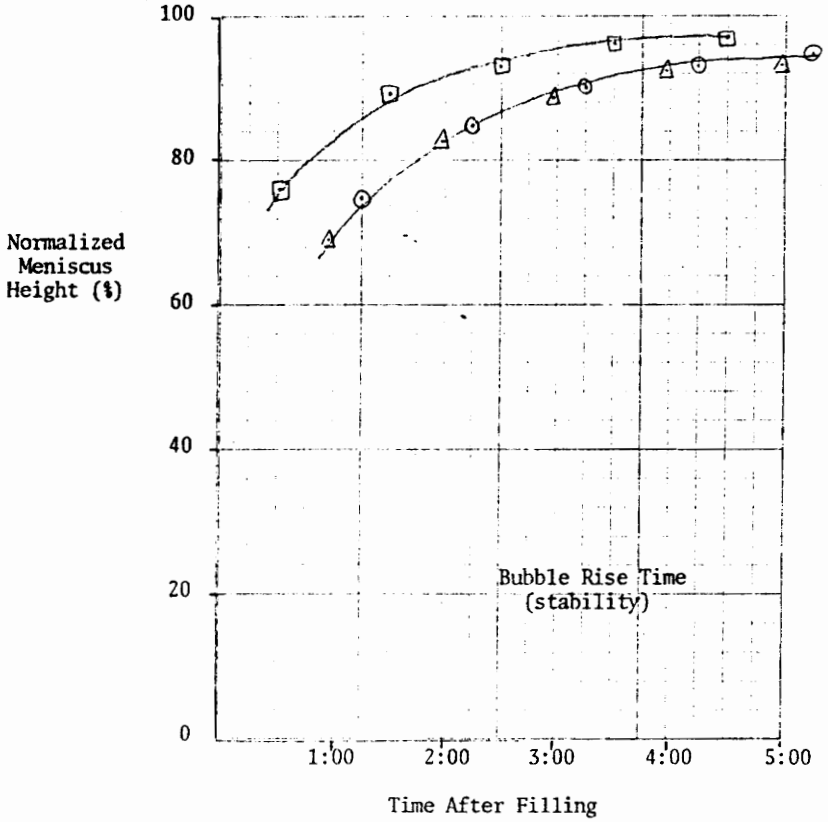

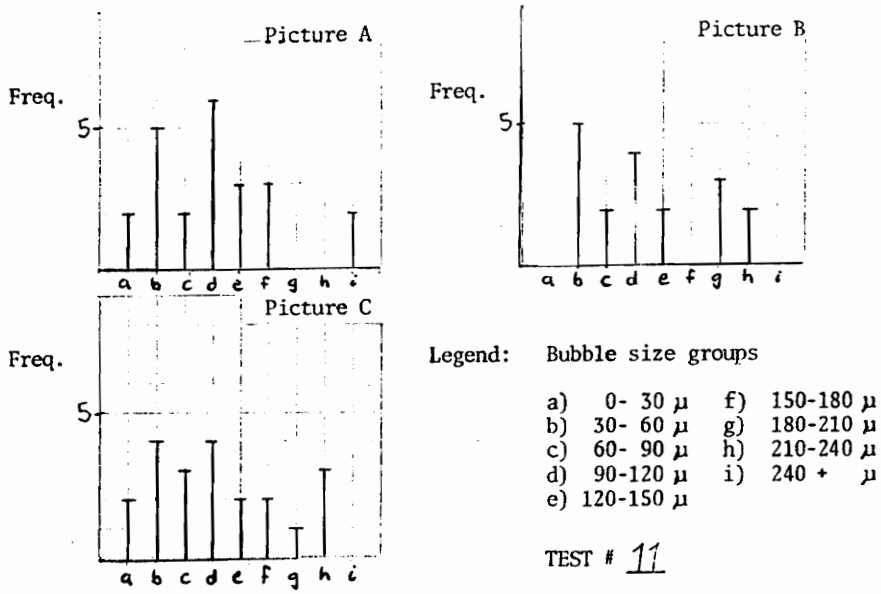

Legend: Bubble size groups

a) 0- 30 μ
b) 30- 60 μ
c) 60- 90 μ
d) 90-120 μ
e) 120-150 μ
f) 150-180 μ
g) 180-210 μ
h) 210-240 μ
i) 240 + μ

TEST # 11

Histograms of Individual Photos

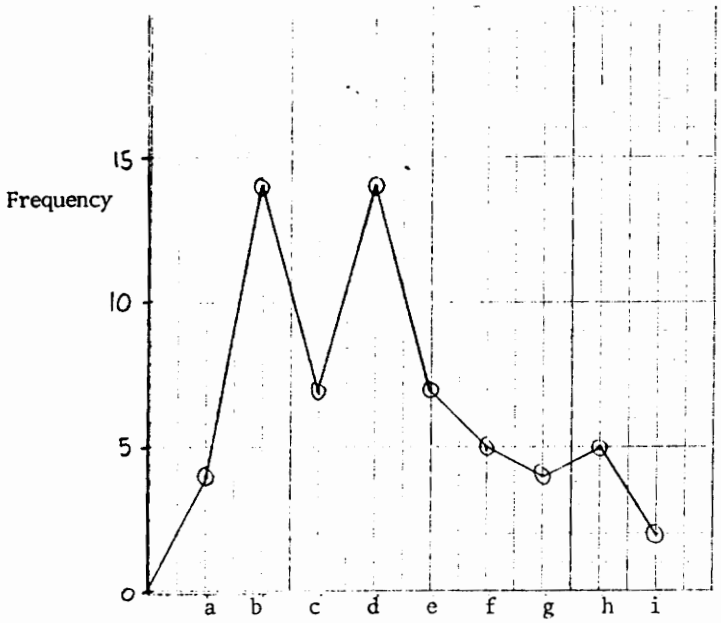

Cumulative Histogram

Data Sheets For Test # 12

Packing Diameter (mm)	:	1.5	Reynolds Number	:	179
Solution Feed Flowrate (L/min)	:	20	Pressure Drop Across Bed (psia)	:	24
Average Quality (% air)	:	72.3			
Solution Concentration (ppm)	:	500	(number of reuses: 1)		
Recycle Ratio (rec/dis)	:	0	System Pressure (psig)	:	13

Notes:

Legend: ○ - Sample A
△ - Sample B
□ - Sample C

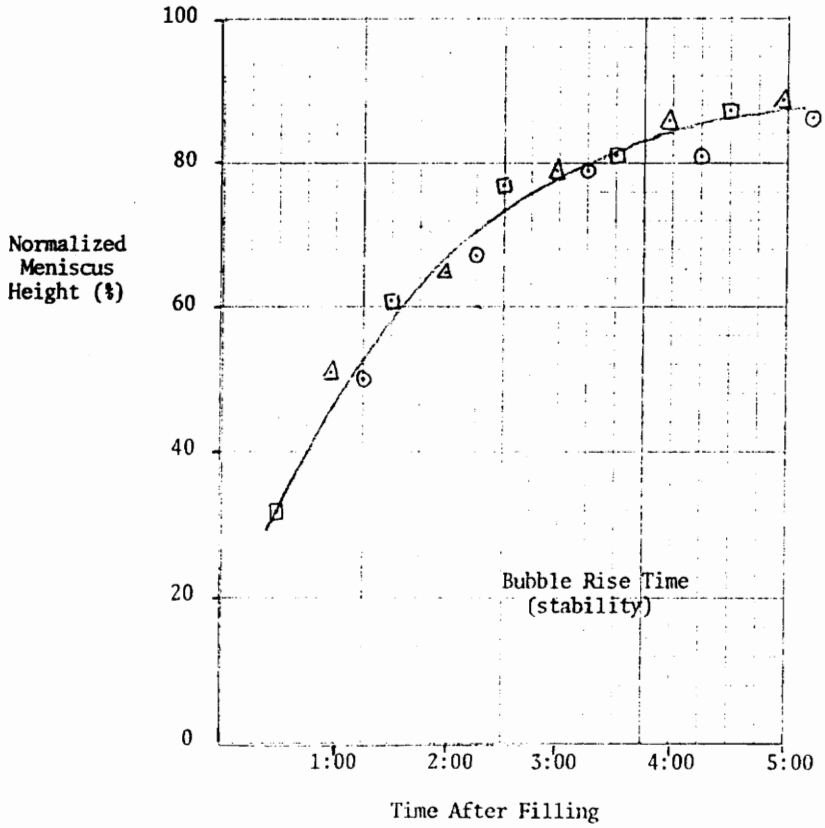

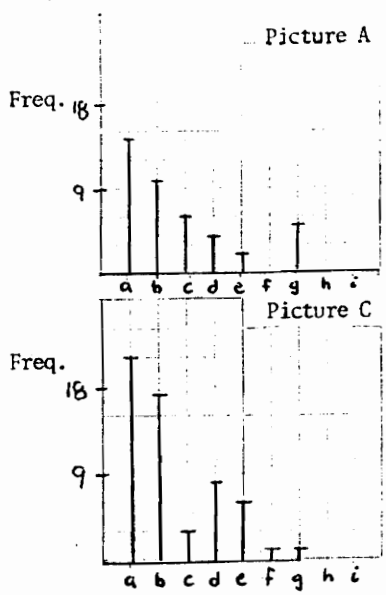

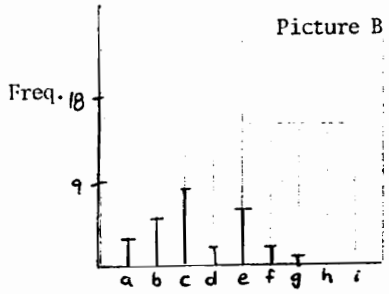

Legend: Bubble size groups

a)	0- 30 μ	f)	150-180 μ
b)	30- 60 μ	g)	180-210 μ
c)	60- 90 μ	h)	210-240 μ
d)	90-120 μ	i)	240 + μ
e)	120-150 μ		

TEST # 12

Histograms of Individual Photos

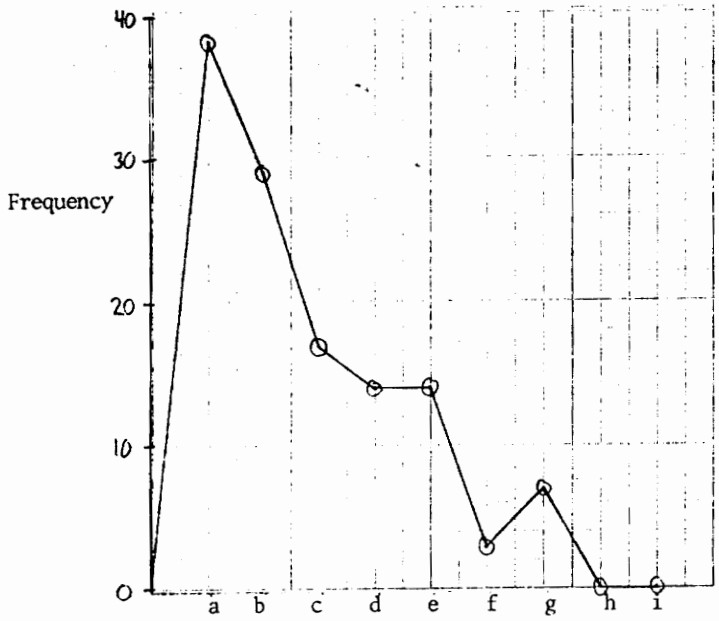

Cumulative Histogram

Data Sheets For Test # 13

Packing Diameter (mm)	: 1.5	Reynolds Number	: 143
Solution Feed Flowrate (L/min)	: 16	Pressure Drop Across Bed (psia)	: 18
Average Quality (% air)	: 67.9		
Solution Concentration (ppm)	: 500	(number of reuses: 1)	
Recycle Ratio (rec/dis)	: 0	System Pressure (psig)	: 10

Notes:

Legend: ○ - Sample A
△ - Sample B
□ - Sample C

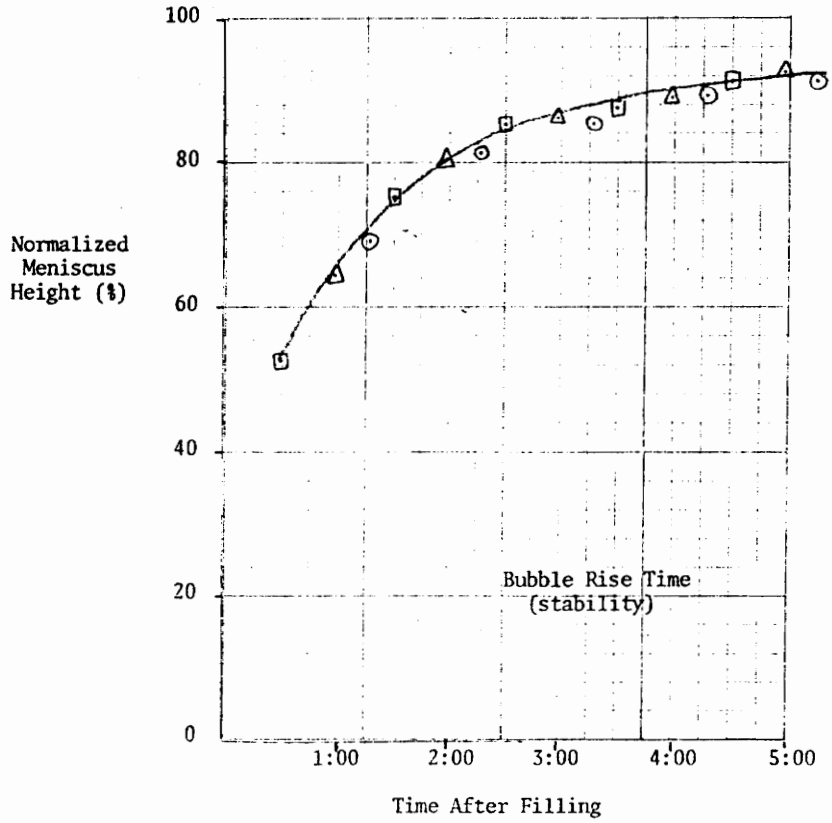

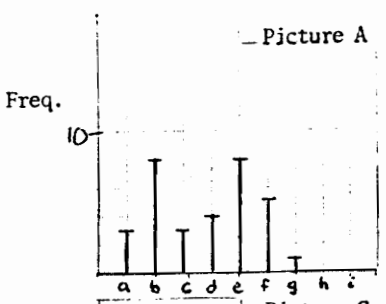

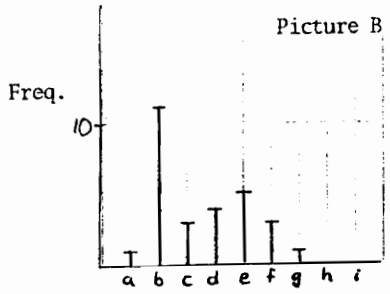

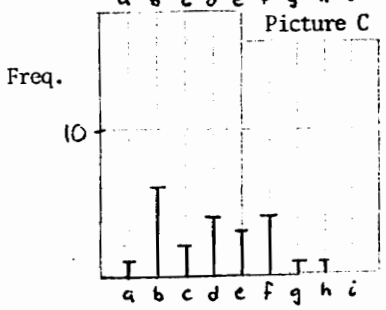

Legend: Bubble size groups

a)	0- 30 μ	f)	150-180 μ
b)	30- 60 μ	g)	180-210 μ
c)	60- 90 μ	h)	210-240 μ
d)	90-120 μ	i)	240 + μ
e)	120-150 μ		

TEST # 13

Histograms of Individual Photos

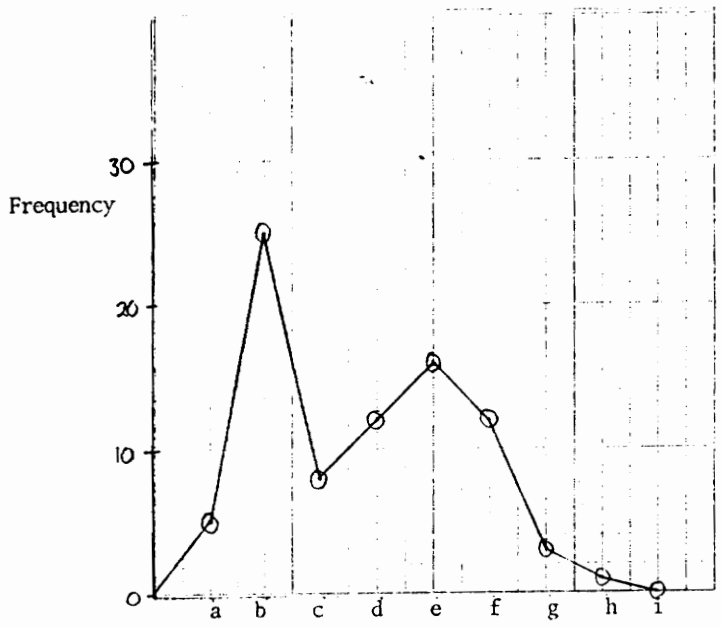

Cumulative Histogram

Data Sheets For Test # 14

Packing Diameter (mm)	: 1.5	Reynolds Number	: 143
Solution Feed Flowrate (L/min)	: 16	Pressure Drop Across Bed (psia)	: 18
Average Quality (% air)	: 67.2		
Solution Concentration (ppm)	: 100	(number of reuses: 0)	
Recycle Ratio (rec/dis)	: 0	System Pressure (psig)	: 10

Notes:

Legend: O - Sample A
Δ - Sample B
□ - Sample C

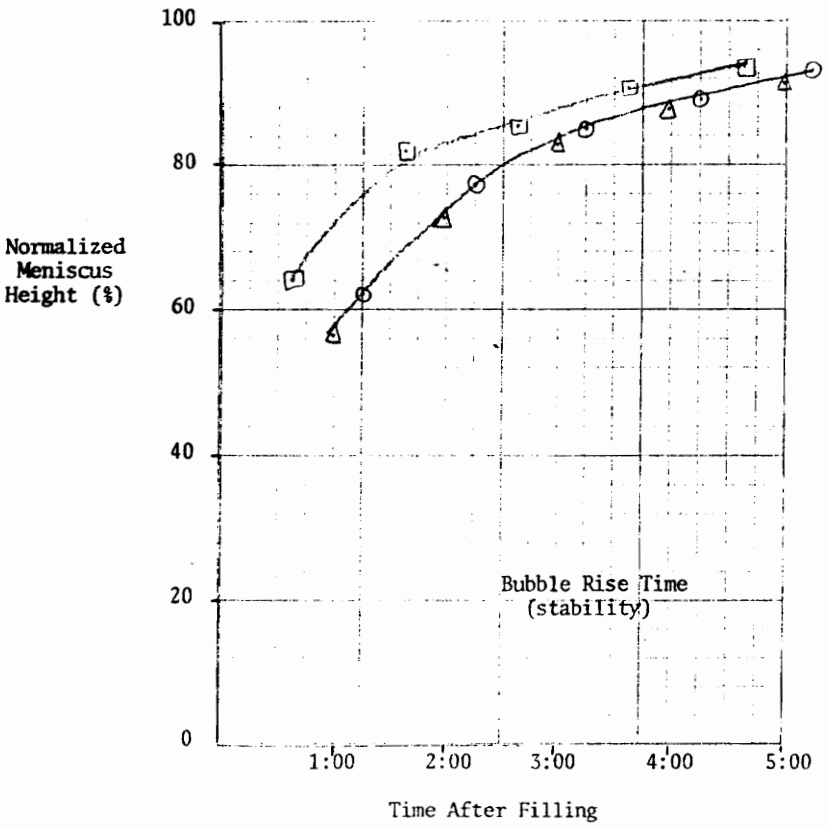

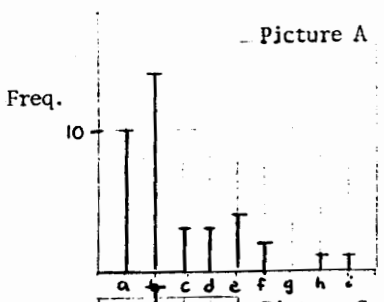

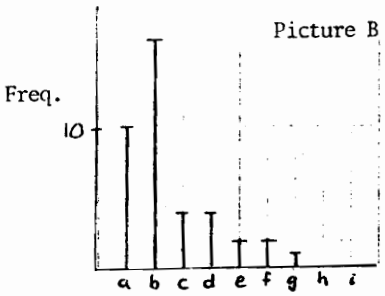

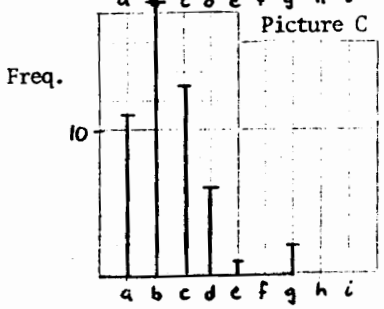

Legend: Bubble size groups

a)	0- 30 μ	f)	150-180 μ
b)	30- 60 μ	g)	180-210 μ
c)	60- 90 μ	h)	210-240 μ
d)	90-120 μ	i)	240 + μ
e)	120-150 μ		

TEST # 14

Histograms of Individual Photos

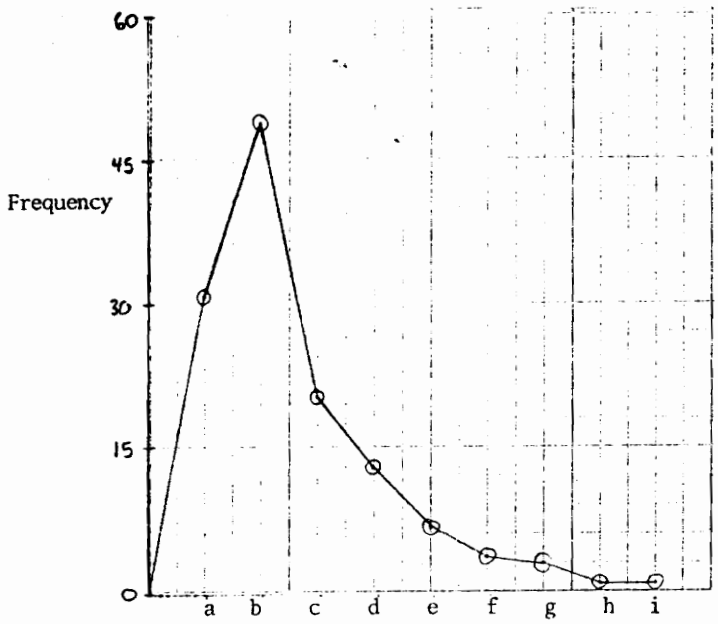

Cumulative Histogram

Data Sheets For Test # 15

Packing Diameter (mm)	:	1.5	Reynolds Number	:	143
Solution Feed Flowrate (L/min)	:	16	Pressure Drop Across Bed (psia)	:	15
Average Quality (% air)	:	68.9			
Solution Concentration (ppm)	:	300	(number of reuses: 0)		
Recycle Ratio (rec/dis)	:	0	System Pressure (psig)	:	16

Notes:

Legend: ○ - Sample A
△ - Sample B
□ - Sample C

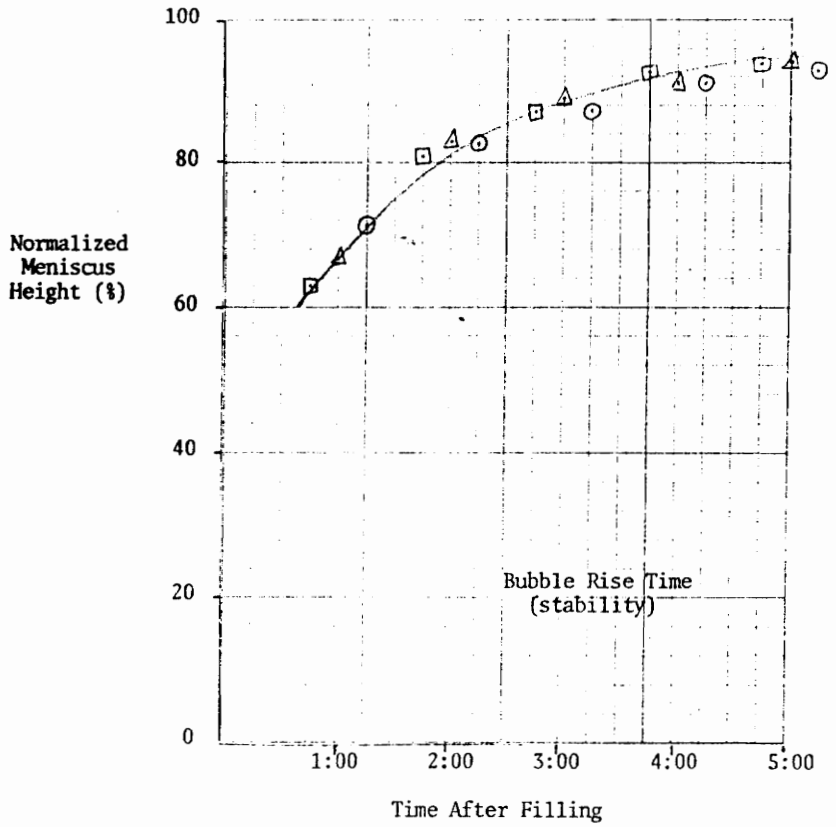

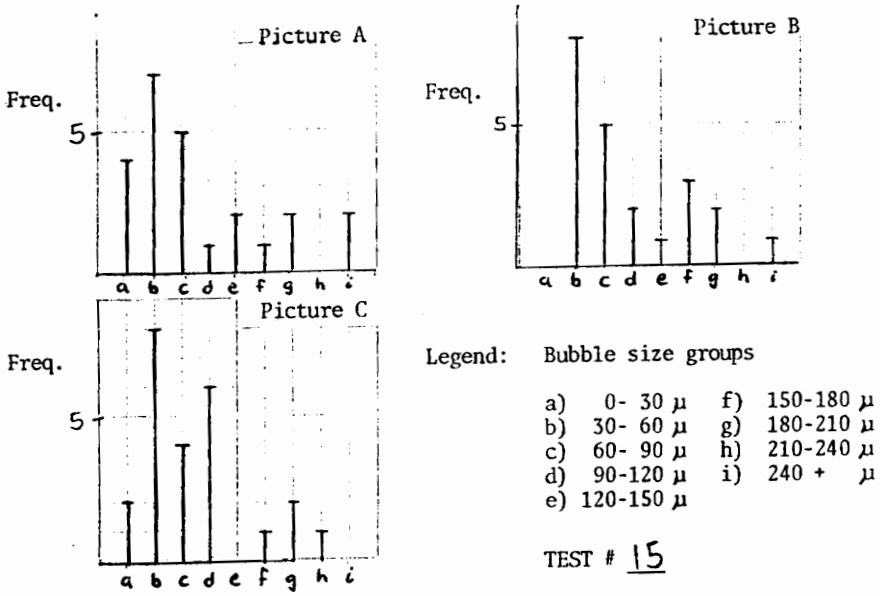

Legend: Bubble size groups

a) 0- 30 μ
b) 30- 60 μ
c) 60- 90 μ
d) 90-120 μ
e) 120-150 μ
f) 150-180 μ
g) 180-210 μ
h) 210-240 μ
i) 240 + μ

TEST # 15

Histograms of Individual Photos

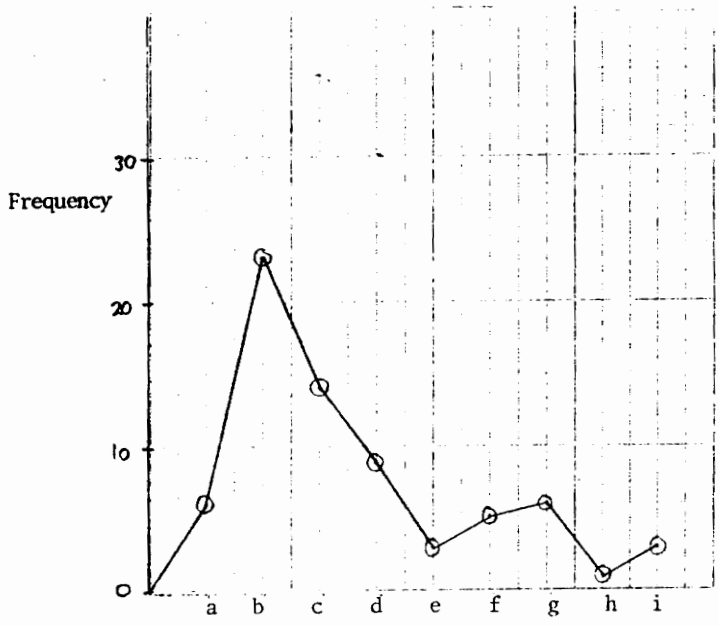

Cumulative Histogram

Data Sheets For Test # 16

Packing Diameter (mm)	: 1.5	Reynolds Number	: 143
Solution Feed Flowrate (L/min)	: 16	Pressure Drop Across Bed (psia)	: 18
Average Quality (% air)	: 65.8		
Solution Concentration (ppm)	: 70	(number of reuses: 0)	
Recycle Ratio (rec/dis)	: 0	System Pressure (psig)	: 10

Notes: Poor bubble stability

Legend: O - Sample A
Δ - Sample B
□ - Sample C

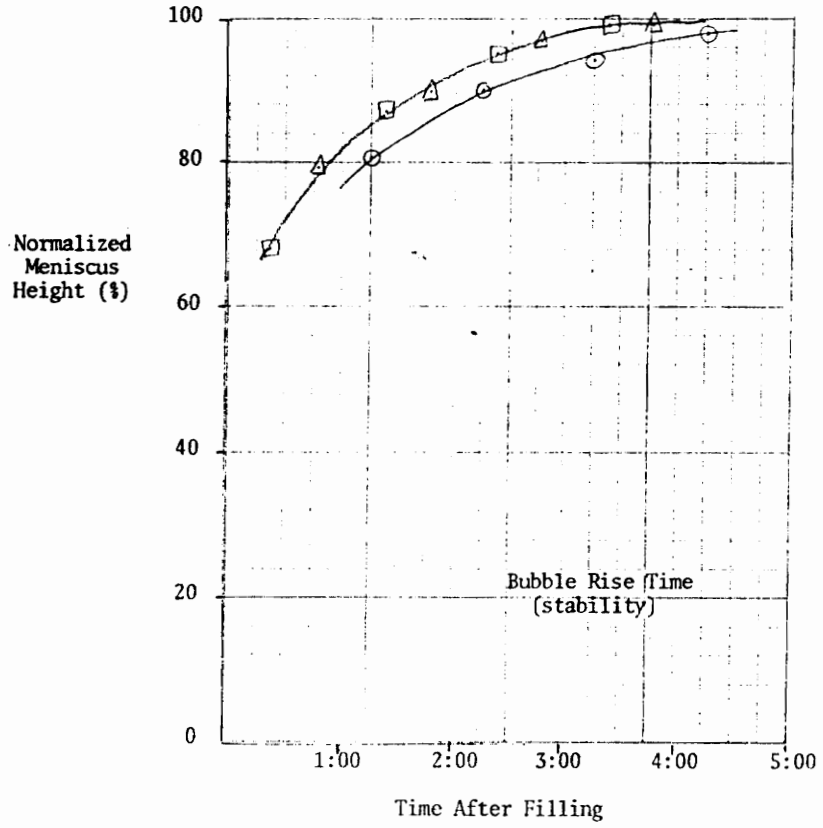

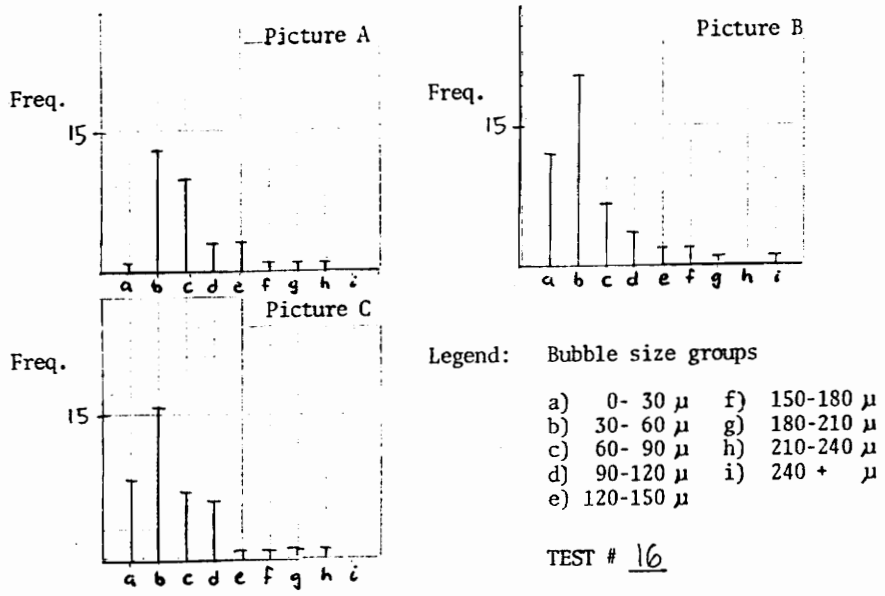

Histograms of Individual Photos

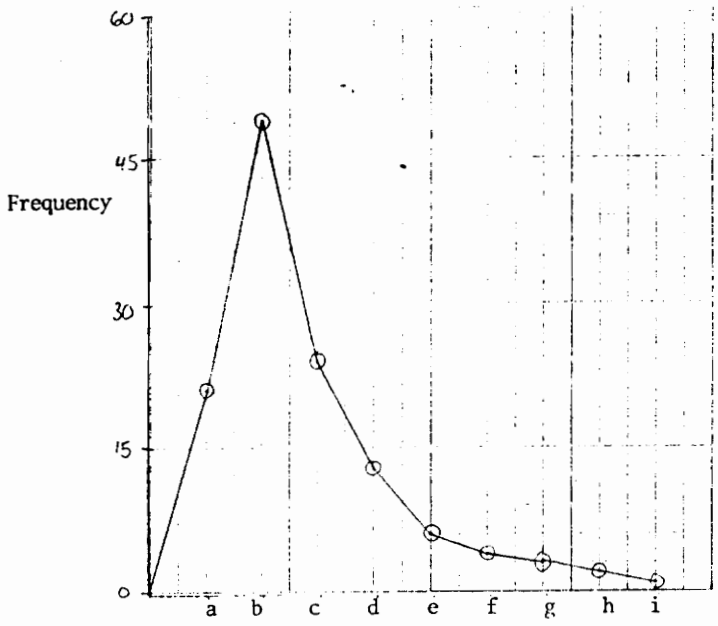

Cumulative Histogram

Data Sheets For Test # 17

Packing Diameter (mm)	:	1.5	Reynolds Number	:	143
Solution Feed Flowrate (L/min)	:	16	Pressure Drop Across Bed (psia)	:	18
Average Quality (% air)	:	66.5			
Solution Concentration (ppm)	:	50	(number of reuses: 0)		
Recycle Ratio (rec/dis)	:	0	System Pressure (psig)	:	10

Notes: No stability

Legend: O - Sample A
Δ - Sample B
□ - Sample C

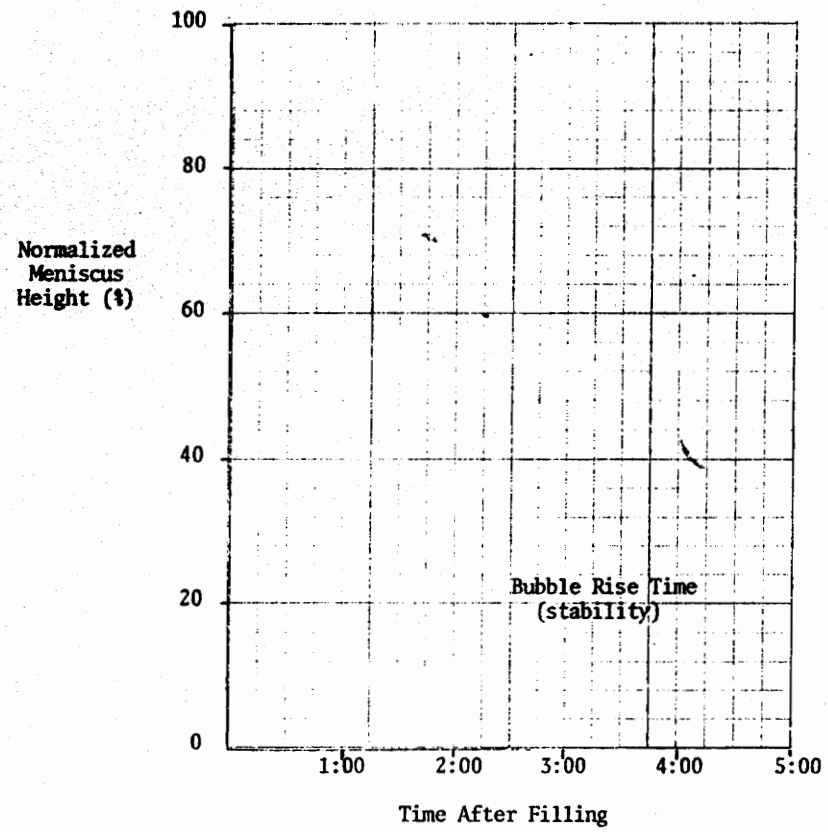

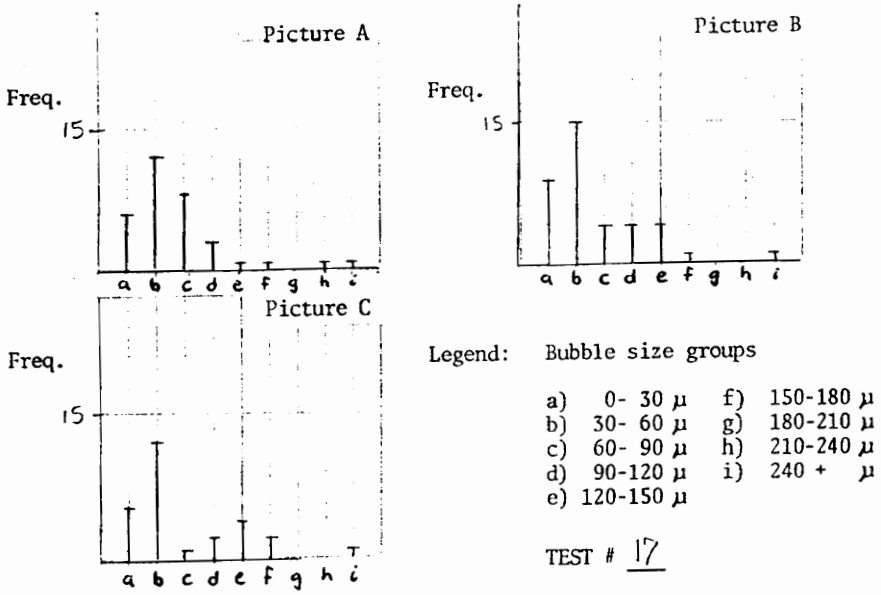

Histograms of Individual Photos

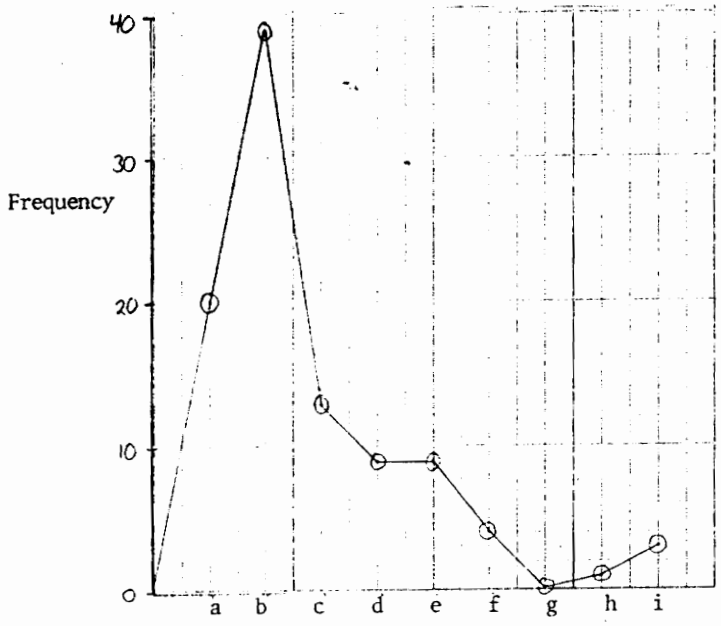

Cumulative Histogram

Data Sheets For Test # 18

Packing Diameter (mm)	: 3.0	Reynolds Number	: 385
Solution Feed Flowrate (L/min)	: 20	Pressure Drop Across Bed (psia)	: 8
Average Quality (% air)	: 71.3		
Solution Concentration (ppm)	: 500	(number of reuses: 0)	
Recycle Ratio (rec/dis)	: .079	System Pressure (psig)	: 16

Notes:

Legend: ○ - Sample A
△ - Sample B
□ - Sample C

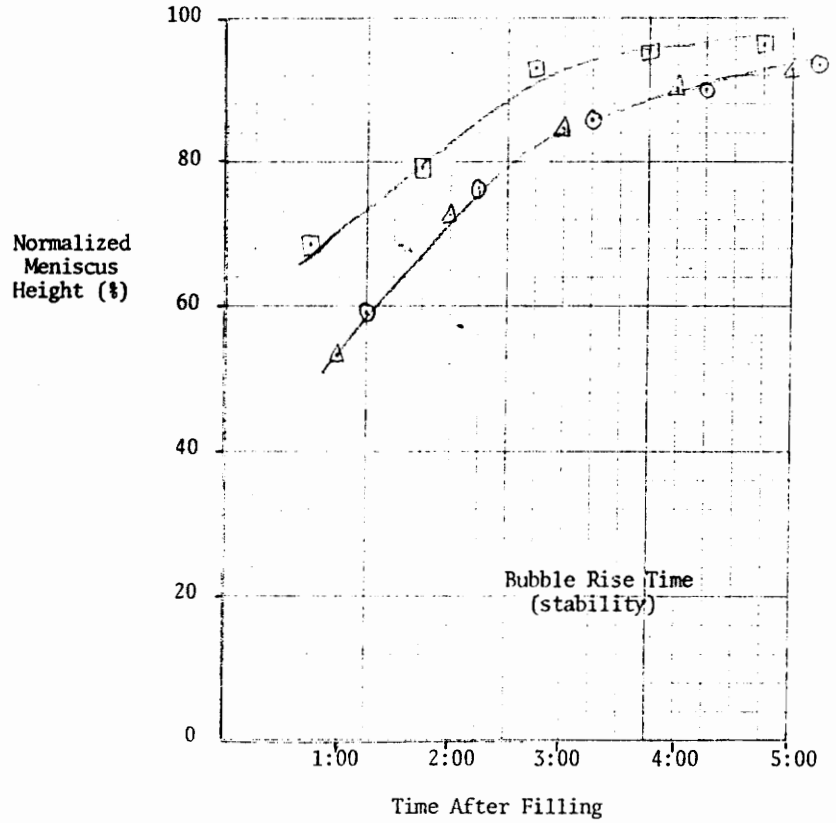

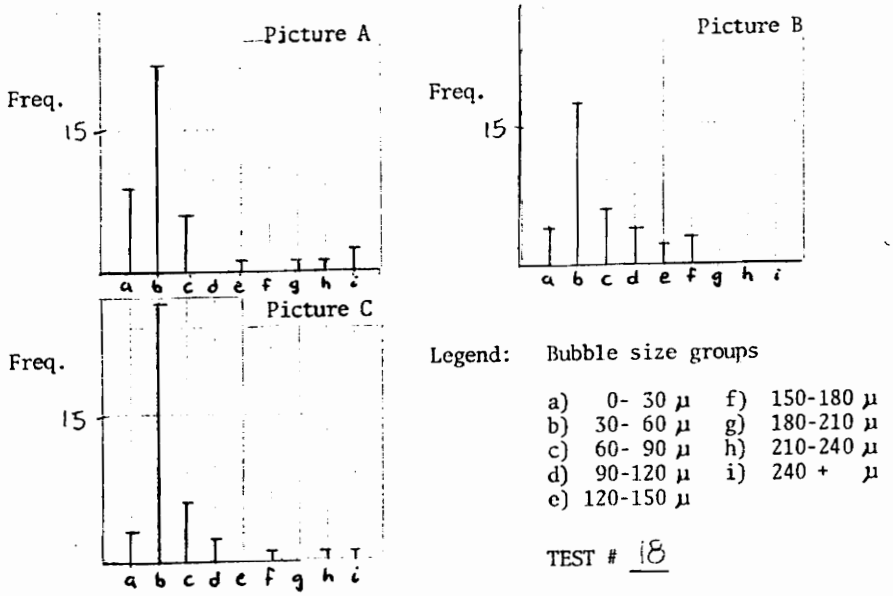

Histograms of Individual Photos

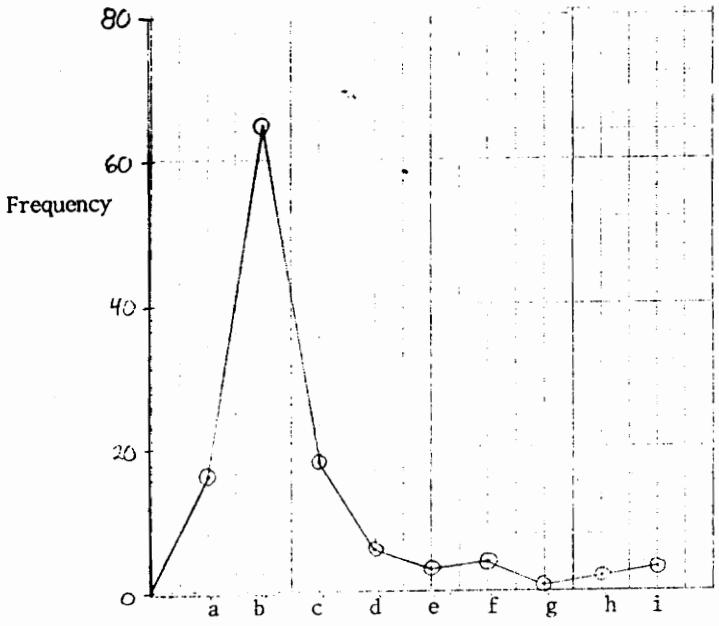

Cumulative Histogram

Data Sheets For Test # 19

Packing Diameter (mm)	: 3.0	Reynolds Number	: 417
Solution Feed Flowrate (L/min)	: 20	Pressure Drop Across Bed (psia)	: 8
Average Quality (% air)	: 68.4		
Solution Concentration (ppm)	: 500	(number of reuses: 0)	
Recycle Ratio (rec/dis)	: .17	System Pressure (psig)	: 16

Notes:

Legend: O - Sample A
Δ - Sample B
□ - Sample C

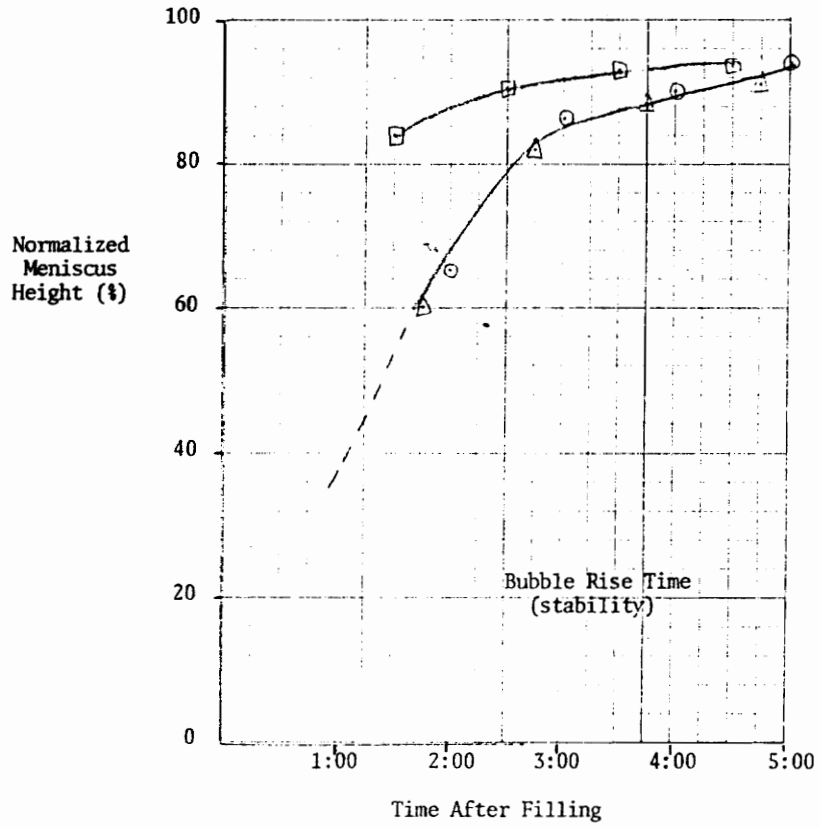

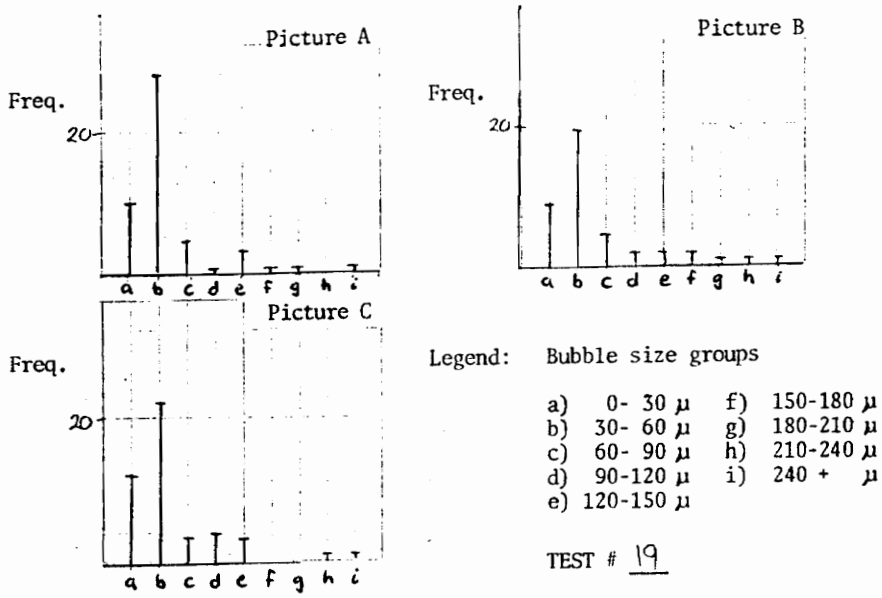

Histograms of Individual Photos

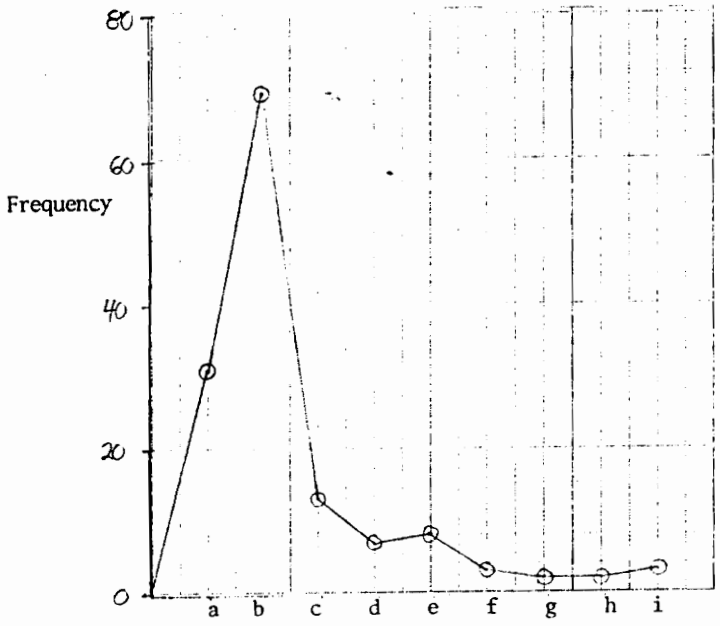

Cumulative Histogram

Data Sheets For Test # 20

Packing Diameter (mm)	:	3.0	Reynolds Number	:	603
Solution Feed Flowrate (L/min)	:	24	Pressure Drop Across Bed (psia)	:	12
Average Quality (% air)	:	61.2			
Solution Concentration (ppm)	:	500	(number of reuses: 1)		
Recycle Ratio (rec/dis)	:	.41	System Pressure (psig)	:	17

Notes:

Legend: O - Sample A
Δ - Sample B
□ - Sample C

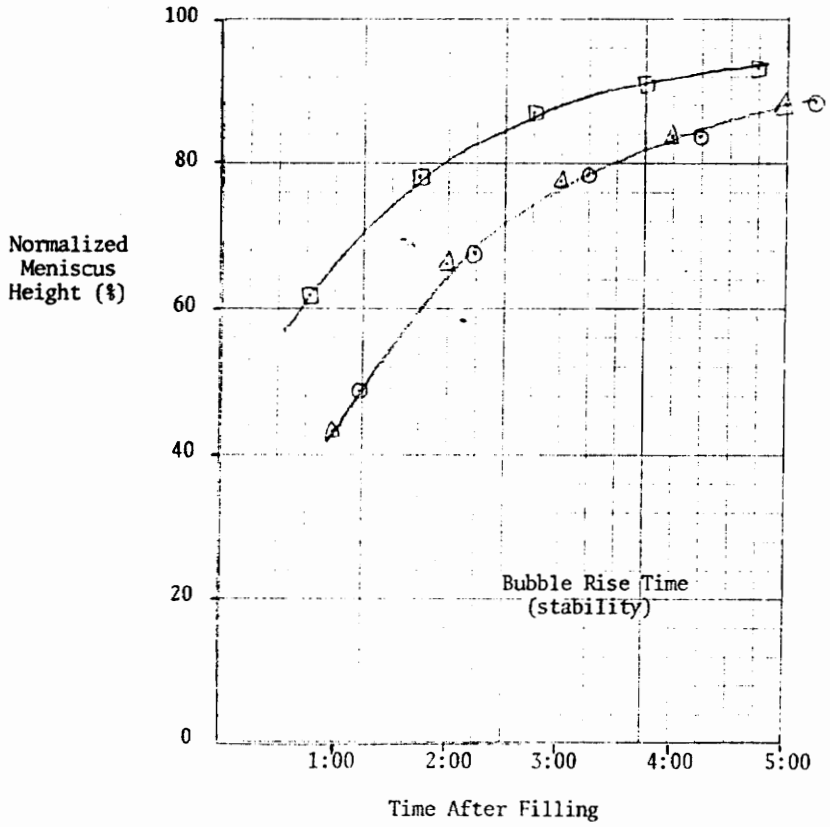

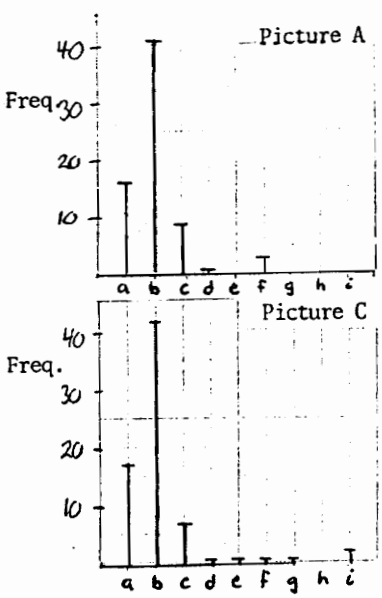

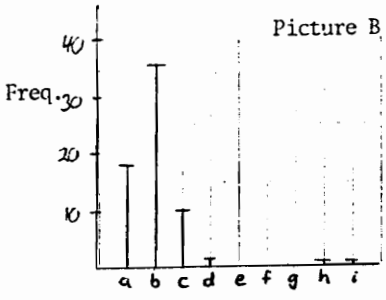

Legend: Bubble size groups

a)	0- 30 μ	f)	150-180 μ
b)	30- 60 μ	g)	180-210 μ
c)	60- 90 μ	h)	210-240 μ
d)	90-120 μ	i)	240 + μ
e)	120-150 μ		

TEST # 20

Histograms of Individual Photos

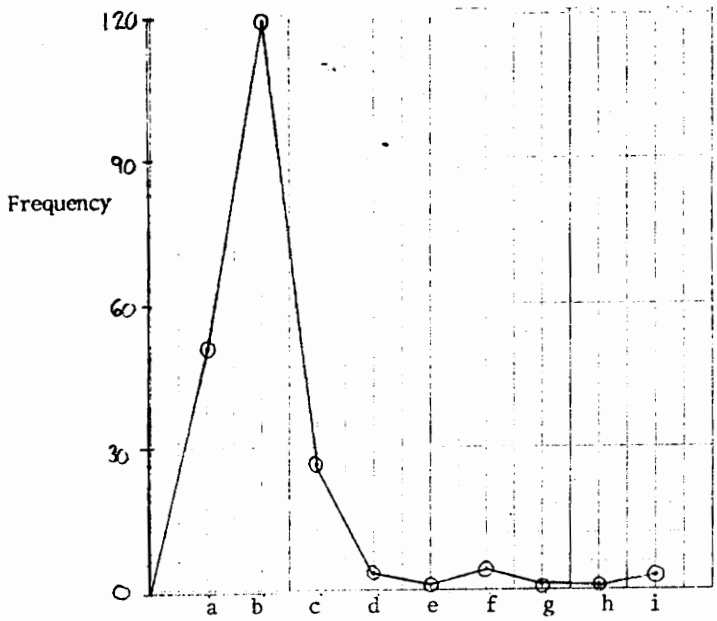

Cumulative Histogram

Data Sheets For Test # 21

Packing Diameter (mm)	:	3.0	Reynolds Number	:	677
Solution Feed Flowrate (L/min)	:	20	Pressure Drop Across Bed (psia)	:	17
Average Quality (% air)	:	61.1			
Solution Concentration (ppm)	:	500	(number of reuses: 2)		
Recycle Ratio (rec/dis)	:	.90	System Pressure (psig)	:	15

Notes:

Legend: ○ - Sample A
△ - Sample B
□ - Sample C

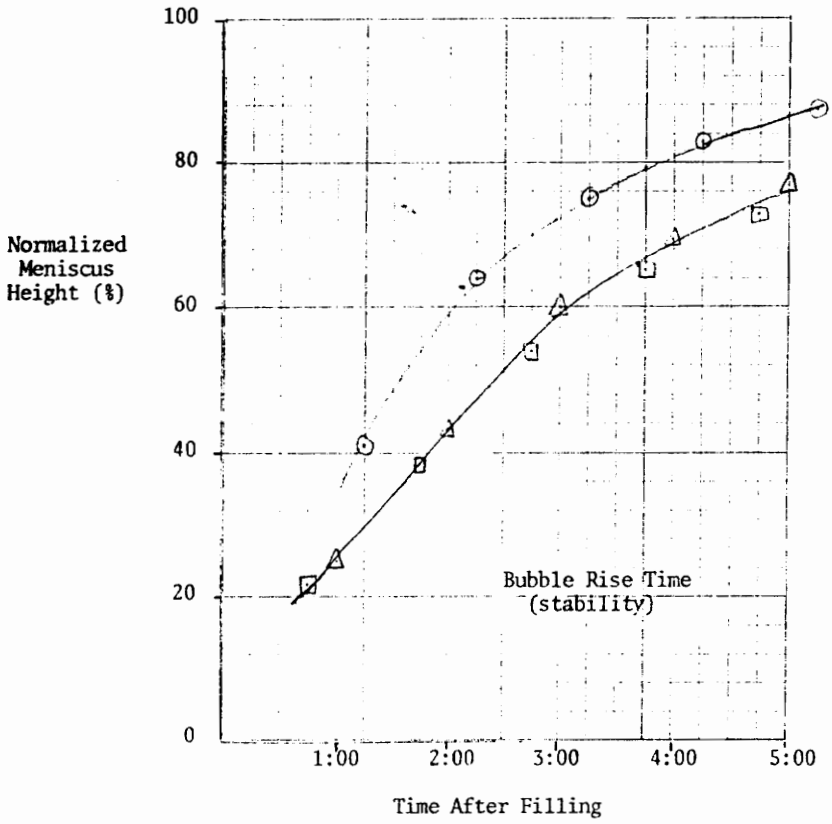

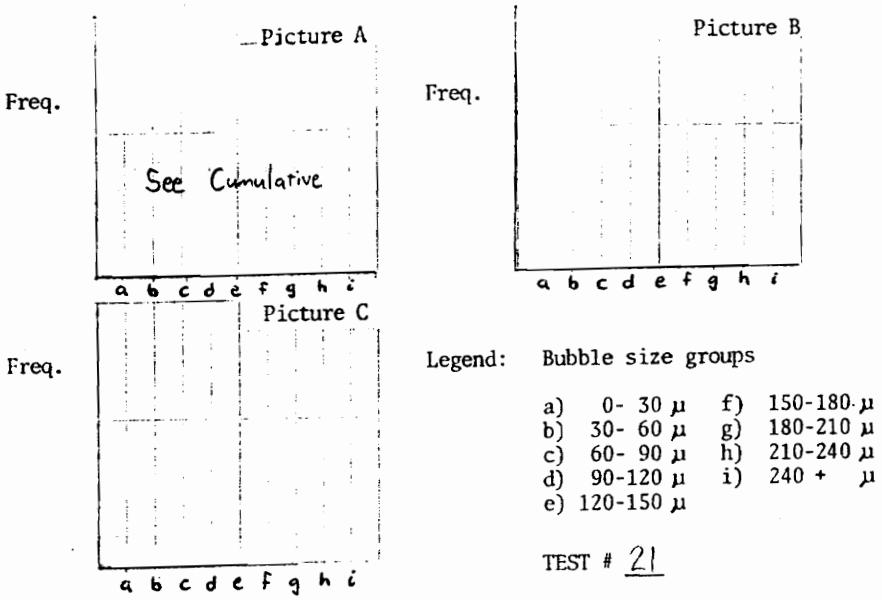

Histograms of Individual Photos

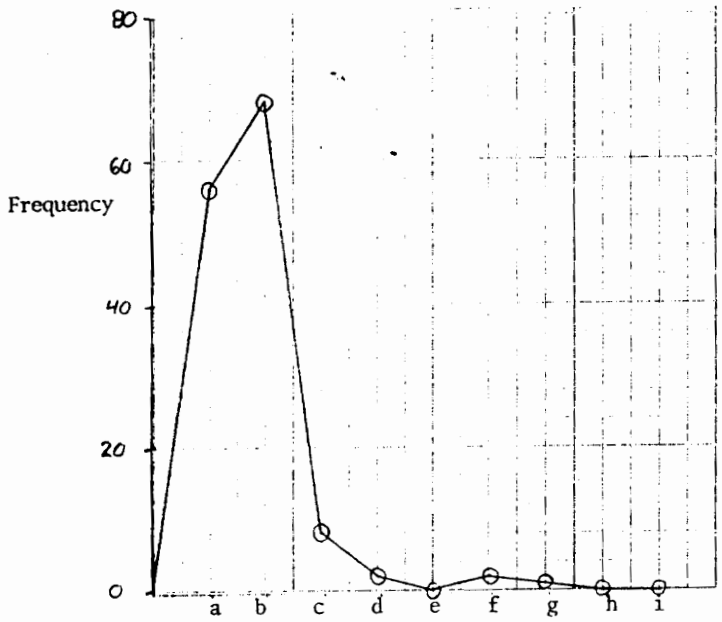

Cumulative Histogram

Data Sheets For Test # 22

Packing Diameter (mm)	:	2.0	Reynolds Number	:	19
Solution Feed Flowrate (L/min)	:	16	Pressure Drop Across Bed (psia)	:	11
Average Quality (% air)	:	64.1			
Solution Concentration (ppm)	:	500	(number of reuses: 0)		
Recycle Ratio (rec/dis)	:	0	System Pressure (psig)	:	9

Notes:

Legend: O - Sample A
Δ - Sample B
□ - Sample C

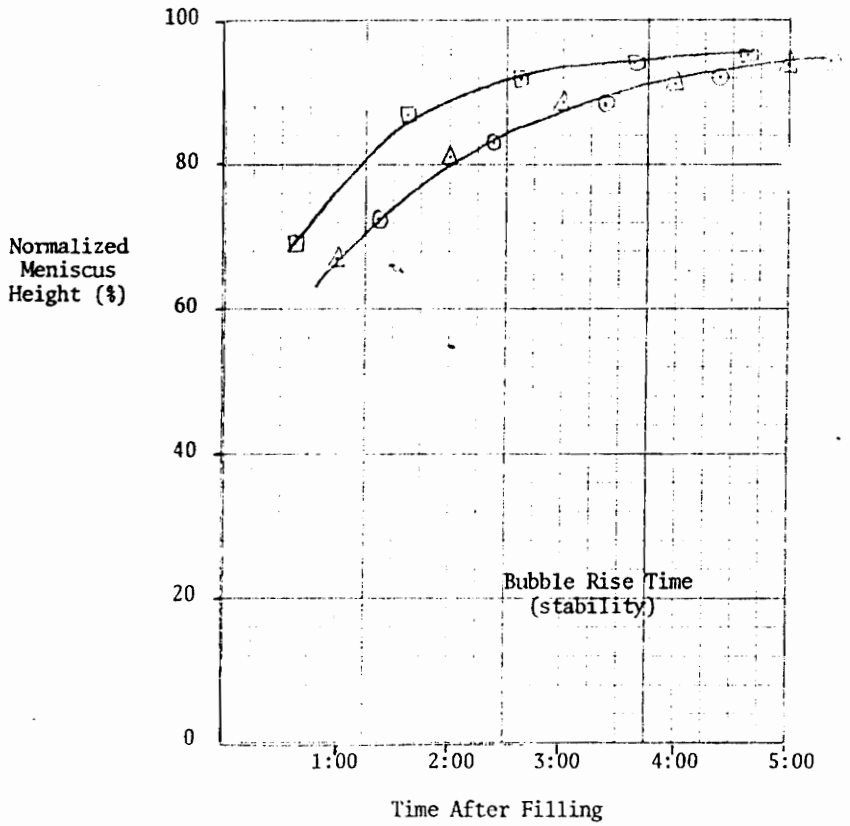

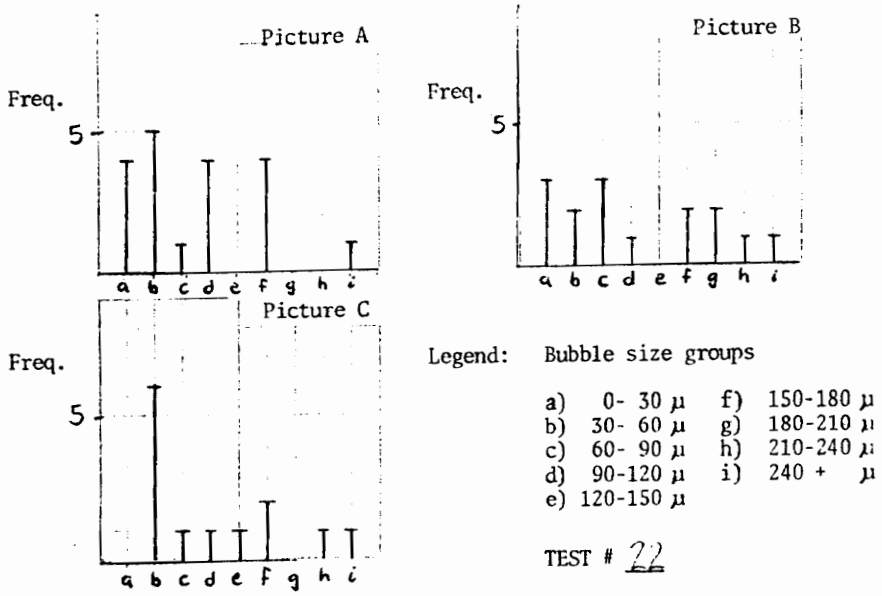

Legend: Bubble size groups

a)	0- 30 μ	f)	150-180 μ
b)	30- 60 μ	g)	180-210 μ
c)	60- 90 μ	h)	210-240 μ
d)	90-120 μ	i)	240 + μ
e)	120-150 μ		

TEST # 22

Histograms of Individual Photos

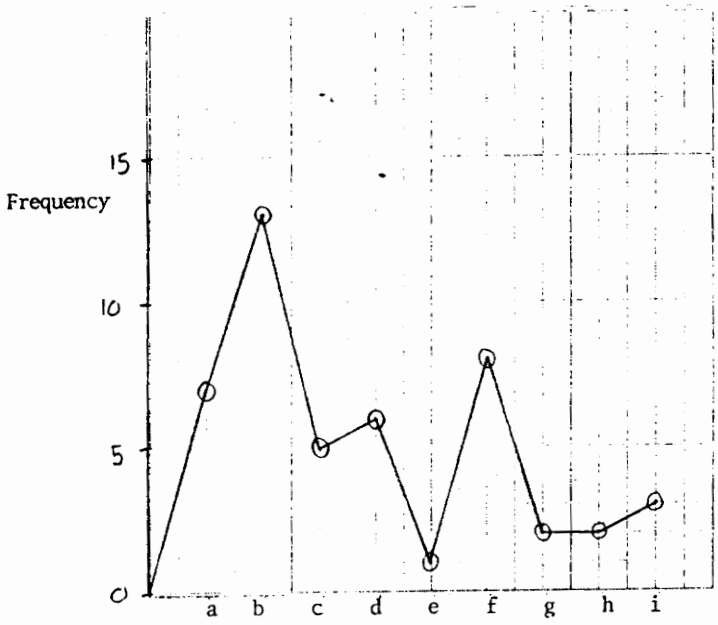

Cumulative Histogram

Data Sheets For Test # 23

Packing Diameter (mm)	:	*	Reynolds Number	:	*
Solution Feed Flowrate (L/min)	:	20	Pressure Drop Across Bed (psia)	:	*
Average Quality (% air)	:	63.4			
Solution Concentration (ppm)	:	500	(number of reuses: 0)		
Recycle Ratio (rec/dis)	:	.719	System Pressure (psig)	:	14

Notes: * No bed. Test to see effect of recycle pump alone.

Legend: O - Sample A
Δ - Sample B
□ - Sample C

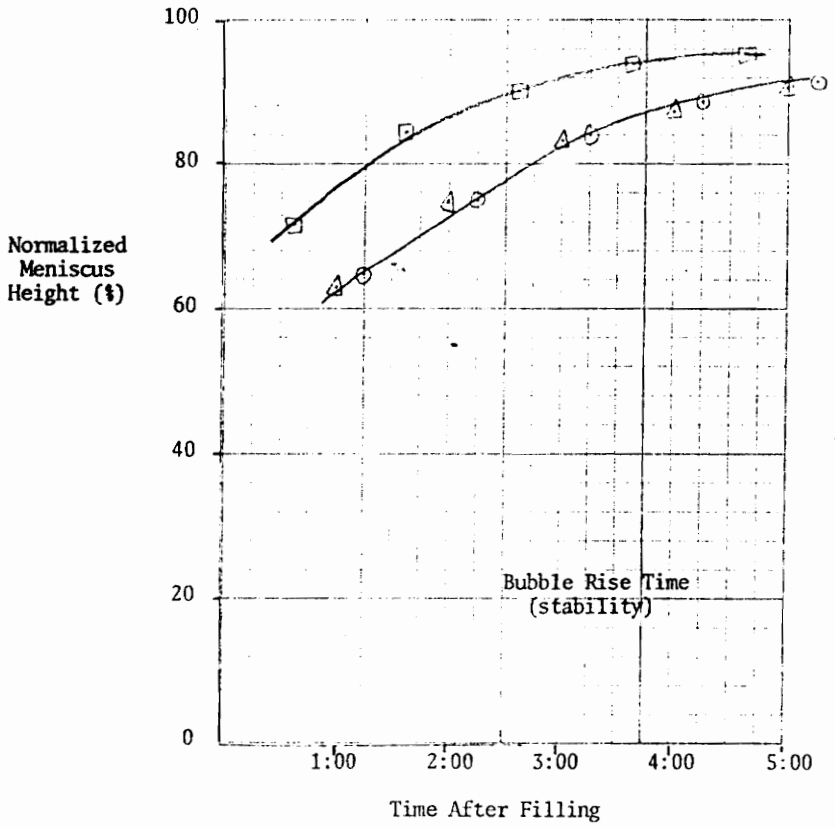

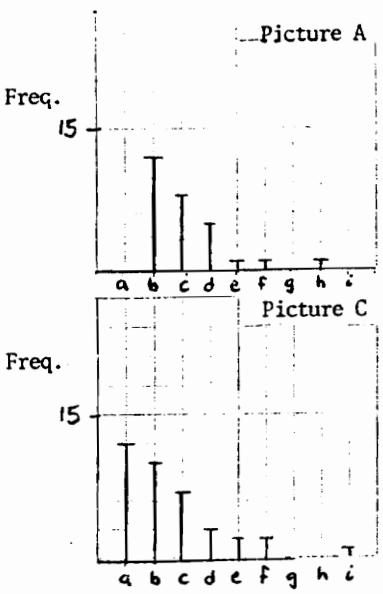

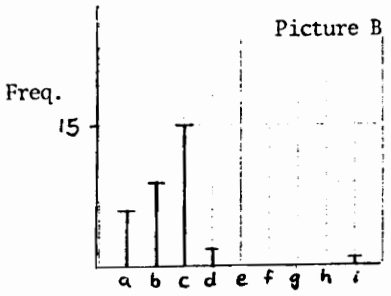

Legend: Bubble size groups

a)	0- 30 μ	f)	150-180 μ
b)	30- 60 μ	g)	180-210 μ
c)	60- 90 μ	h)	210-240 μ
d)	90-120 μ	i)	240 + μ
e)	120-150 μ		

TEST # 23

Histograms of Individual Photos

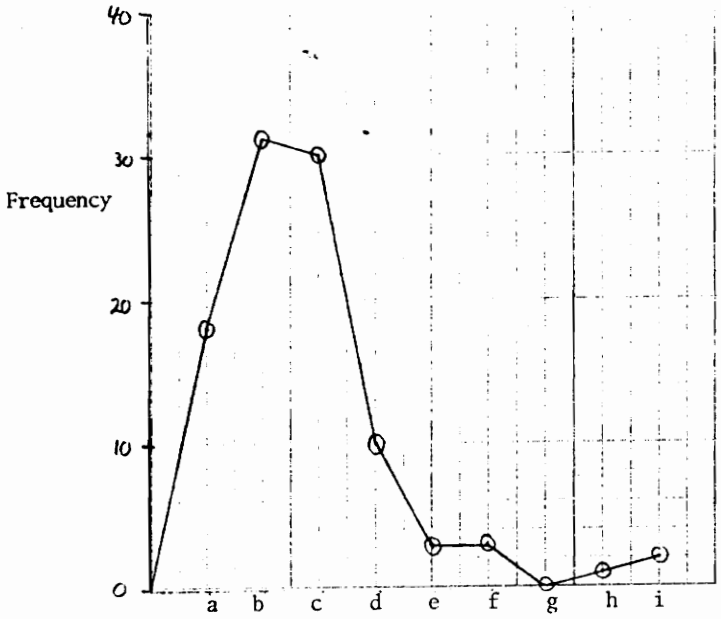

Cumulative Histogram

Data Sheets For Test # 24

Packing Diameter (mm)	: *	Reynolds Number	: *
Solution Feed Flowrate (L/min)	: 20	Pressure Drop Across Bed (psia)	: *
Average Quality (% air)	: 64.4		
Solution Concentration (ppm)	: 500	(number of reuses: 0)	
Recycle Ratio (rec/dis)	: .854	System Pressure (psig)	: 15

Notes: * No bed. Test to see effect of recycle pump alone

Legend: ○ - Sample A
△ - Sample B
□ - Sample C

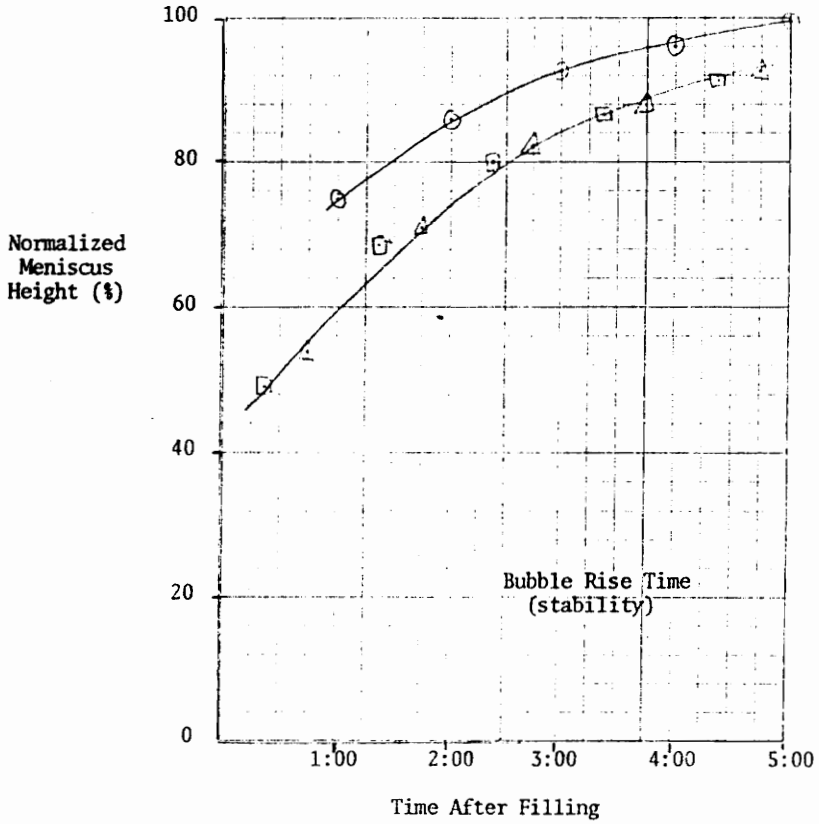

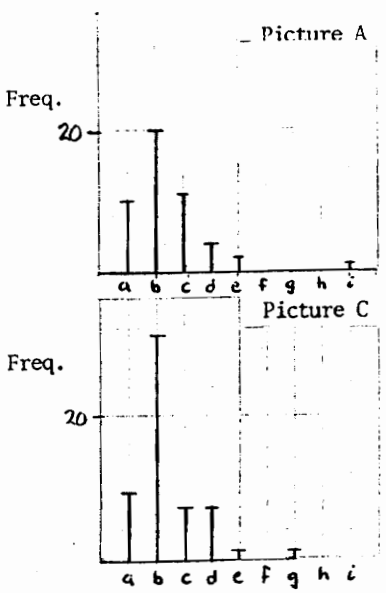

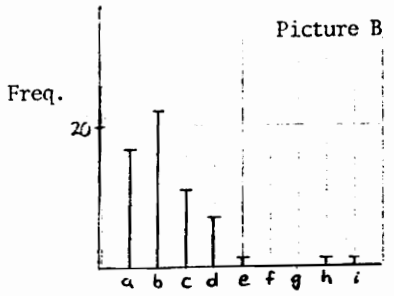

Legend: Bubble size groups

a)	0- 30 μ	f)	150-180 μ
b)	30- 60 μ	g)	180-210 μ
c)	60- 90 μ	h)	210-240 μ
d)	90-120 μ	i)	240 + μ
e)	120-150 μ		

TEST # 24

Histograms of Individual Photos

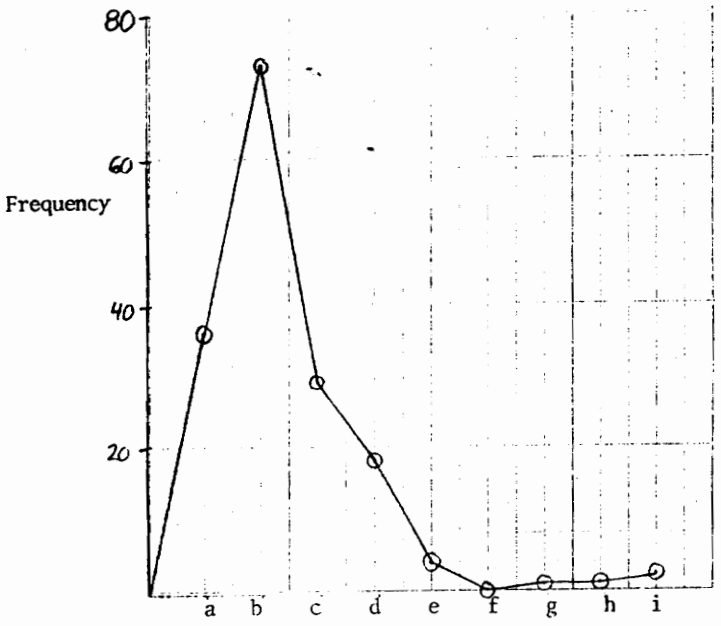

Cumulative Histogram

Data Sheets For Test # 25

Packing Diameter (mm)	: 2.0	Reynolds Number	: 249
Solution Feed Flowrate (L/min)	: 20	Pressure Drop Across Bed (psia)	: 11
Average Quality (% air)	: 67.7		
Solution Concentration (ppm)	: 500	(number of reuses: 0)	
Recycle Ratio (rec/dis)	: 0	System Pressure (psig)	: 14

Notes:

Legend: O - Sample A
Δ - Sample B
□ - Sample C

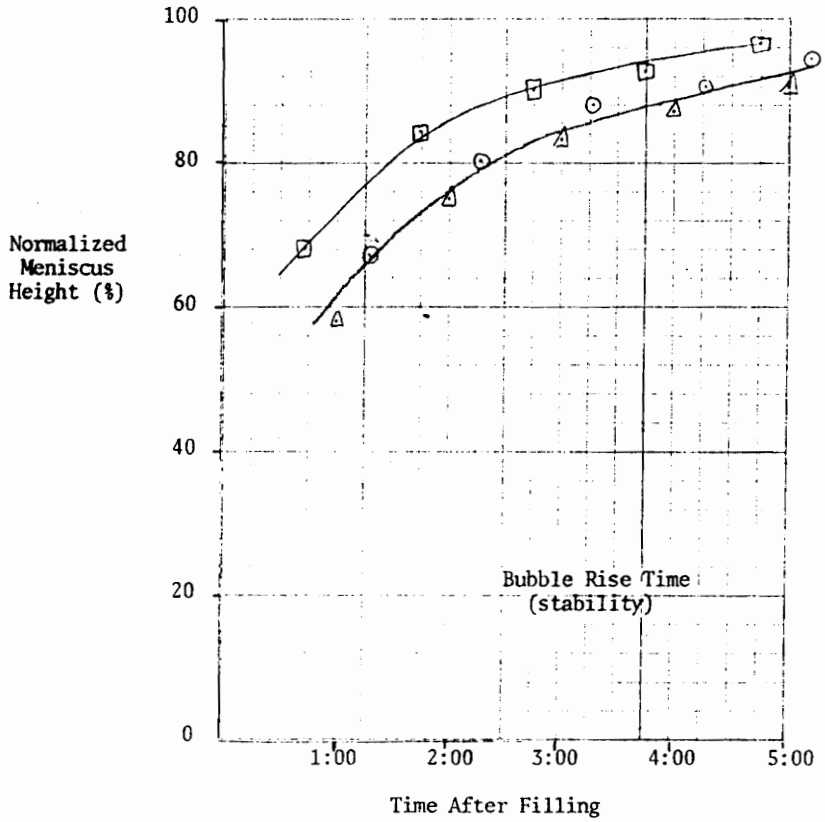

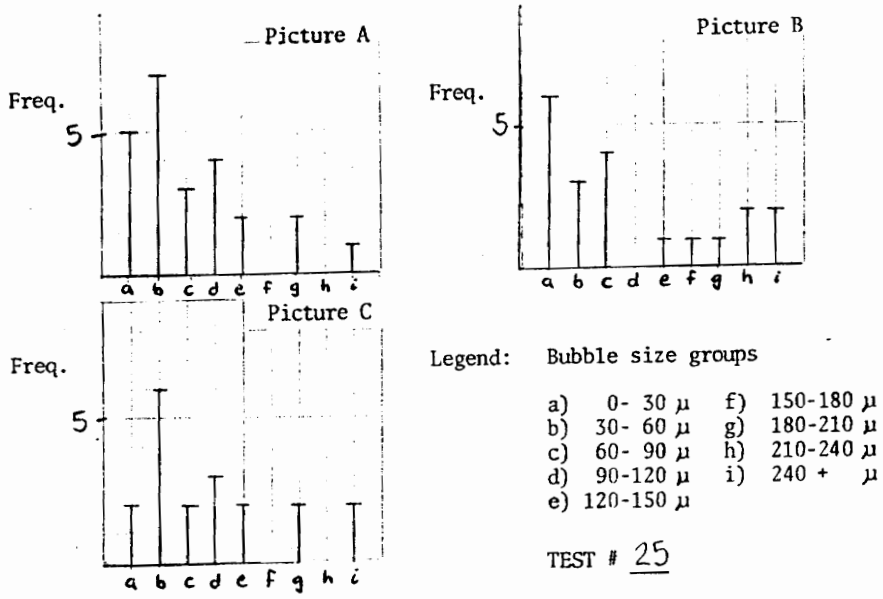

Histograms of Individual Photos

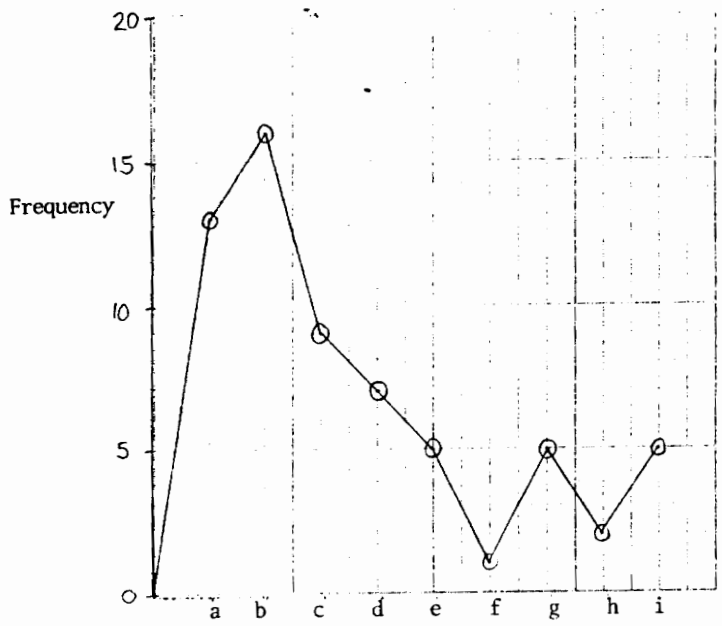

Cumulative Histogram

Data Sheets For Test # 26

Packing Diameter (mm)	:	2.0	Reynolds Number	:	249
Solution Feed Flowrate (L/min)	:	20	Pressure Drop Across Bed (psia)	:	10
Average Quality (% air)	:	67.6			
Solution Concentration (ppm)	:	500	(number of reuses: 0)		
Recycle Ratio (rec/dis)	:	0	System Pressure (psig)	:	13

Notes: Air introduced upstream.

Legend: ○ - Sample A
△ - Sample B
□ - Sample C

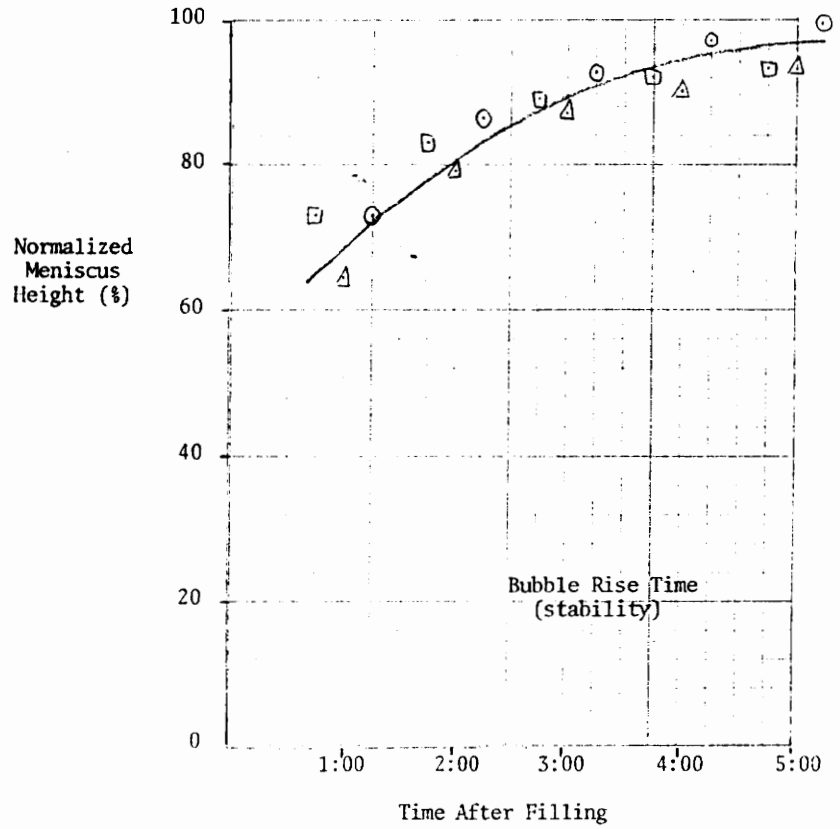

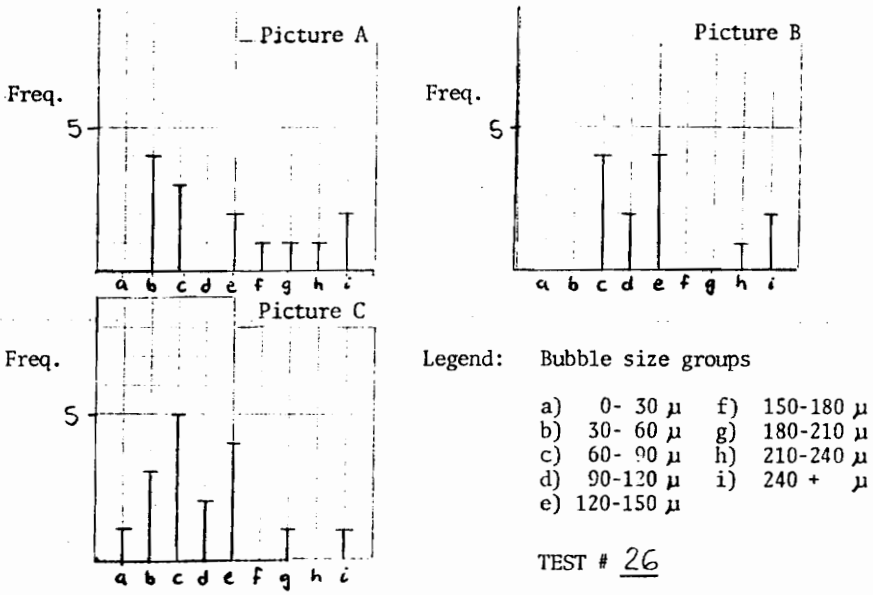

Histograms of Individual Photos

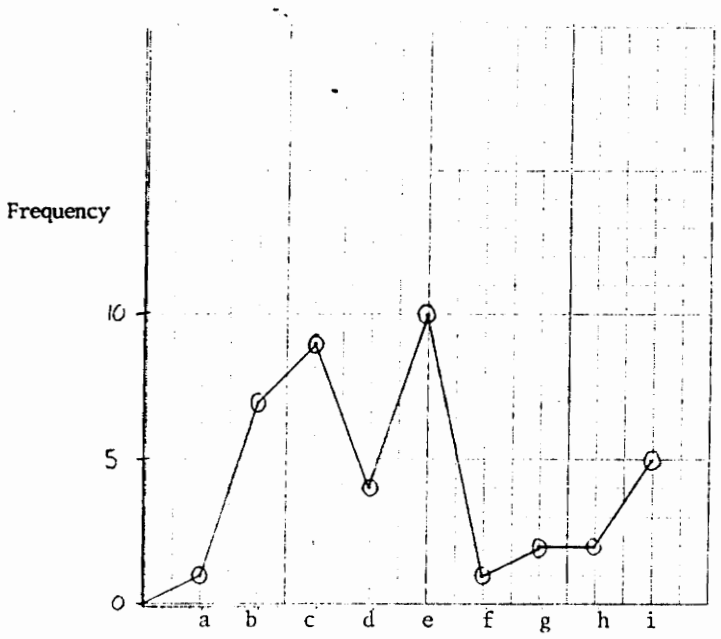

Cumulative Histogram

Appendix E. Photomicrographs

The following contains photomicrographs of 26 runs. Only one of the three pictures of each run is included.

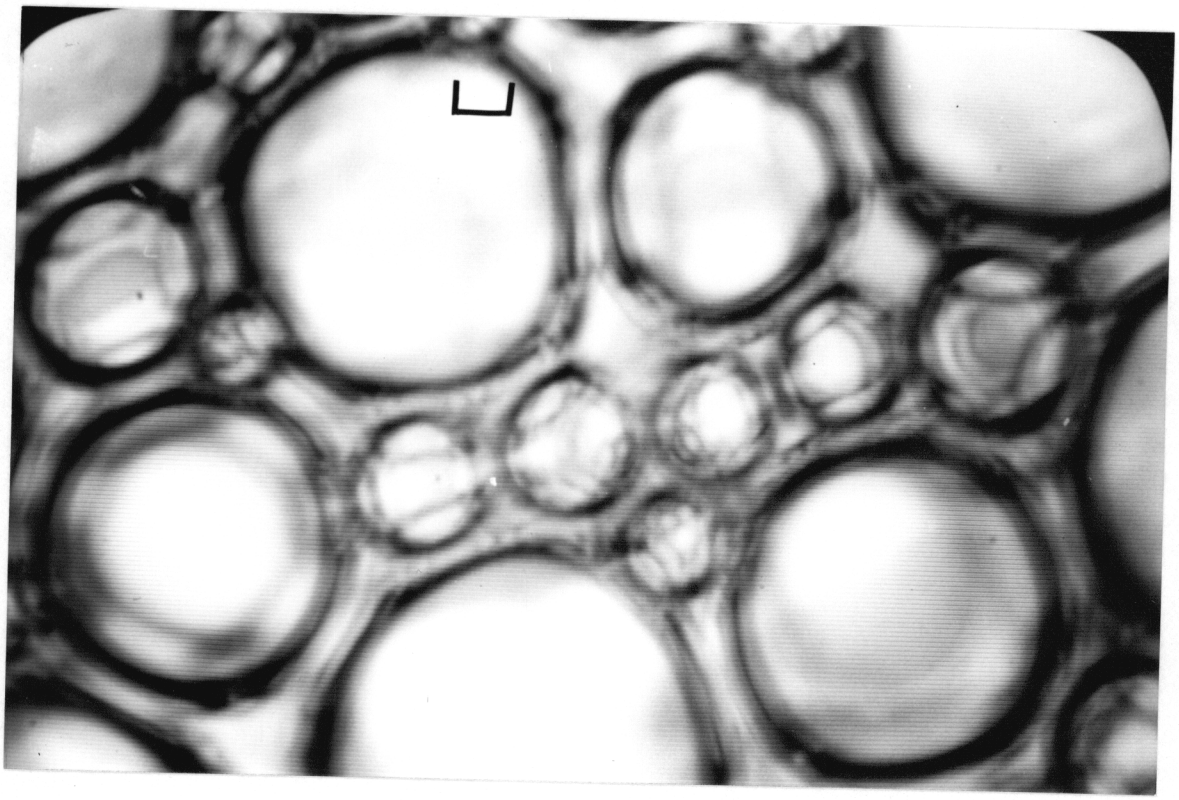

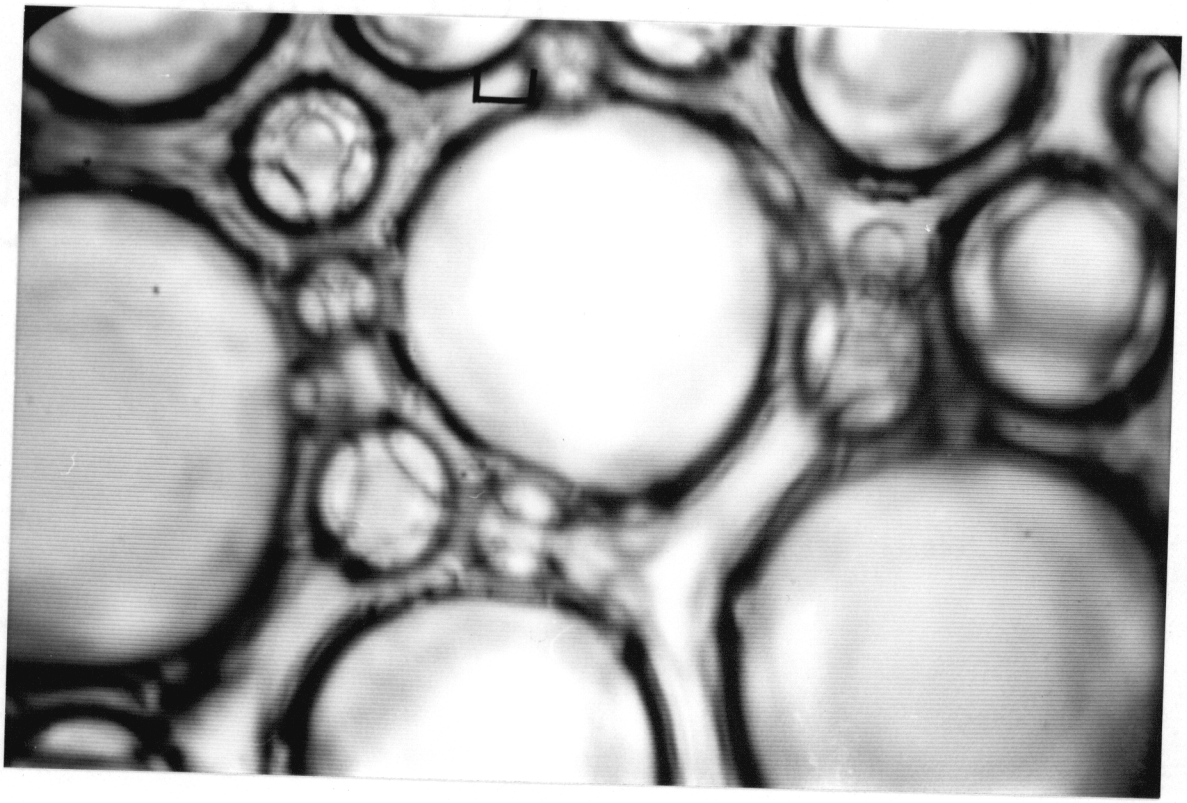

2

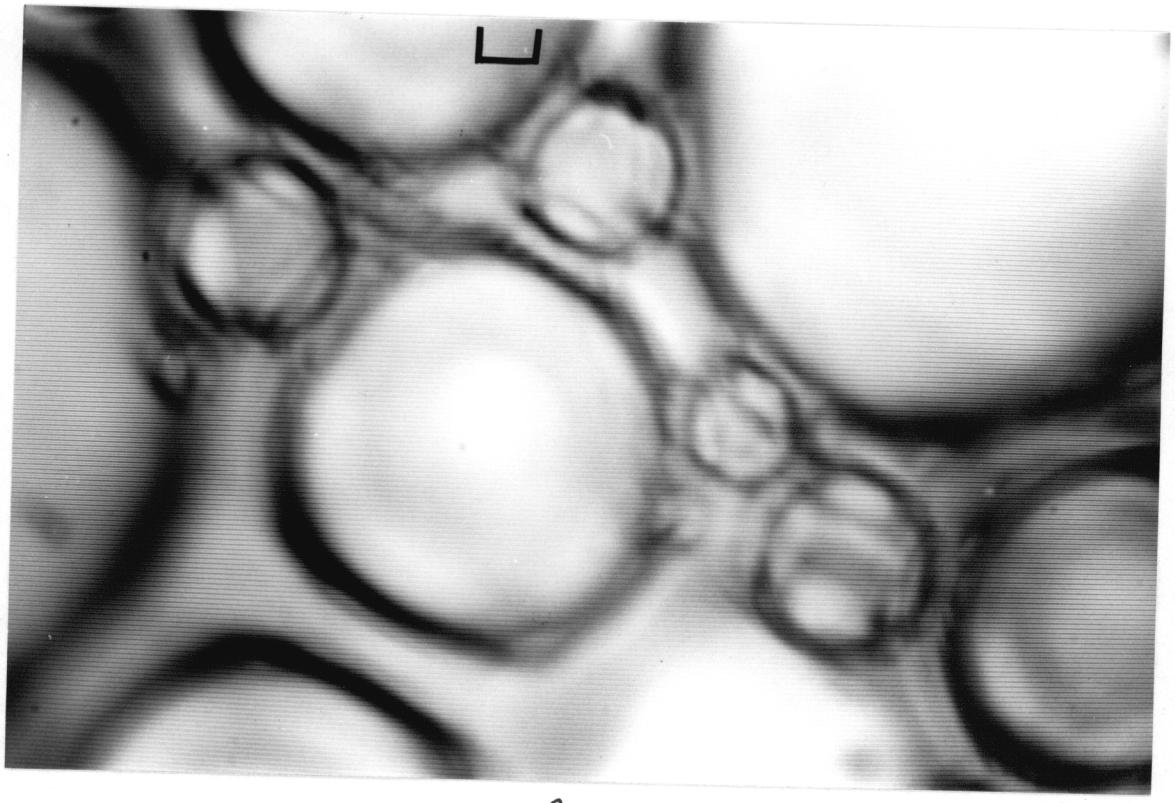

3

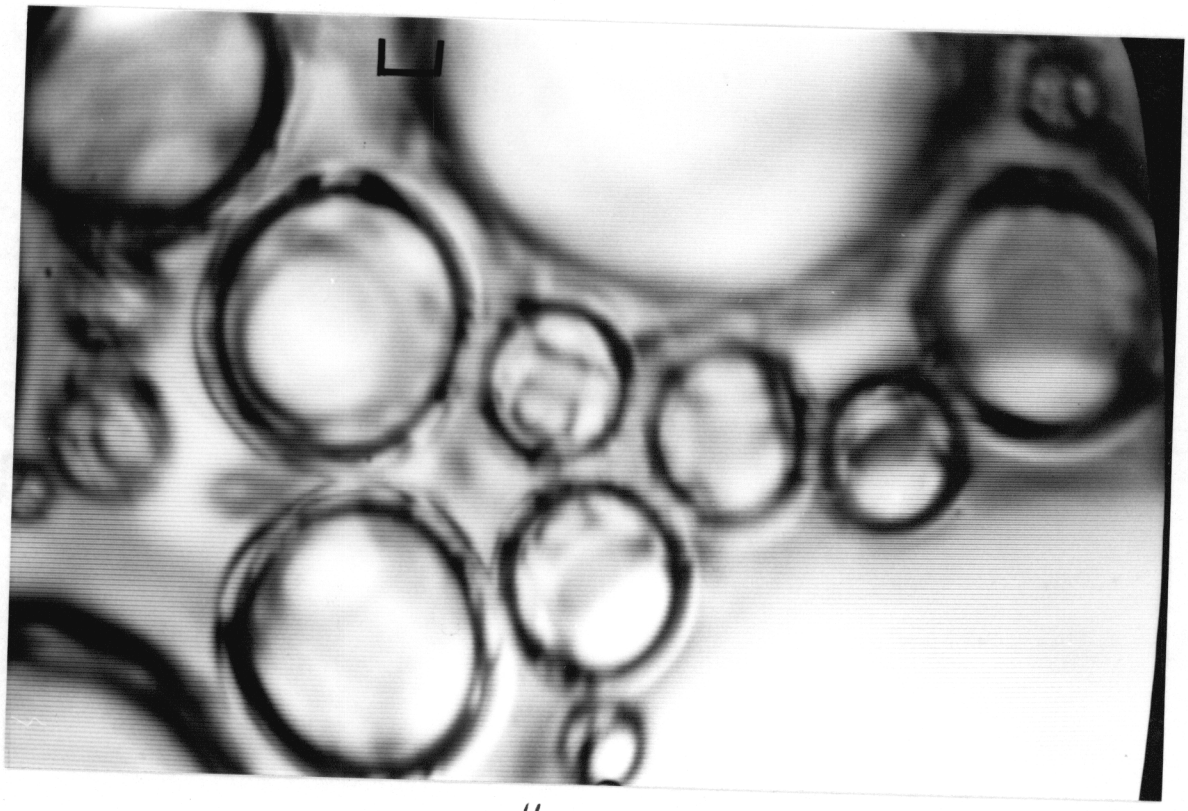

4

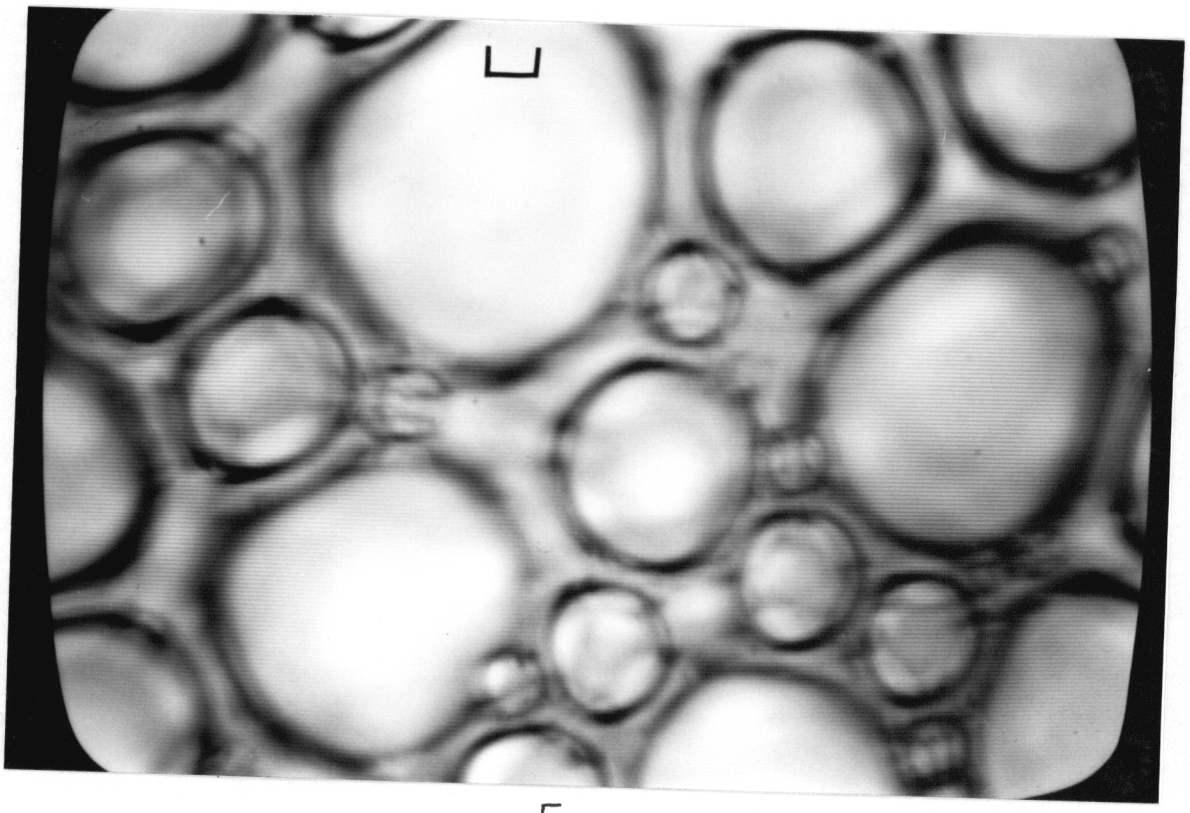

5

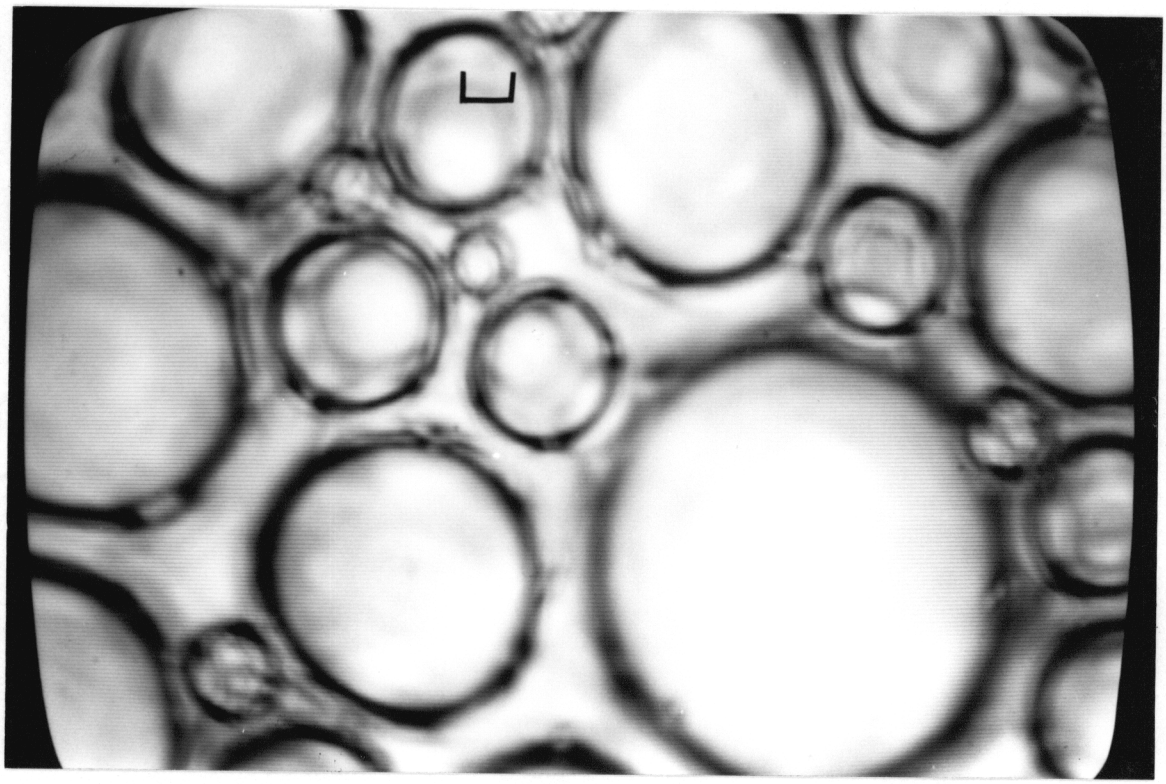

6

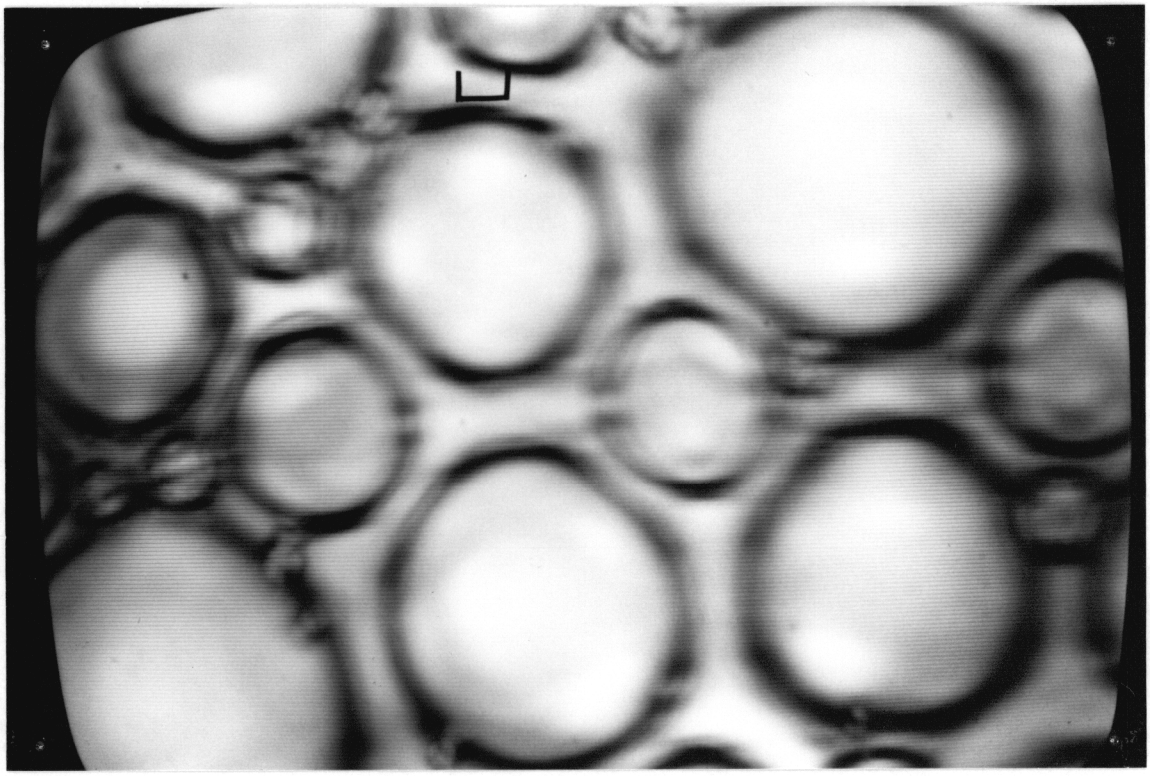

7

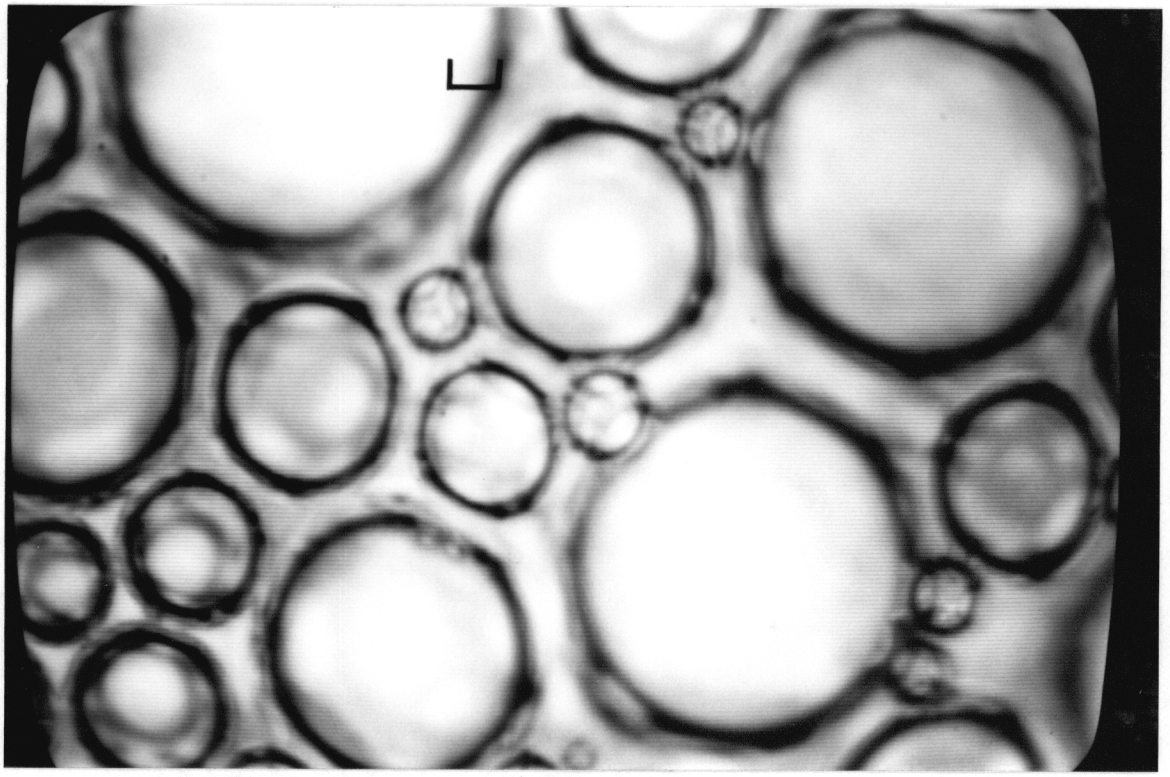

8

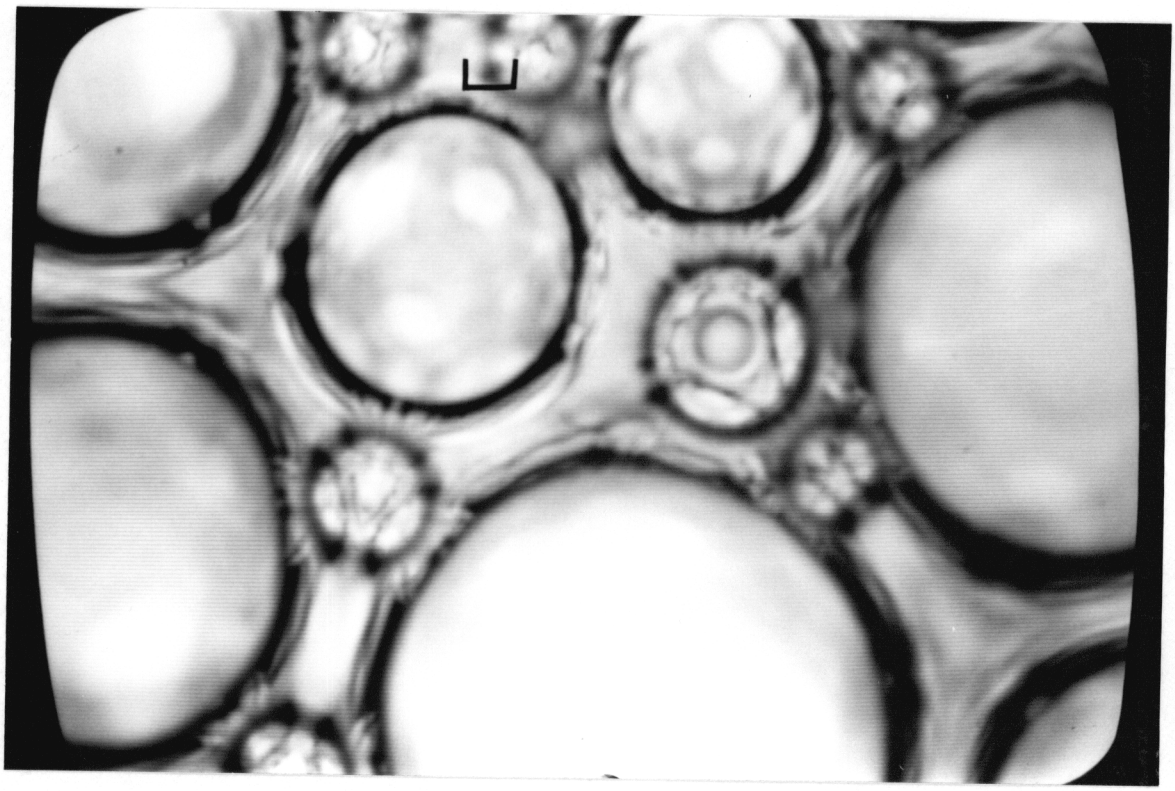

9

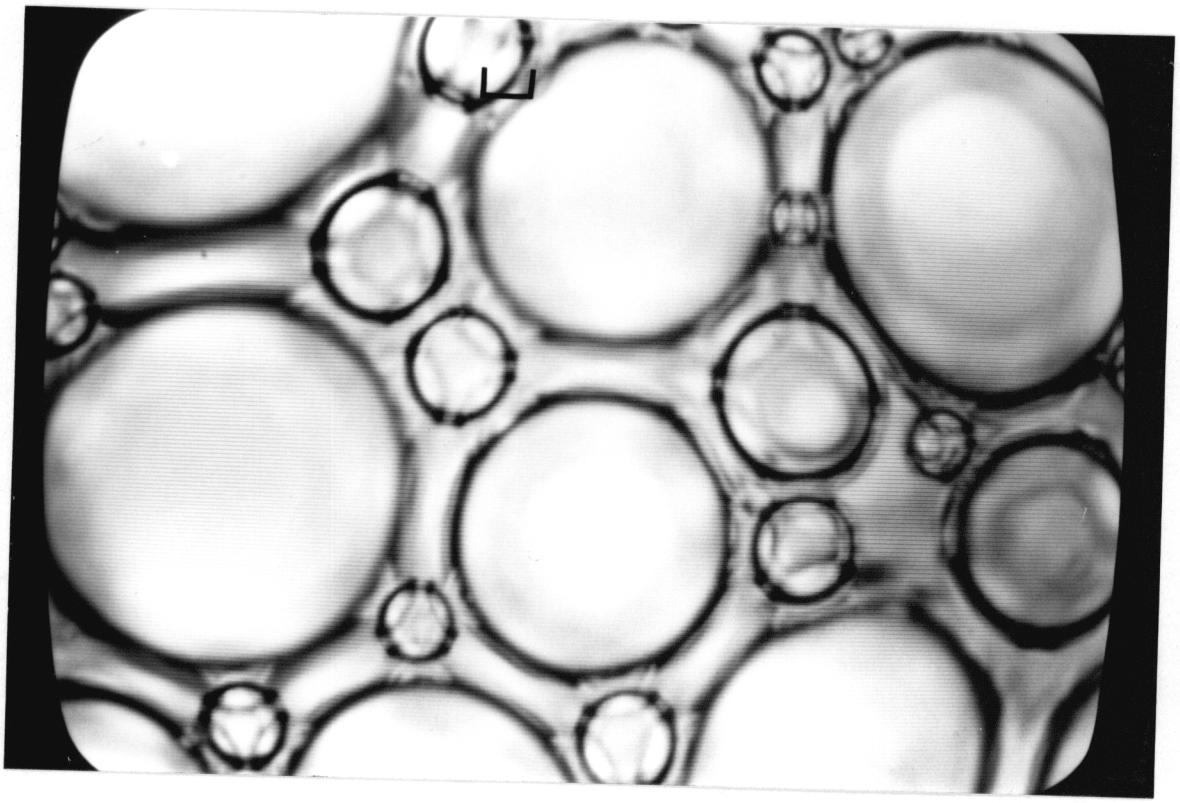

10

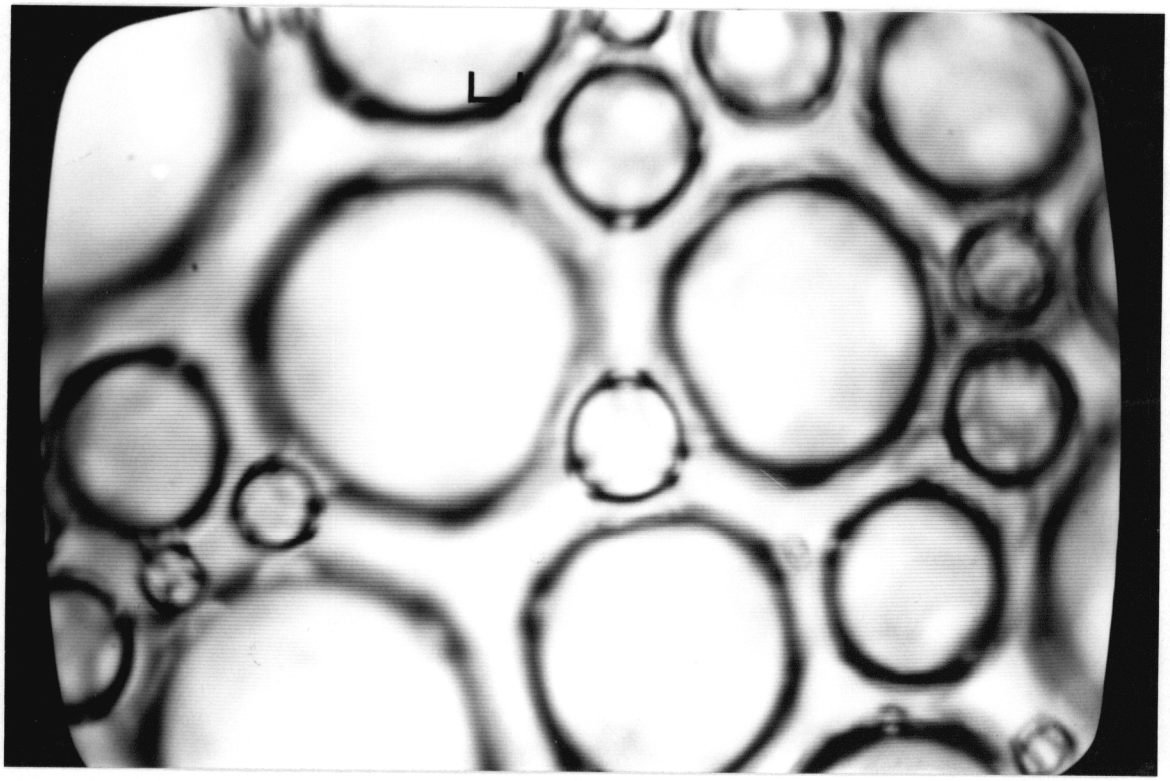

11

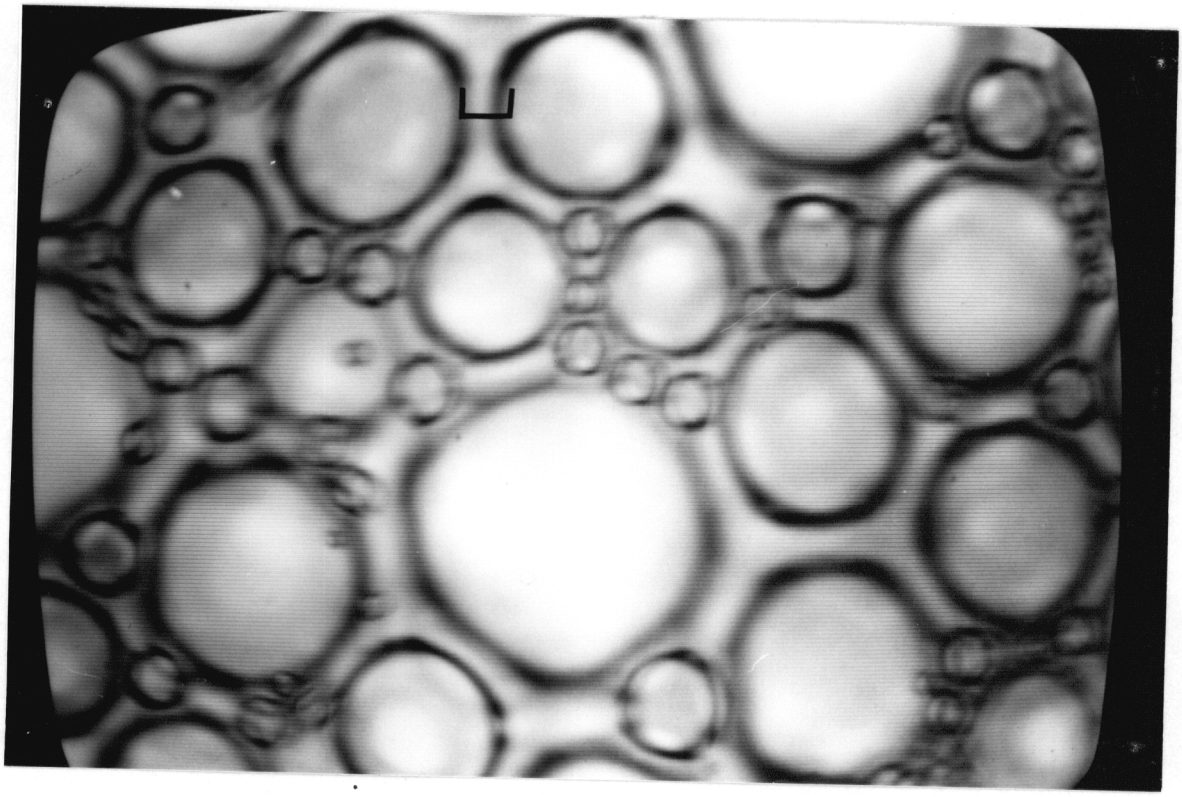

12

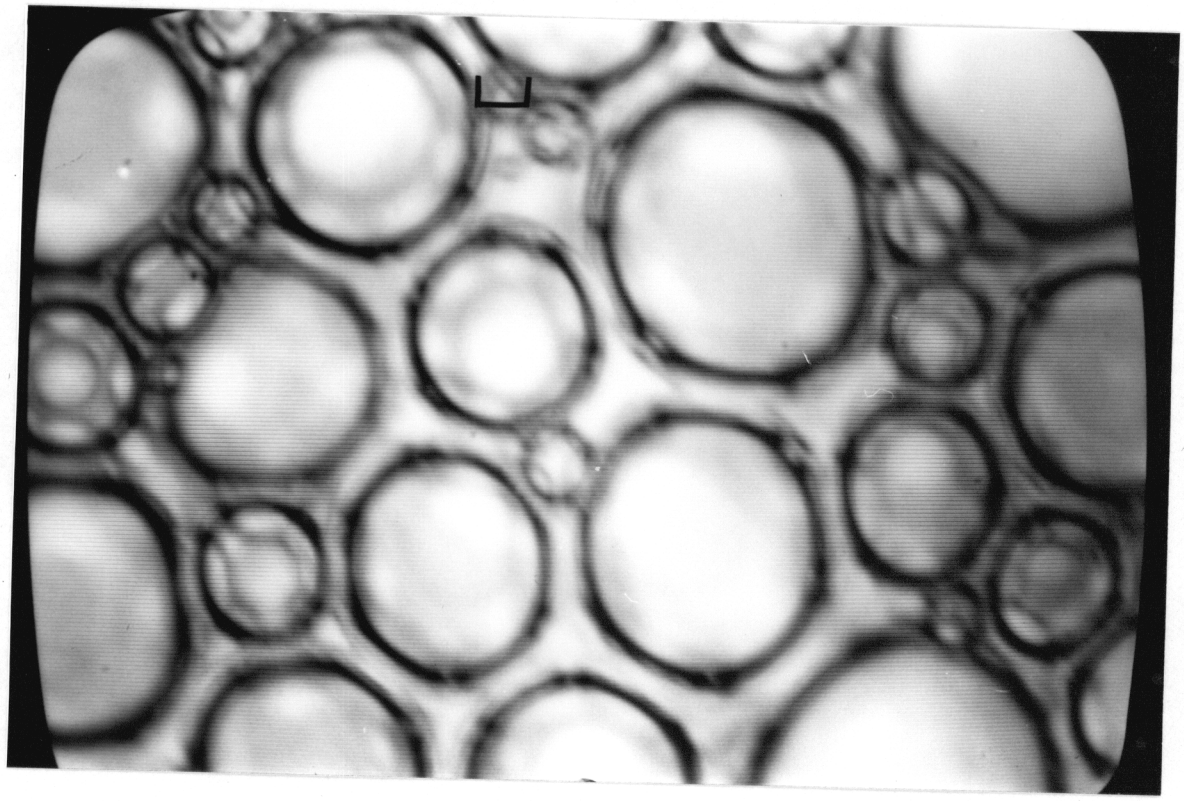

13

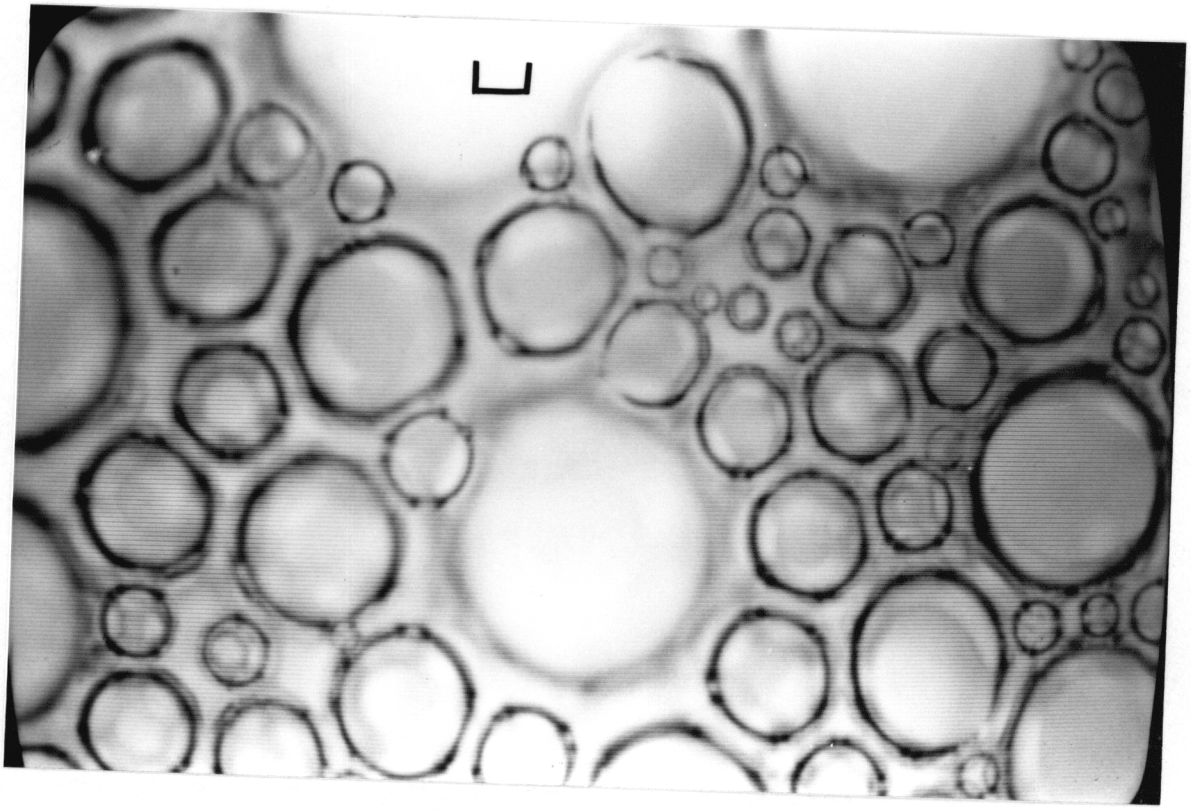

14

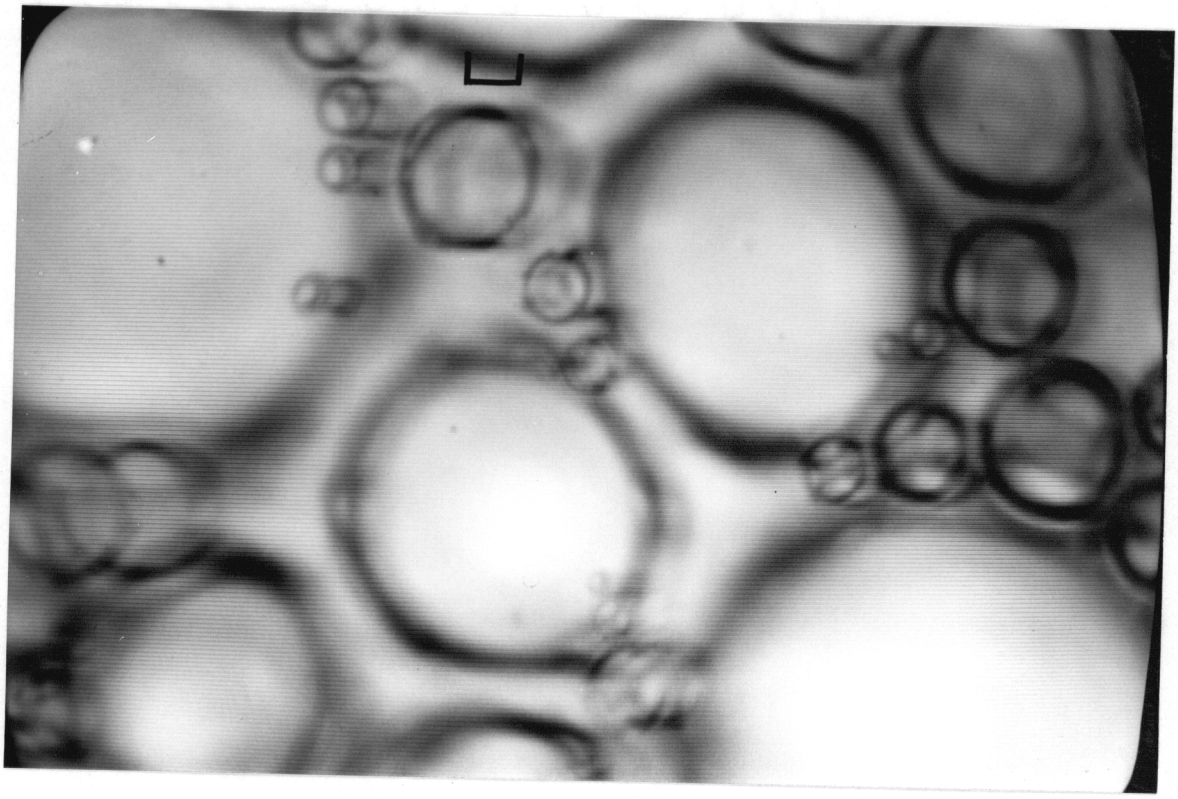

15

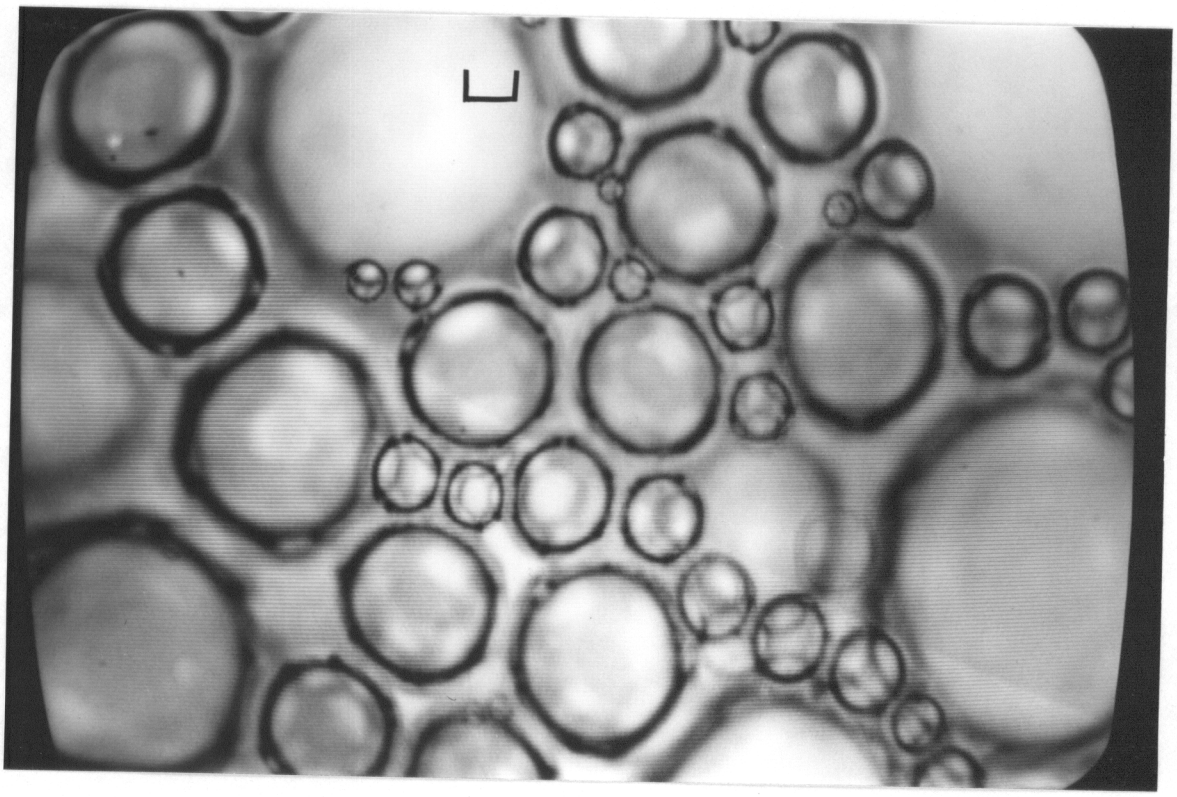

16

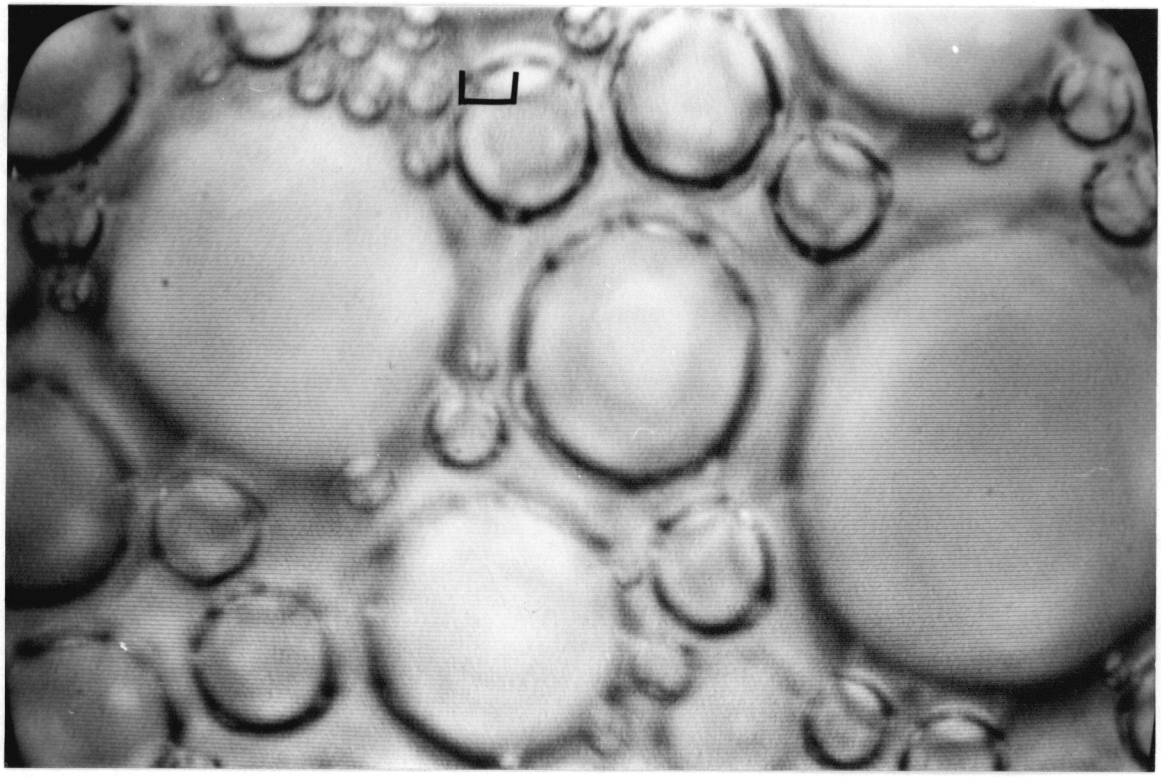

17

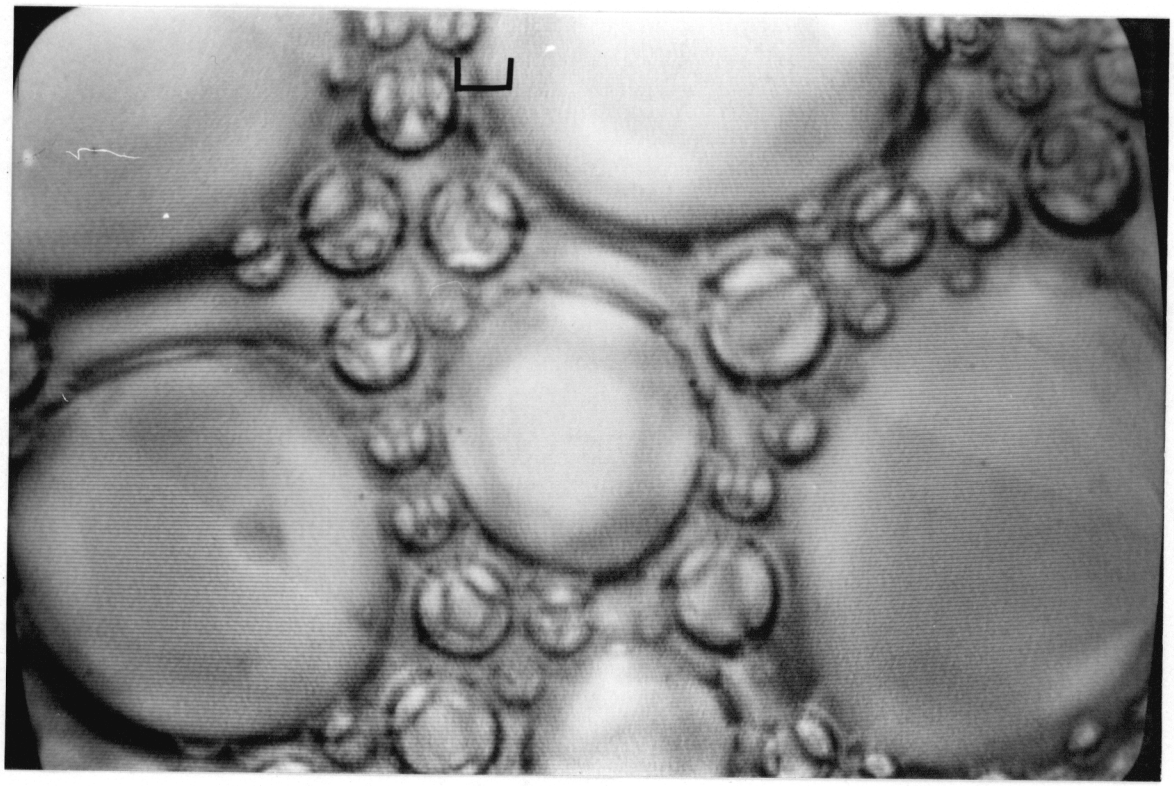

18

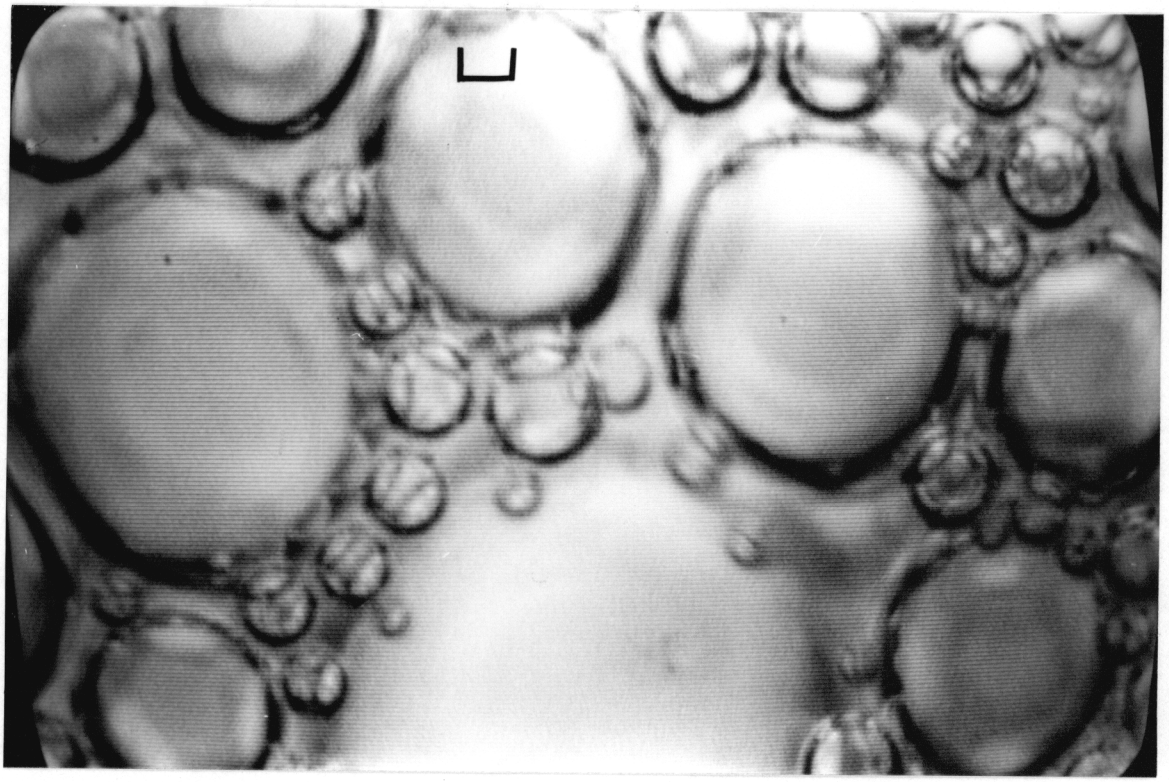

19

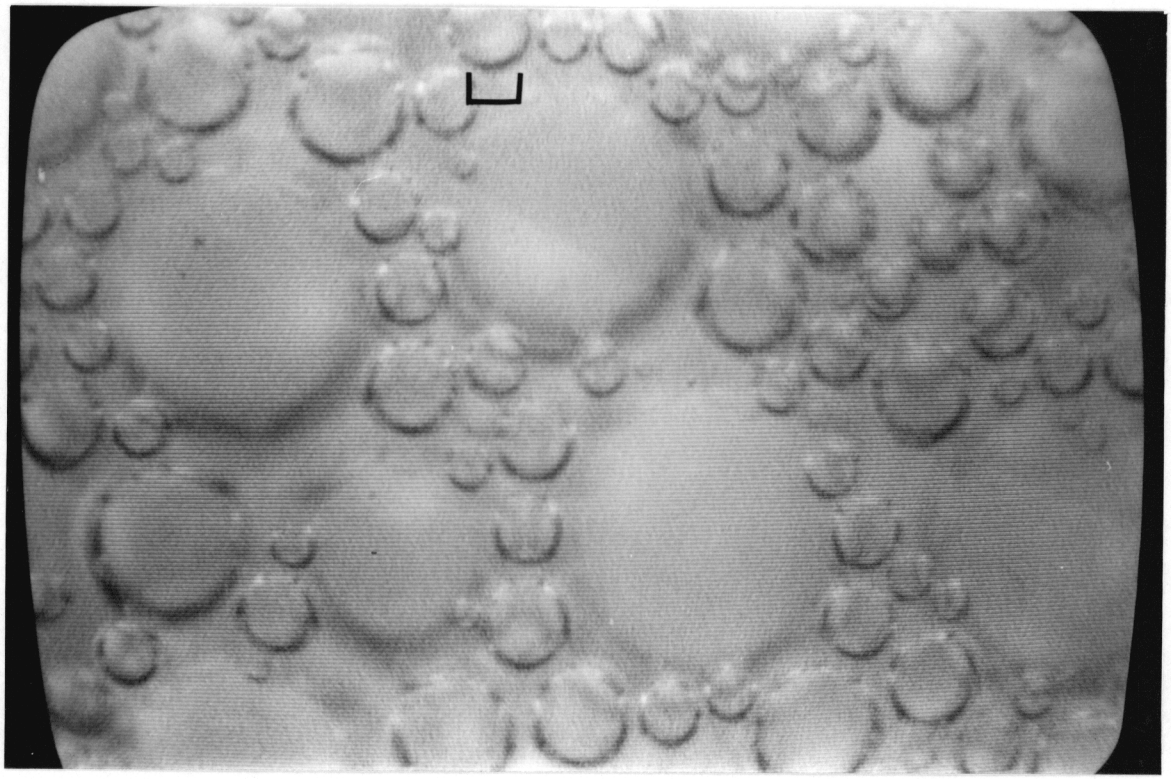

20

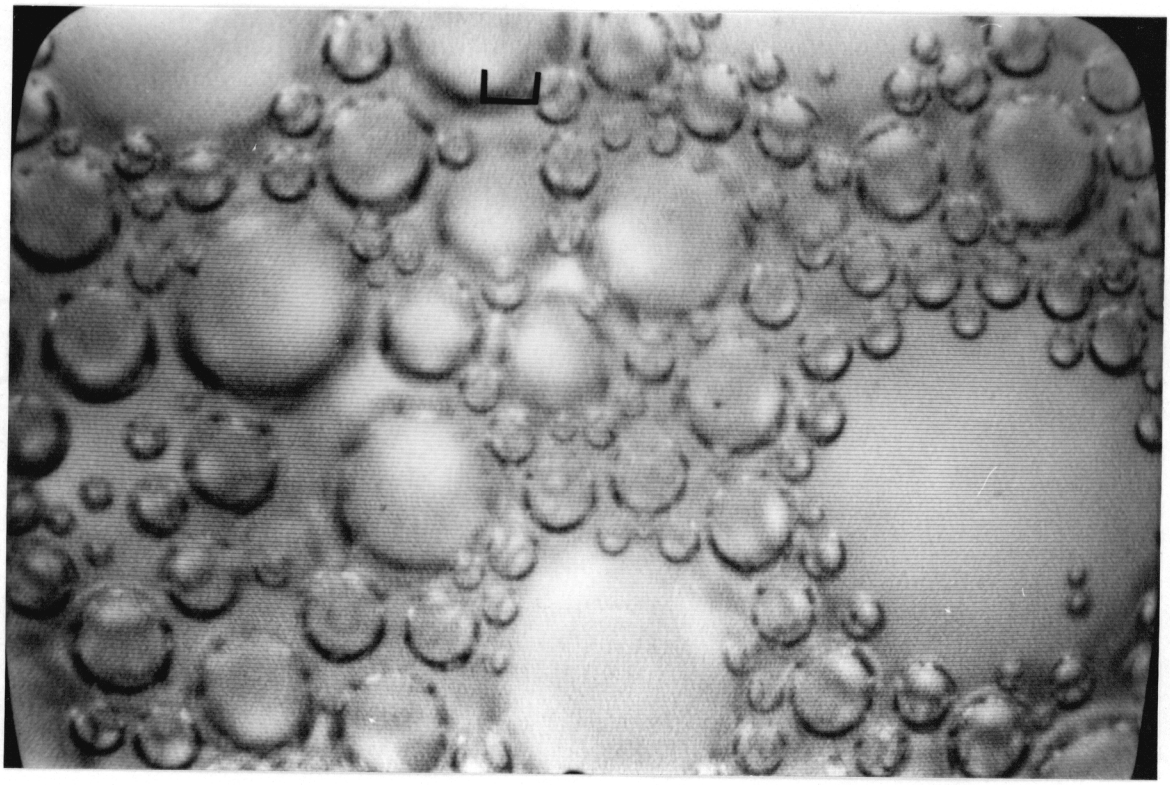

21

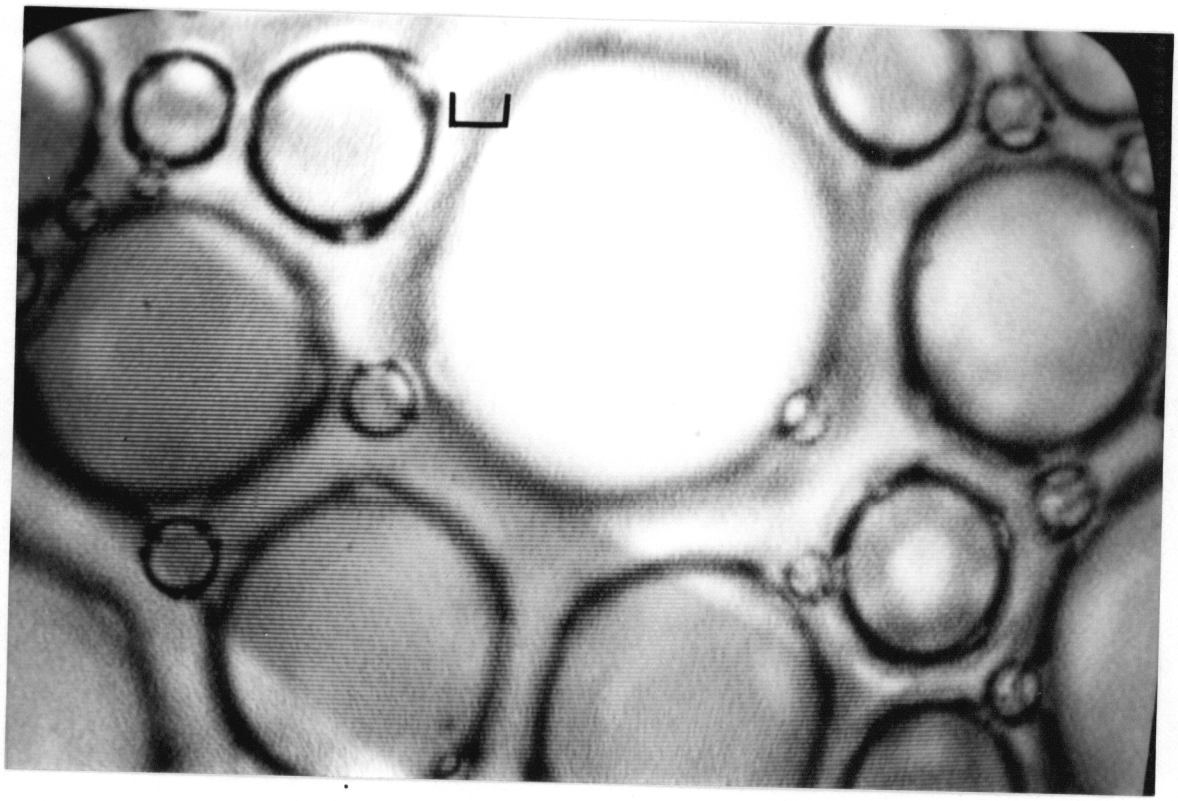

22

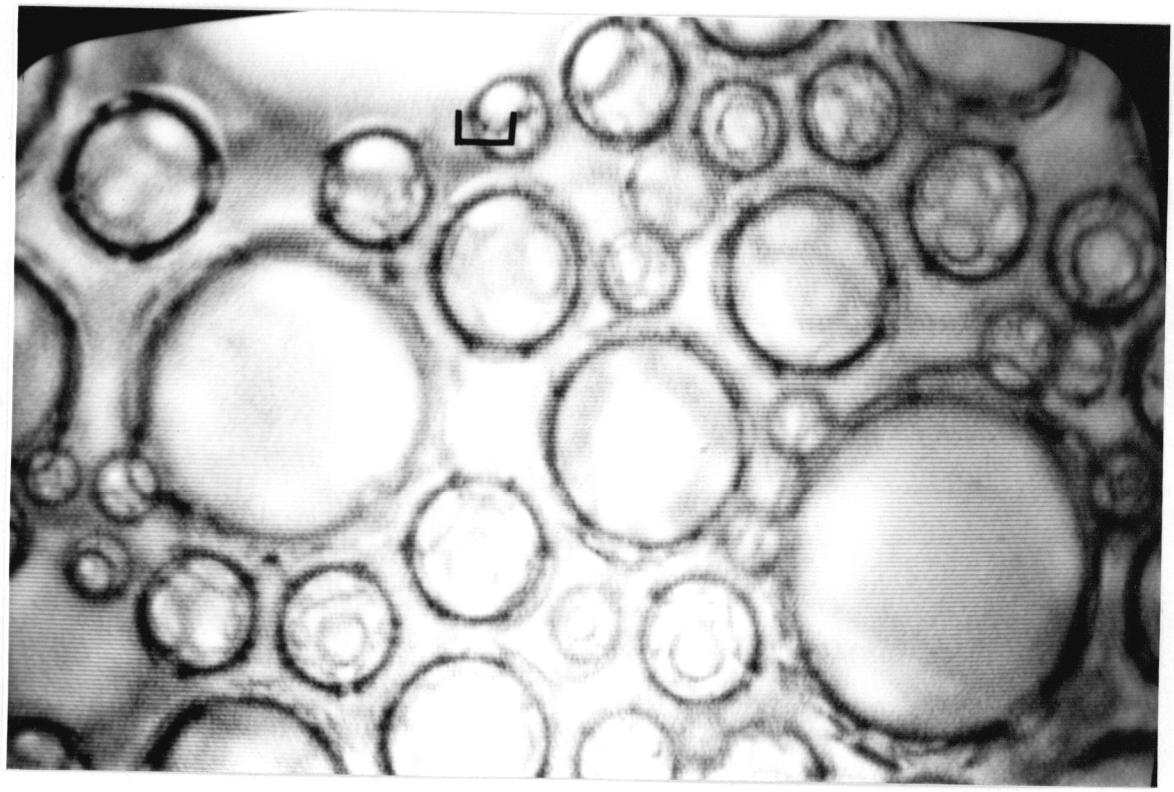

23

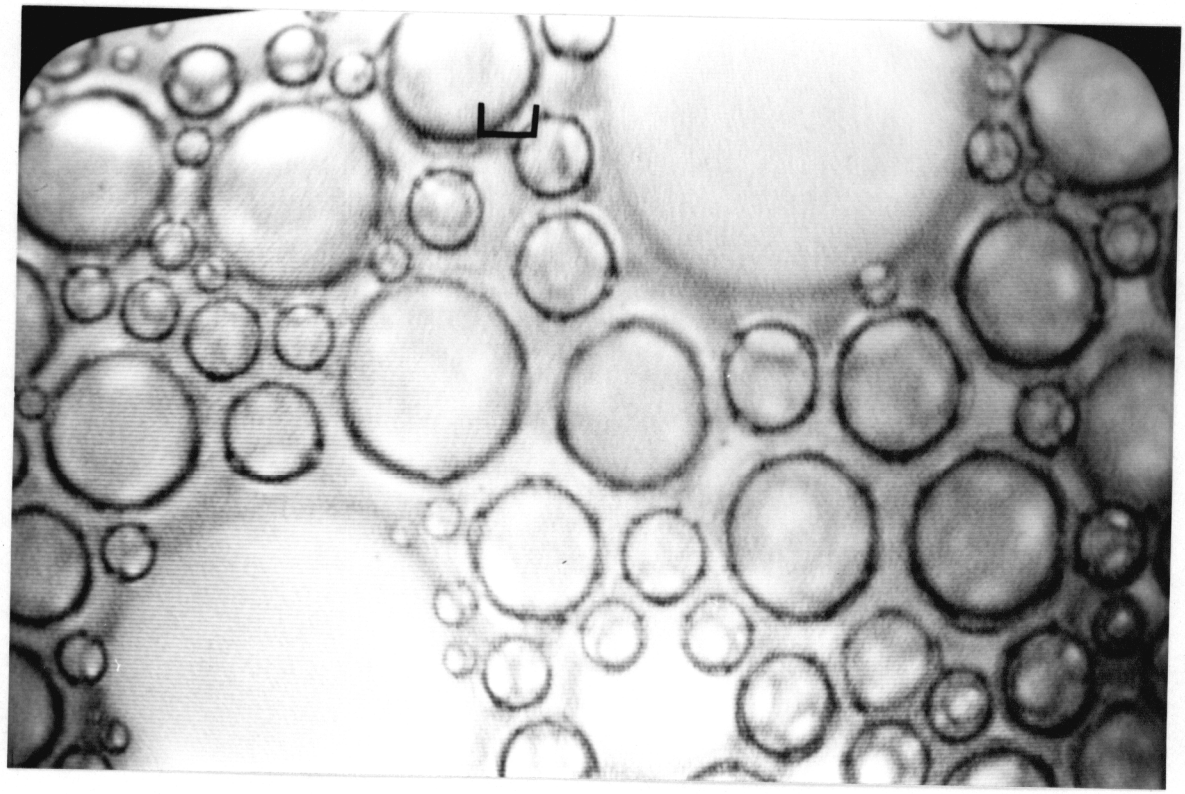

24

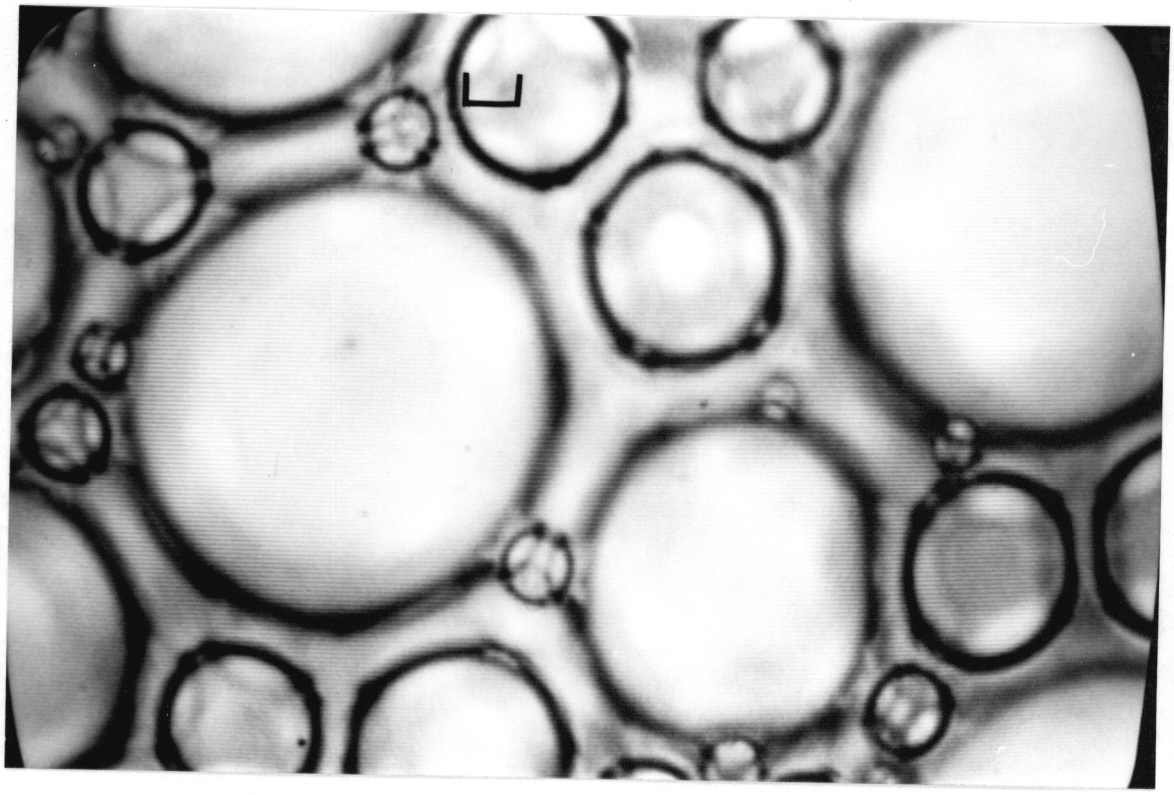

25

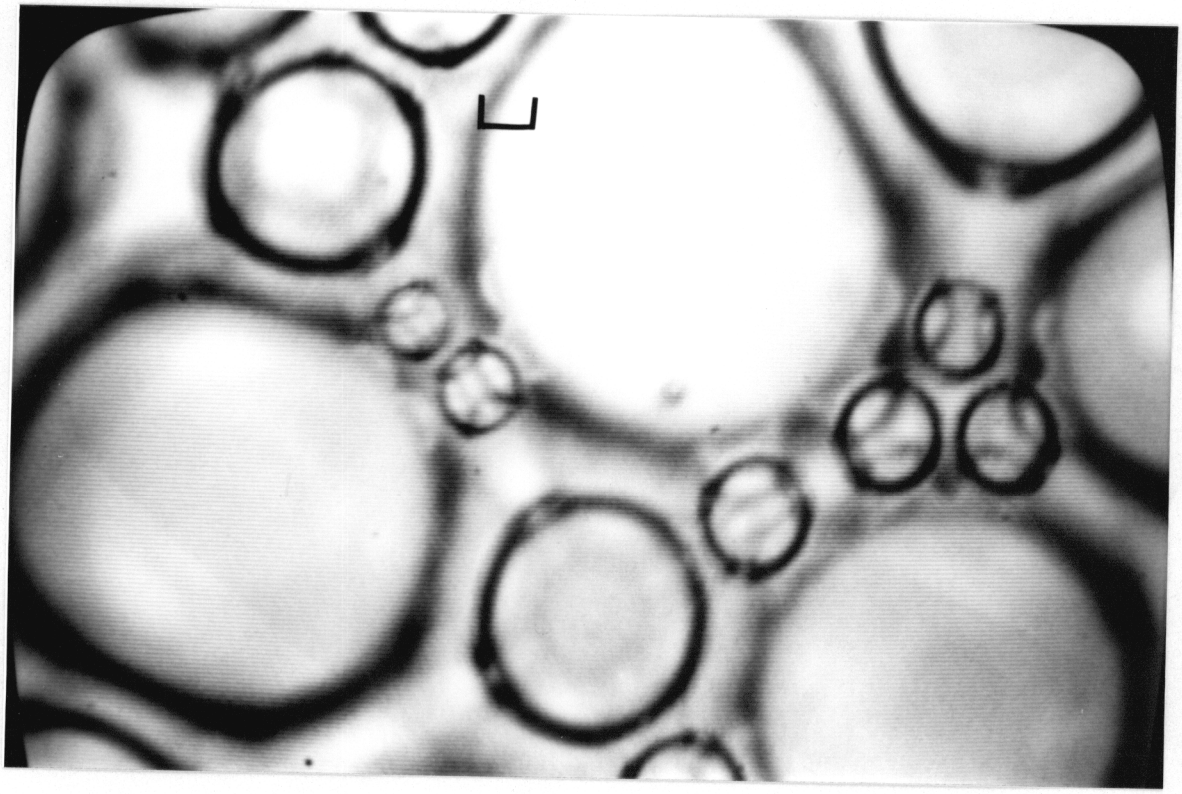

26

Vita

James A. Suggs was born in Nashville, Tennessee, April 11 1963; however, Nashville was his home for only 11 months. As the son of an Air Force officer, his childhood was spent in many different places, including the Philippine Islands. The family's last move was to College Station, Texas, where Jim attended and graduated from A&M Consolidated High School.

After graduating from high school he went to North Carolina State University in Raleigh to study Chemical Engineering. At NC State, Jim was an active member of both Tau Beta Pi and the student chapter of the American Institute of Chemical Engineers. In May of 1985, he graduated cum laude with a BS in Chemical engineering. In September of the same year Jim entered the Master of Science program at Virginia Polytechnic Institute and State University to further his chemical engineering education. During the interim between schools, he worked as a research chemical engineer for Research Triangle Institute in Research Triangle Park, North Carolina.

Jim has accepted employment with E.I. DuPont de Nemours, and after graduation will be working as a member of the Naval Fuels Product Team at the Savannah River Plant in Aiken, South Carolina.